uOttawa

L'Université canadienne
Canada's university

FACULTÉ DES ÉTUDES SUPÉRIEURES ET POSTOCTORALES

uOttawa

L'Université canadienne
Canada's university

FACULTY OF GRADUATE AND POSDOCTORAL STUDIES

Patrick Dumond
AUTEUR DE LA THÈSE / AUTHOR OF THESIS

M.A.Sc. (Mechanical Engineering)
GRADE / DEGREE

Department of Mechanical Engineering
FACULTÉ, ÉCOLE, DÉPARTEMENT / FACULTY, SCHOOL, DEPARTMENT

Towards Improving the Manufactured Consistency of Wooden Musical Instruments Through Frequency Matching

TITRE DE LA THÈSE / TITLE OF THESIS

Natalie Baddour
DIRECTEUR (DIRECTRICE) DE LA THÈSE / THESIS SUPERVISOR

CO-DIRECTEUR (CO-DIRECTRICE) DE LA THÈSE / THESIS CO-SUPERVISOR

Robert Langlois

Dan Necsulescu

Gary W. Slater
Le Doyen de la Faculté des études supérieures et postdoctorales / Dean of the Faculty of Graduate and Postdoctoral Studies

TOWARDS IMPROVING THE MANUFACTURED CONSISTENCY OF WOODEN MUSICAL INSTRUMENTS THROUGH FREQUENCY MATCHING

Patrick Dumond

A thesis submitted to the Faculty of Graduate and Postdoctoral Studies
in partial fulfilment of the requirement for the degree of

MASTER OF APPLIED SCIENCE

in Mechanical Engineering

Ottawa-Carleton Institute for Mechanical and Aerospace Engineering
University of Ottawa
Ottawa, Canada

January 2010

Your file Votre référence
ISBN: 978-0-494-65993-9
Our file Notre référence
ISBN: 978-0-494-65993-9

Abstract

Although many improvements in the manufacturing of musical instruments have been made recently, one aspect that has often been overlooked is that of the acoustic consistency of the final manufactured product. The aim of this thesis is to create a method in which a soundboard can be frequency matched to a brace in order to meet a set standard after assembly.

A simple analytical model is created in order to study the effect of the plate's stiffness and brace thickness on the combined system. The assumed shape method is used in the analysis.

Results show that by adjusting the thickness of the brace in order to compensate for the stiffness of the plate, one of the natural frequencies can be adjusted to meet a certain value. However, matching multiple natural frequencies cannot be done with a rectangular brace. Therefore modifications to the shape of the brace are suggested.

***

Bien que, récemment, plusieurs améliorations ont été mises en place dans la fabrication des instruments musicaux, un aspect souvent négligé est l'uniformité dans la qualité acoustique du produit final. Le but de cette thèse est de créer une méthode dans laquelle la table d'harmonie d'un instrument peut être unie à une barre afin d'atteindre un standard de fréquence prédéterminé après l'assemblage.

Un modèle analytique simple est créé afin d'étudier l'effet de la rigidité de la table d'harmonie ainsi que l'épaisseur de la barre sur le system combiné. La méthode de mode supposé est utilisée durant l'analyse.

Les résultats démontrent qu'en ajustant l'épaisseur de la barre, afin de compenser pour la rigidité de la table d'harmonie, une fréquence naturelle peut être ajustée à une valeur spécifique. Cependant, plusieurs fréquences ne peuvent être harmonisées avec une barre rectangulaire. Subséquemment, des modifications à la barre sont suggérées.

Acknowledgments

I would like to thank my mom for always pushing me to strive for my best even though the procrastination doesn't help. I would like to thank my dad for always going along with all my crazy ideas and always having my best interest in mind. I would like to thank my sister for being awesome and for being my partner in crime. I would like to thank Gen for promoting my creativity and always being up to the challenge. I would like to thank my mom, my dad, my sister and Gen for always supporting me and knowing when to let me do my thing, for being there when I need you and knowing when to get out of the way. You are the very best of the best and I couldn't ask for more.

I would like to thank my supervisor, Dr. Natalie Baddour, for helping me focus all my ideas and not letting me get too far off the road which led to finishing this thesis. For being there at the deadline right along with me and also, for making me realise that vibrations is a fascinating subject. Somehow, I paid attention and stayed somewhat quiet for three hours a week in vibration class.

I would like to thank Dr. Frank Vigneron for really advancing my fundamental understanding of vibrations and mechanics in general and for also helping me with certain aspects of this thesis.

I would like to thank Michel Labrosse for helping me setup my finite element model and showing me how to use prep7.

I would like to thank all my office mates for putting up with me and for generally making every school day awesome, it was well worth the ride.

Finally, I would like to thank Robert Godin of Godin Guitars for giving me important insight into the guitar manufacturing industry.

Thanks to everyone for helping me check this one off the old bucket list.

Table of Contents

Chapter 1 Background **1**
1.1 Current Techniques 2
1.2 Instrument Construction 3
1.3 Optimisation Process 6
1.4 Psychoacoustics and Frequency Measurements 9
1.5 Musical Instrument Research 10
1.6 Musical Acoustics 11
1.7 Wood 12
1.8 Technology in the Industry 14
Chapter 2 Motivation **16**
2.1 Motivation 16
2.2 Problem Statement 17
2.3 Methodology 18
2.4 Outline of the Thesis 19
Chapter 3 Analysis of a Simple Mass-Spring Model **21**
3.1 Motivation 21
3.2 System Layout and Setup 21
3.3 Case 1 – Two Masses With No Link Between Them 22
3.4 Case 2 – Two Masses With a Solid Link Between Them 23
3.5 Case 3 - Two Masses With a Link of Stiffness k_3 Between Them 24
3.6 Understanding the Effect of Stiffness k_3 25
Chapter 4 Analysis of Continuous Models **31**
4.1 Beam Theory 32
4.2 Plate Theory 33

4.3 Higher Order Solutions 38
4.4 Orthotropic Plates 39
4.5 Modified Plate Energies 41
4.6 The Assumed Shape Method 44
4.7 Alternate Method 54
Chapter 5 Results 57
5.1 Software 57
5.2 System Properties and Dimensions 59
5.3 Exact Values of the Natural Frequencies 62
5.4 Number of Trial Functions Used 63
5.5 Validation 65
5.6 Simple Mass-Spring Model Comparison 67
5.7 Frequency Matching 69
Chapter 6 Discussion 72
6.1 Material Properties 72
6.2 Dimensions 73
6.3 Exact Solutions 73
6.4 Trial Function Convergence 74
6.5 Assumed Shape versus Finite Element Method 78
6.6 Two Degree of Freedom versus Continuous 79
6.7 Frequency Matching 81
6.8 Interesting Insight 83
6.9 Sources of Error 84
Chapter 7 Analysis of a Scalloped Brace 86
7.1 Modeling of the Scalloped Brace 87
7.2 Results 88
7.3 Discussion 88
Chapter 8 Summary, Conclusions and Future Work 90
8.1 Summary 90
8.2 Conclusions 91
8.3 Recommendations for Future Work 91

Appendix A Derivation of a Simple Mass – Spring System **93**
A.1 Calculation of the System's Natural Frequencies 94
A.2 Calculation of the System's Mass 97
A.3 Calculation of the Beam's Stiffness 97
A.4 Calculation of the Plate's Stiffness 98
A.5 Maple Code for Calculating the Stiffness of the Plate 100
A.6 Maple Code for Calculating Natural Frequencies 101
Appendix B Hamilton's Principle for a Simply Supported Plate **102**
B.1 Kinetic Energy 103
B.2 Strain Energy 103
B.3 Hamilton's Principle 104
B.4 Solving the Plate's Equation of Motion 111
Appendix C Assumed Shape Method for a Beam Divided into Two Equal Sections [23] **113**
Appendix D Maple Code for the Assumed Shape Method Plate Models **137**
D.1 Maple Code for the Simply Supported Isotropic Rectangular Plate 138
D.2 Maple Code for the Simply Supported Orthotropic Rectangular Plate 143
D.3 Maple Code for the Simply Supported Isotropic Modified Plate 148
D.4 Maple Code for the Simply Supported Orthotropic Modified Plate 153
Appendix E Maple Code for the Assumed Shape Method Scalloped Brace Plate Model **159**
Appendix F ANSYS Code for the Finite Element Method Plate Models **166**
F.1 Prep7 Input File for the Simply Supported Isotropic Modified Plate 167
F.2 Prep7 Input File for the Simply Supported Orthotropic Modified Plate 168
References **170**

List of Figures

Figure 1.1: Construction of a typical violin [1] 4
Figure 1.2: Construction of a typical guitar [1] 4
Figure 1.3: Underside of a braced guitar soundboard 5
Figure 1.4: Shape of a scalloped brace 8
Figure 1.5: Orthogonal axes of wood 13
Figure 1.6: Quartersawn wood 13
Figure 3.1: Mass - spring system 22
Figure 3.2: Test specimen 26
Figure 3.3: 1st natural frequency versus the stiffness k_3 29
Figure 3.4: 2nd natural frequency versus the stiffness k_3 30
Figure 4.1: Plate problem 33
Figure 4.2: Modified simply supported rectangular plate with cross brace across its width 41
Figure 4.3: Orthotropic rectangular plate fitted with brace across its width 44
Figure 4.4: Modified plate divided into sections along the x-axis 55
Figure 5.1: Brace showing pertinent dimensions 60
Figure 5.2: Plate and brace showing pertinent dimensions 61
Figure 6.1: Comparison of the first mode for the simply supported plate with and without a brace 75
Figure 6.2: Modeshapes required in calculating the fundamental frequency of the modified plate 76
Figure 6.3: Modeshapes required in calculating the second natural frequency of the modified plate 77

Figure 7.1: Scalloped brace with the modes of vibration it affects 87
Figure A.1: Mass - spring system 93
Figure B.1: Simply supported rectangular plate 102
Figure F.1: Location of keypoints on the modified plate model..... 166

List of Tables

Table 3.1: Properties of Sitka Spruce (12% moisture) [14] 26
Table 3.2: Dimensions of the test specimens 27
Table 3.3: Mass and stiffness of each system 27
Table 3.4: Natural frequencies for various values of k_3 28
Table 5.1: Material properties for the isotropic plate and brace [14] 59
Table 5.2: Material properties for Sitka spruce as an orthotropic material [14] 60
Table 5.3: Test specimen dimensions 61
Table 5.4: Natural frequencies of the exact solution to the isotropic and orthotropic brace 62
Table 5.5: Natural frequencies of the exact solution to the simply supported isotropic plate 62
Table 5.6: Natural frequencies of the isotropic plate using 6 trial functions 63
Table 5.7: Natural frequencies of the orthotropic plate using the assumed shape method 64
Table 5.8: Natural frequencies of the isotropic modified plate using the assumed shape method 64
Table 5.9: Natural frequencies of the orthotropic modified plate using the assumed shape method 65
Table 5.10: Comparison of results for the assumed shape vs. the finite element method (isotropic) 66
Table 5.11: Comparison of results for the assumed shape vs. the finite element method (orthotropic) 67
Table 5.12: Comparison of the isotropic brace, plate and combined system natural frequencies 68

Table 5.13: Comparison of the orthotropic brace, plate and combined system natural frequencies 68
Table 5.14: Results of the 1st and 4th natural frequency when varying E_R ($h_b = 0.012\ m$) 70
Table 5.15: Results of the 1st and 4th natural frequency when varying h_b ($E_R = 850\ MPa$) 70
Table 5.16: The system is compensated so that the 1st natural frequency is held constant 71
Table 5.17: The system is compensated so that the 4th natural frequency is held constant 71
Table 7.1: Comparison of brace geometry on a simply supported isotropic modified plate 88

Nomenclature

A: Magnitude vector

D: Stiffness function

E: Young's modulus

G: Shear modulus

h: Thickness

k: Stiffness

K: Stiffness matrix

K_s: Shear correction factor

m: Mass

M: Mass matrix

L: Longitudinal axis parallel to the wood grain

L_x: Length along the x axis

L_y: Length along the y axis

m: Mode number

n: Trial function number

q: Generalized coordinates

Q: Generalized non-conservative forces

R: Radial axis normal to the growth rings and perpendicular to the wood grain

S: Stiffness components

t: Time

T: Kinetic energy of the system

T: Tangential axis tangent to the growth rings and perpendicular to the wood grain

u: Displacement along the x axis

U: Strain energy of the system

v: Displacement along the y axis

V: Potential energy of the system

w: Displacement along the z axis

w_o: Displacement along the z axis of the plate's neutral plane

W: Work

x: Axis direction and position

y: Axis direction and position

z: Axis direction and position

γ: Shear strain

ε: Normal strain

μ: Density

ν: Poisson's ratio

ρ: Mass per length or mass per area

σ: Normal stress

τ: Shear stress

φ: Discrete spatial trial functions

ω: Natural frequency

Chapter 1

Background

For hundreds of years, craftsmen around the world have been making and perfecting musical instruments. Knowledge and skill passed on from generation to generation have allowed the art to progress and flourish. Today, high end musical instruments are still surprisingly made predominantly by hand.

The use of traditional methods for making musical instruments has always been considered the only way of tuning and optimizing the individual wood pieces as well as the whole instrument in order to make each individual instrument sound its best. Scientific study of musical instruments has proven to be extremely complex with most sound subtleties unable to be measured to this day [1].

The musical instrument manufacturing industry is one that likes to cling to tradition. Many customers of the industry still cite tradition as a key component in the manufacturing of superior instruments which, in many regards, holds a certain truth. This is primarily due to a lack of technology in the industry, which would permit the reproduction of the skills used by traditional instrument makers for building instruments with consistently good tone. This is also the reason that little effort has been made to improve mass produced manufactured instruments.

1.1 Current Techniques

In the industry today, two main techniques for building wooden stringed musical instruments exist. The first technique involves hand building of the instrument by an instrument craftsman or a luthier. The second technique is much more industrialised and involves the mass production of instruments using automatic or semi-automatic machinery. Both techniques are described in further detail.

1.1.1 Hand-Built Musical Instruments

Hand-built musical instruments are built by instrument craftsmen, which in the case of stringed instruments are called luthiers. Instrument building techniques and methods are often passed down from one luthier to another and gained over years of experience. Current techniques have been perfected over hundreds of years, yet there are so many variables that luthiers still modify instruments so as to add their personal touch. A hand built instrument does not necessarily mean that no power tools have been used in the creation of the instrument, simply that each individual piece has been custom tailored by the luthier to form a whole instrument. High precision machinery is also generally not used. For this reason, while being very similar, most hand-built instruments are usually one of a kind in appearance and sound.

The overall quality of the instrument benefits from the ability to optimise each part. It is clear that a mediocre luthier will produce a mediocre instrument. However, only those who are experienced and who have developed a finely tuned ear are able to manually adjust every part of an instrument so as to optimise it. This leads to a much better playing and sounding instrument once completed [2]. The optimisation process is explained in greater detail in section 1.3.

1.1.2 Factory Built Musical Instruments

Factory built instruments considered here are those that are masse produced using automatic or semi-automatic machinery. This is the second and newer technique in the production of instruments. The motivation behind mass produced instruments is to lower their cost and make them available to more people. This is achieved by automating part or all of the building process. To do so, lumber is run through the machinery and is accurately cut and assembled to predefined dimensions and specifications. The advantage of this process is that instruments come out structurally and aesthetically very similar. The disadvantage is that because of the variable nature of wood, musical instruments come out of the process sounding acoustically quite different from instrument to instrument. There is, therefore, a great lack of consistency in the acoustical characteristics of manufactured instruments.

Once completed, the mass-produced instruments do not generally go through an optimisation process. This is considered to require the most skill and to be the most time-consuming part of instrument construction by most luthiers and is therefore completely overlooked in manufactured instruments in order to save time and money.

1.2 Instrument Construction

Most wooden stringed instruments have similar features that allow them to produce sound. While it has been shown numerous times that all parts of an instrument contribute to the overall sound, there is general agreement that it is the soundboard, also known as the top plate, of the instrument that is most acoustically active and for which the highest inconsistency exists [3]. The construction of a typical violin and guitar is shown in figure 1.1 and figure 1.2.

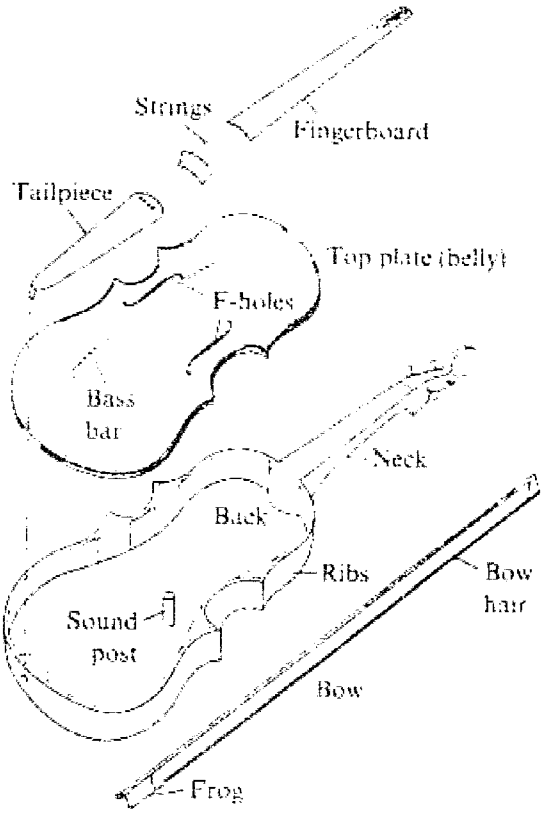

Figure 1.1: Construction of a typical violin [1]

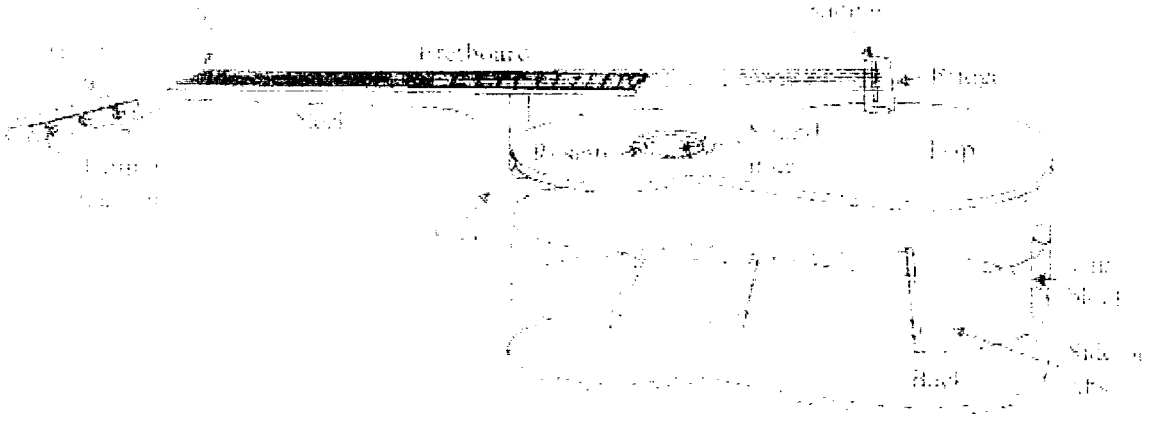

Figure 1.2: Construction of a typical guitar [1]

A stringed instrument is built so that the strings are connected to the soundboard via the bridge. The energy produced when the strings vibrate causes the bridge to rock. This energy is then transferred to the soundboard because it is coupled to the bridge. This in turn causes the soundboard to vibrate. The design of the soundboard serves two purposes. The first is to structurally resist the immense tension of the strings and the second is to

produce the sound or tone which is associated with each individual stringed instrument (e.g. the sound of a violin versus the sound of a guitar).

In order for the soundboard to be flexible enough to vibrate at the desired frequencies, it is made thin. This makes the soundboard structurally unsuitable to resist the immense string tension. In order to compensate for this, braces are added to the underside of the soundboard. While these are structural in nature, they can also be adjusted so as to produce the desired frequencies. This is discussed further in section 1.3.

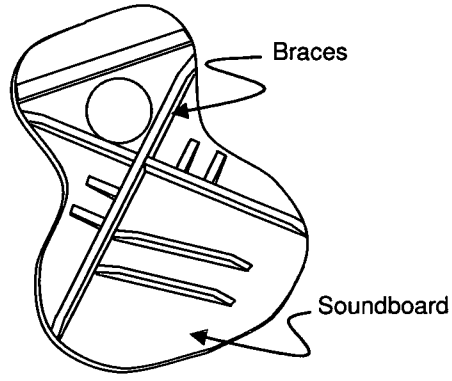

Figure 1.3: Underside of a braced guitar soundboard

The soundboard produces sound in two main ways. Both sound-producing methods involve the soundboard pushing the mass of air around it. The first method in which the soundboard produces sound is by acting as a bellow displacing the air within the cavity of the body. Having nowhere to go, the air leaves the cavity through the aperture(s), known as the sound hole(s). This method of sound production is known as a Helmholtz resonator and it has been shown that the important factors in such sound production are the cubic volume of the space in the cavity, as well as the size of the aperture [4]. Using modern technology, the cavity within the instrument's body, as well as the aperture can have very precise dimensions. Therefore the acoustic properties of the sound produced by the Helmholtz resonator are considered to be constant.

The second method of sound production is of the soundboard moving the air on its outside surface. The predominant factor which influences the sound produced here is the natural frequencies of the vibrating soundboard itself. Therefore, so that there is acoustic consistency in the final product, there must be consistency in the vibration properties of

the soundboard itself. This is seen as a difficult task because of wood's inherently inconsistent properties.

The soundboard itself is assembled around its edges to the instrument's sides. The sides of the instrument are also known as ribs. The boundary conditions of the soundboard are probably somewhere between a simply supported and clamped edge [1]. This is primarily due to flexibility in the ribs. These ribs are also assembled to a back which closes off the body cavity. The body is then connected to a neck which also has a head. Strings are attached to the instrument's head and run along the length of the neck where they attach to the bridge, as seen in figure 1.1 and figure 1.2.

It is all these parts assembled as a whole and tuned to specific frequencies which allow the production of harmonious sound known as music in the hands of a trained musician.

1.3 Optimisation Process

The most widely used method for optimising musical instruments is known as tap tuning. Tap tuning involves the manual adjustment of braces placed on an instrument's soundboard by removing brace material until a desired sound or frequency is obtained. It is important to note that by removing brace material, the natural frequencies are lowered [5]. This is because by removing material from the brace, its stiffness is reduced as well as its mass, however the removal of wood has a larger impact on the brace's stiffness then it does on its mass. Thus, looking at basic vibration theory as seen in equation (1.1), if the stiffness k is reduced by a greater factor then is the mass m, the natural frequencies ω are also reduced.

$$\omega^2 = \frac{k}{m} \tag{1.1}$$

For the greater part of the stringed instrument's history, the optimisation process has been performed by ear. The luthier generally holds the soundboard at a known node (location of zero displacement) for a given vibration mode. The specific mode chosen for tap tuning is usually based on the luthiers preference. There is common consensus

however, that the lower modes are of greater importance [6]. The luthier then holds the soundboard up to his ear and taps it at the chosen mode's anti-node (location of maximum displacement). Based on what is heard, the luthier removes material from the soundboard's braces in order to obtain the desired sound. It evidently takes a lot of practice and years of experience to know what to listen for and where to remove material during the optimisation process.

More recently, instrument builders have started looking at the modal patterns produced at the various natural frequencies of a given instrument. Often referred to as Chladni patterns, they are the visual representation of the way in which the instrument vibrates at different frequencies. Much research has been done in this area using both sand and laser interferometry in order to visualize these Chladni patterns [7]. Some luthiers have even gone as far as trying to adjust the soundboard braces based directly on the patterns seen and the frequencies at which they are seen. The soundboard is usually excited at a certain frequency and the braces adjusted until the expected pattern appears. This has however proven to be an extremely complex task where only a detailed study on violins has enabled a set of instructions for the modification of the 1^{st}, 2^{nd} and 5^{th} modes for improving the sound quality [6]. No other guide is available for the mode tuning of instruments besides the violin. More recent studies have in fact demonstrated that it is the natural frequencies that are more important than the modal patterns, due to the fact that modes can be re-ordered by way of dimensional changes in the specimen being adjusted [8].

A more intuitive approach, based on old methods and new technology, is also becoming popular [5]. The soundboard is held similar to the tap-tuning method described above, but instead of tapping the anti-nodes, each brace is tapped in sequence. The frequency spectrum is recorded using a microphone. Each brace is then adjusted to a pre-determined frequency. The pre-determined frequencies are based on those which create a harmonious frequency spectrum for the overall soundboard. Alternatively, the soundboard can be supported around its perimeter, similar to the way in which it will be installed on the instrument, during the tapping process. The use of strobe tuners, oscilloscopes or frequency spectrum software reduces the amount of experience required by the luthier. The method also describes removing material from the centre of the brace

to quickly lower the natural frequencies and to remove material from the ends so as to fine tune to the final desired frequency. This often leads to what is known as scalloped braces, as shown in figure 1.4.

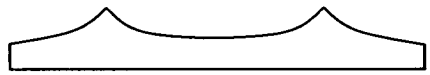

Figure 1.4: Shape of a scalloped brace

Much debate exists in the industry as to whether or not scalloped braces improve the sound of musical instruments based directly on its shape or whether it is the result of the tuning process itself, which more often than not leads to this shape. Proponents exist for both sides of the argument but little is known scientifically about the effects of the scalloped shape.

Interestingly enough, some builders have taken the relationship between frequency and stiffness seriously, and have developed what is called deflection tuning [5]. This method, which lends itself more useful to manufacturing, is based on the idea that since a soundboard that is stiffer produces a higher frequency, then lowering its stiffness should also lower the frequency. While the actual process of brace adjustment is just as time consuming as previous methods, the skill required to understand what needs to be adjusted is less important. This is because a simple deflection measurement is taken under a known force and compared to a set standard. Material is then removed until the deflection matches this standard. This method is ideal for instrument makers who have not yet developed a finely-tuned ear or for a noisy manufacturing environment which makes it difficult to take frequency measurements. This method is still quite time consuming and still requires human intervention, therefore it is not generally used for low cost instruments.

1.4 Psychoacoustics and Frequency Measurements

Psychoacoustics is the science of the human perception of sound. The study of how the human hearing system perceives the sound produced by musical instruments is an extremely important factor. Studies clearly show that what is measured by scientific instruments is not necessarily what is perceived by the builder or the player [9]. Their interpretation of such auditory stimulus provided by a musical instrument can also be different. While most people cannot agree as to what exactly makes a musical instrument sound good, most agree upon what instruments do sound good [10]. This leads some to believe that there are indeed specific factors that make great sounding instruments. However, these factors are as of yet unknown.

In psychoacoustics, pitch is generally referred to as the perceived frequency heard by the listener. Because the ear is a complex system, the pitch may not be the same as the frequency measured using scientific instruments. This seems to be increasingly true above 1 kHz as the gap between the frequency and pitch widen up to the hearing threshold [9].

Research into the necessary frequency accuracy during modeling and analysis seems to point to about a 1% margin due to the ear's sensitivity to pitch [11].

Some people are able to finely tune their ear's sensitivity through training and are able to distinguish and pinpoint specific pitches. This is especially useful to a luthier who wishes to optimise the sound produced by his instruments. For those without such a talent, new tools and techniques exist to help them. The most useful of these tools is frequency spectrum analysis software. Software such as this allows a luthier to record the sound produced by an instrument and then to plot the frequency spectrum of the sound.

Avoiding the whole perception of sound all together, some luthiers prefer to use the Chladni pattern approach. This reduces the psychoacoustic effects, as described above.

1.5 Musical Instrument Research

While musical instruments have been around for millenniums, their scientific study has only begun. Since the middle of the 20th century, a few researchers have been trying to understand the physical workings of musical instruments, notably the violin. Early research focused mainly on identifying the key factors which give violins their tone and what differentiates good instruments from great ones. To do so, researchers consider the methods used to construct violins, the vibration properties of the strings, the way in which the strings interact with the instrument through the bridge, the effect of braces and the properties of the wood used itself [12]. This has led to a widespread focus on the actual vibration properties of the instrument, notably the soundboard. Visual methods were developed based on Chladni patterns, which allow researchers to see the modes of vibration at various frequencies. Based on what they observe, researchers attempt to reproduce instruments which are considered to be of high sound quality. Finally, a lot of effort has been spent studying the radiation of the sound produced by the instrument, since it is the sound radiation of the instrument which is heard by both the player and the audience [7].

More recently, researchers have discovered that the understanding gained on the violin translates fairly well to other wooden stringed instrument. Therefore, a wider variety of instruments are now being scrutinized. Also, with recent advances in computer technology many researchers are now focusing their attention on numerically modeling musical instruments. More computing power is still necessary in order to refine models enough for the higher frequency range [11].

Over the entire period of time that researchers have been building theoretical models of musical instruments, another set of researchers have been continuously improving experimental methods to test them. This has allowed the science to progress by validating what little is in fact known about musical instruments.

1.6 Musical Acoustics

The understanding of musical acoustics has also made leaps and bounds in understanding what makes music different from noise. Researchers agree that music is produced by a mathematical arrangement of frequencies which is pleasing to the ear.

Most instruments are played one note at a time or with chords (i.e. an assembly of notes played at once). Even when only one note is played, a whole set of characteristic frequencies are excited. These sets of characteristic frequencies are what help differentiate the sound of various instruments. The lowest characteristic frequency is known as the fundamental frequency. The other characteristic frequencies help give the sound body and are known as partials. These partials give the sound its flavour and are considered to be one of the determining factors in giving an instrument its specific tone. Through experimental study, it has been shown that in instruments of similar design it is the ratios of these partials to the fundamental which are related.

When partials are integral multiples of the fundamental, they are known as harmonics. The pitch of a set of characteristic frequencies is assigned to the pattern created by the fundamental and its harmonics. Any given number of these harmonics, including the fundamental can be missing from a set of characteristic frequencies while still being able to assign a specific pitch to the sound heard by the ear. In general, a minimum of two are necessary for the nervous system to recognize the pattern [13].

Furthermore, damping properties or the decay time of specific partials have also recently been shown to help give an instrument its tone [11]. This helps explain the reasons for the lack of success in fully reproducing the sound of a wooden stringed instrument using composite materials. Although the structural properties can be matched quite successfully, the tone of a composite instrument is quite different from that of a wooden instrument due primarily to the different damping properties of the materials used.

1.7 Wood

Wood is a naturally occurring material obtained from trees. As with almost any natural material, wood's properties vary highly from specimen to specimen, usually requiring compensation for these statistical variations. When using wood as a structural material, an engineer simply overcompensates using the weakest known property of the statistical distribution. However, when it comes to getting consistent acoustical properties, overcompensating in fact dampens the beautiful acoustic properties that are usually sought.

From an engineering point of view, it is important to understand these variations so as to be able to better control manufacturing with these materials. All types of wood have grain that run in one direction, which make it stiffer in that particular direction. This grain is due to the annual growth ring of trees. Growth rings occur because trees grow at a quicker pace in the early season, expanding width wise. The wood that grows during this period is known as earlywood and is characterized by cells having thin walls leaving large cavities. Latewood occurs during the late growing season when a tree's physical growth slows down creating a much denser wood characterized by thick walled, small cavity cells. This denser wood is what becomes visible as annual rings or grain. Depending on the climate and weather, more or less earlywood is produced, increasing or decreasing the number of growth rings per area or what is known as grain count [14].

Because of this grain, wood is considered to be an orthotropic material. This means that wood has different constant properties in each of the three orthogonal axes. We name the three axes as follows [14]:

- Longitudinal axis L (parallel to the grain)
- Radial axis R (normal to the growth rings, perpendicular to the grain)
- Tangential axis T (tangent to the growth rings, perpendicular to the grain)

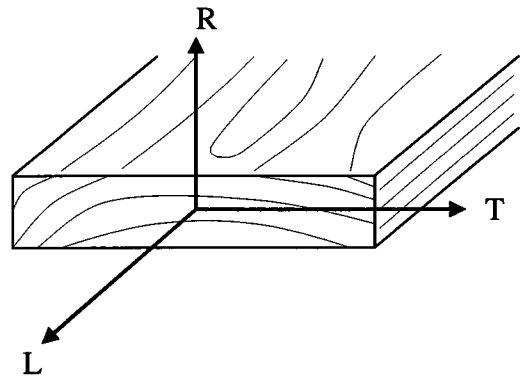

Figure 1.5: Orthogonal axes of wood

Instrument makers recognize the importance of grain direction and generally agree that for best instrument wood, the tree should be quartersawn [2]. This means that the wood is sawn so that the grain is as parallel as possible to the tangential axis across the wood's thickness. The closer the grain is to being parallel to the tangential axis across the thickness, the stiffer the wood will be in both the longitudinal and radial directions. Luthiers normally use this degree of grain straightness and uniformity as one important measure of the wood's quality [2]. This leads to two important property directions for the instrument maker as seen in figure 1.6.

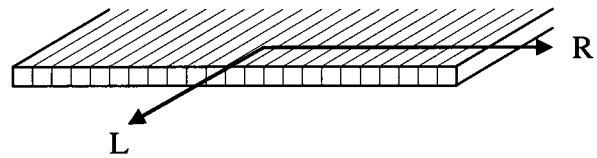

Figure 1.6: Quartersawn wood

Wood is generally stiffer in the longitudinal direction because the grains act as fibres in that direction. The important properties in each direction are Young's modulus and Poisson's ratio. It is these properties along with the density of the wood that vary from specimen to specimen and which need to be adjusted in order to obtain better consistency of the final manufactured product.

It is interesting to note that for over a century the preferred wood used for backs and sides by builders of musical instruments, notably guitars is that of rosewood. A recent study has shown that out of seven typically used hardwoods, rosewood produces the most

consistent natural frequencies in a finished instrument built using very tight dimensional tolerances [10]. This may in fact point to the importance of natural frequency consistency in the instrument building process.

Although consistent material would make the task easier, master classical guitar player and renowned luthier, Richard Bruné, who is considered by some to be in the best position to give insight on the matter, states that great instruments can always be made from less than ideal wood [10]. This gives light to the fact that natural frequencies are adjustable and can be matched to those which are considered to produce great instruments.

1.8 Technology in the Industry

Over the last decade or so, many larger manufacturers have started to look at ways to improve the consistency of their manufacturing processes. Most have taken the approach of increasing the accuracy of their tooling in order to improve their dimensional building consistency. To do so, many manufacturers have brought in numerically controlled machinery, lasers and robots as well as custom-built jigs which ensure greater accuracy and consistency [10]. This has increased the number of good instruments that come out of the manufacturing process and decreased the number of rejected instruments unsuitable for sale.

Acoustical consistency is, however yet to be addressed. This is primarily due to the complexity in understanding the sound produced by musical instruments. Techniques proven to help improve acoustical consistency are as of yet too time consuming and require too much manual skill for a typical manufacturing production. Therefore manufacturers are usually reticent to incorporate any of them as a step in the building process.

A recent visit to the Godin acoustic guitar factory has verified the claims in literature that the acoustical quality of a soundboard plate is tested by measuring its stiffness across the grain. During the manufacturing process, the deflection across the soundboard's grain without braces is measured under a known load. Based on a certain set of deflection

ranges, the soundboards are judged to be of higher or lower acoustical quality and are therefore used in different product lines. This test gives an idea as to the soundboards stiffness and thus the resulting frequency of the final product. Although not a robust scientific verification of the soundboard's potential, this method has been used and has worked to a certain degree for many generations of musical instruments. Since the manufacture is aware of the range of soundboards for which its specifically dimensioned braces produce decent instruments, a certain quality control is obtained.

Chapter 2

Motivation

2.1 Motivation

A significant amount of research has been performed over the last half century on modeling musical instruments, figuring out what they do and how they do it, deciphering the factors that make a great instrument great and improving the dimensional consistency of the manufacturing process. However, little has been done to improve the acoustical consistency of the final product and this is what forms the motivation behind this research.

It is also the purpose of this research not to stray too far from current industry practice, with the intent of keeping manufacturing costs to a minimum. As mentioned in section 1.8 on current industry technology, the only acoustic quality control performed on the soundboard during production is to test its stiffness across the grain. For the purposes of this research, it is assumed that a precise measurement of this stiffness is available. Current manufacturing practice involves using dimensionally identical braces on soundboards. This research seeks to exploit the availability of advanced manufacturing techniques, such as CNC manufacturing or other, which permit the fabrication of custom-made braces. The idea behind this is that based on its measured stiffness, it should be possible to frequency match a given soundboard with a set of custom-made braces to produce an instrument that meets a set standard. In industry, the information obtained

through the deflection stiffness measurement can be analysed via software to produce the required brace dimensions. This information can then be passed on to CNC machinery which can cut the frequency matched braces for the given soundboard.

The idea of frequency matching discussed throughout this thesis refers to the adjustment of natural frequencies in individual systems, so that when combined these systems produce a set of natural frequencies which are matched to a set standard. In essence, in using and adjusting the natural frequencies of these individual systems, it is possible to predict the combined system's natural frequencies before assembly. In musical terms, this is usually referred to as tuning of the individual components.

2.2 Problem Statement

It is assumed that a great instrument exists and can be used as a benchmark for which the natural frequencies of other manufactured instruments can be compared. It is also assumed that the soundboard is given, along with knowledge of its stiffness across the grain as a precise measurement and not a range of measurements. The question is then to determine the shape and dimensions of the braces that will be matched to this soundboard so that the coupled soundboard/brace system has the same natural frequencies as the benchmark instrument. This calculated shape of the brace can then be easily manufactured with modern manufacturing techniques to produce a custom brace for that particular soundboard.

To the best of the author's knowledge, no work has been done on the problem as formulated above, with the current solution consisting of custom, hand manufacturing and tuning by a luthier as explained in chapter 1.

2.3 Methodology

The manufacturing problem as stated above can be rephrased in terms of a vibrations problem. The problem then becomes one of combining two separate vibrating elements, consisting of the brace(s) and the soundboard, to produce a coupled system with desired or specified frequencies of vibration. As stated above, it is assumed that the soundboard is given and cannot be modified, while it is sought to determine the shape and dimensions of the brace so that the combined system has the desired frequencies.

As explained in chapter 1, current state-of-the-art thinking is that it is the first few modes of the coupled system that are necessary in order to tune the soundboard during manufacturing. Therefore, it is the first few modes of the combined brace/soundboard system that will be of interest and the approach taken to solving the problem will make use of this fact.

While the finite element method is seemingly the industry standard for modeling, it is not necessarily the best choice to gain insight as to the interactions between the soundboard and its braces. Other methods are therefore also considered.

The first attempt to gain insight into the problem starts with the simplest possible model in order to understand how the coupled system interacts. Thus, the analysis begins with a simple two degree of freedom system. In this first model, the soundboard and its braces have been simplified to a plate and a single brace, where the first degree of freedom is allocated to the fundamental frequency of the plate and where the second degree of freedom is the fundamental frequency of the brace.

Using the insight gained from such a simplistic problem, a continuous model of the brace and plate setup is then developed and analyzed. Since no exact solution exists for such a setup, different solution approaches must be considered.

To solve the aforementioned continuous problem, numerical methods such as the finite element or finite difference methods are often used [11]. Numerical methods are popular because they are able to model extremely complex shapes accurately. The disadvantage to using such numerical models is the lack of insight that would otherwise

be obtained by observing how the model reacts to changes in the overall structure. This is due to the fact that the method of analysis uses finite functions to construct the solution.

However, in this thesis, methods which use global functions such as the Rayleigh-Ritz, assumed shape and weighted residuals methods shall be used, as they offer insight into the overall behaviour of the model as changes are applied. Although limited to less complex shapes than the numerical methods, they are still able to model many coupled systems that do not have exact solutions. Furthermore, the assumed shape method has specifically been chosen as the analysis tool because of its direct approach and ease of use. It is also preferred because of the vibration insight it gives about the model's natural frequencies, as well as its corresponding vibration modes [15].

The insight gained from this model will further the understanding of the brace-soundboard interaction and will enable the development of more complex models through future research.

2.4 Outline of the Thesis

The thesis begins by looking at the simple mass-spring system used to model the plate and brace in chapter 3. Chapter 4 gives the theory for the continuous system model by developing the exact solution for each of the brace and the plate. It also describes the kinetic and strain energy of a plate for both isotropic and orthotropic materials. Higher order solutions are also discussed. Finally the assumed shape method is explained. Chapter 5 gives the results of the analysis for the analytical solutions of the brace and plate along with a comparison of the solutions from the assumed shape and finite element methods. The ability to frequency match a brace to a plate is also investigated. Chapter 6 discusses the results obtained through the analysis and also discusses the insight gained throughout the research. Chapter 7 develops and discusses the possibility of using a brace having a scalloped shape in order to frequency match more than one natural frequency in the combined system. Finally, conclusions and recommendations for future work are given in chapter 8.

It is hoped, that through this research, a complete and efficient method for improving the acoustical consistency of manufactured wooden stringed musical instruments, without dramatically altering their cost, can eventually be developed.

Chapter 3

Analysis of a Simple Mass-Spring Model

3.1 Motivation

We begin our analysis by looking at a simple mass-spring system. The motivation behind developing such a simple system is to observe the fundamental interactions that occur between the vibrating plate and brace. To do so, system 1 will be used as representative of the plate and system 2 will be representative of the brace. The insight gained herein will be used in developing a continuous model. It is also the purpose of this simple model to observe the effects that the connection between the plate and the brace has on the combined system's natural frequencies.

3.2 System Layout and Setup

The simple mass-spring system can be seen in figure 3.1. The setup involves two mass–spring systems having each one degree of freedom (1DOF). Three different cases will be used to analyse the systems. The first involves no coupling between mass – spring systems. The second involves a rigid link between both systems. Finally, the third is coupled using a link of certain stiffness. We have chosen to analyse this simple example to better understand the effect the coupling stiffness between the two systems has on the natural frequencies of the overall system. A mass – spring system can be used as a simple

representation of the actual system and helps lay down the ground work for our understanding of the systems behaviour.

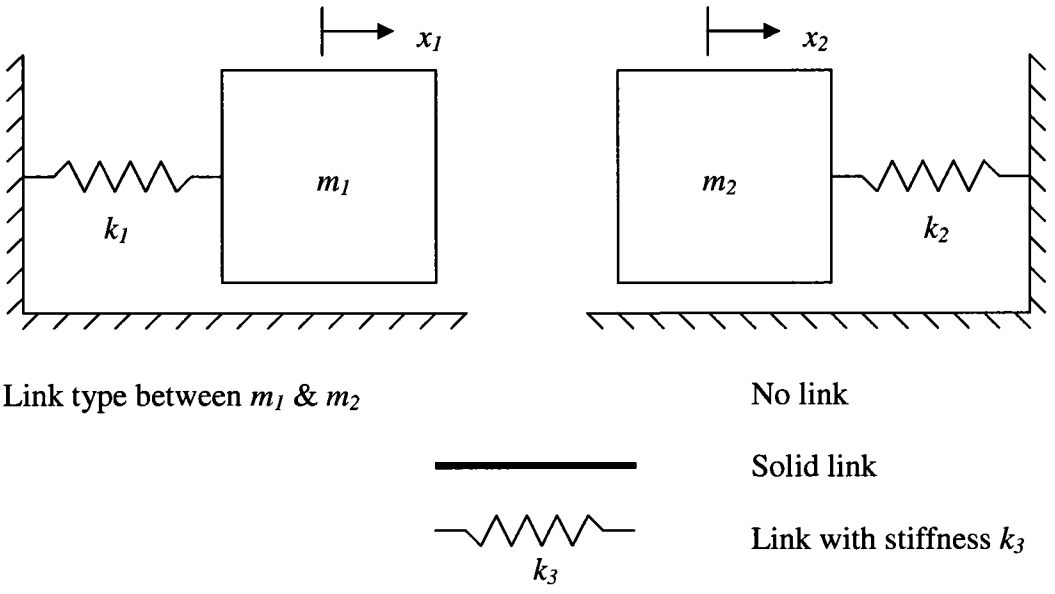

Figure 3.1: Mass - spring system

The Lagrange method is used to solve the natural frequencies for all three cases. We must begin by finding the kinetic and potential energy of each case. A detailed derivation of each case can be found in appendix A. We look at each case individually.

3.3 Case 1 – Two Masses With No Link Between Them

The first case we look at involves two mass–spring systems that have no coupling between them. Writing the kinetic and potential energy for both systems gives

System 1	System 2	
$T_1 = \frac{1}{2} m_1 \dot{x}_1^2$	$T_2 = \frac{1}{2} m_2 \dot{x}_2^2$	(3.1)
$V_1 = \frac{1}{2} k_1 x_1^2$	$V_2 = \frac{1}{2} k_2 x_2^2$	

Using Lagrange's method, the natural frequencies for each of the two systems can be found as

$$\begin{array}{ll} \text{System 1} & \text{System 2} \\ \omega_1 = \sqrt{\frac{k_1}{m_1}} & \omega_2 = \sqrt{\frac{k_2}{m_2}} \end{array} \tag{3.2}$$

The natural frequencies above represent those for each uncoupled system. Because no link is present between them they do not influence each other in any way.

3.4 Case 2 – Two Masses With a Solid Link Between Them

The second case involves two mass–spring systems which are coupled using a solid link. The solid link means that both individual systems now act as one large single system having only one displacement variable and one natural frequency. Developing the kinetic and potential energy for the system gives

$$T = \frac{1}{2}(m_1 + m_2)\dot{x}_1^2 \qquad V = \frac{1}{2}(k_1 + k_2)x_1^2 \tag{3.3}$$

Using Lagrange's method, the natural frequency for the overall system (subscript '*s*' for solid link) is given by

$$\omega_s = \sqrt{\frac{(k_1 + k_2)}{(m_1 + m_2)}} \tag{3.4}$$

Since a solid link couples both systems, each individual system now moves as one entity. There is therefore only one natural frequency for the system as it remains a 1DOF system. It is evident that it is nothing more than the sum of both the stiffness and mass of each system.

3.5 Case 3 - Two Masses With a Link of Stiffness k_3 Between Them

The third case couples the two mass–spring systems using a link of stiffness k_3. The individual natural frequencies of each system influence each other to create natural frequencies of the coupled system. The kinetic and potential energy for the coupled system can be expressed as

$$T = \frac{1}{2}m_1\dot{x}_1^2 + \frac{1}{2}m_2\dot{x}_2^2 \qquad V = \frac{1}{2}k_1x_1^2 + \frac{1}{2}k_2x_2^2 + \frac{1}{2}k_3(x_2 - x_1)^2 \tag{3.5}$$

Using Lagrange's equation, it can be seen that because the system now has two degrees of freedom, there are two natural frequencies for the coupled system. The subscript '*p*' is for the plus root and the subscript '*m*' indicates the minus root

$$\omega_p^2 = -\frac{1}{2m_1m_2}\left(-m_1(k_3+k_2) - m_2(k_3+k_1) + \sqrt{m_1^2(k_3^2+k_2^2+2k_2k_3) + m_2^2(k_3^2+k_1^2+2k_1k_3) + 2m_1m_2(k_3^2 - k_1k_3 - k_2k_3 - k_1k_2)}\right) \tag{3.6}$$

$$\omega_m^2 = -\frac{1}{2m_1m_2}\left(-m_1(k_3+k_2) - m_2(k_3+k_1) - \sqrt{m_1^2(k_3^2+k_2^2+2k_2k_3) + m_2^2(k_3^2+k_1^2+2k_1k_3) + 2m_1m_2(k_3^2 - k_1k_3 - k_2k_3 - k_1k_2)}\right) \tag{3.7}$$

Theses two natural frequencies are those associated with the 2DOF of the new coupled system. They are complicated by the fact that they are coupled by a link of stiffness k_3. The effect that each system has on each other as well as the effect the link has on the system is not yet clear. However it is obvious that the natural frequencies are a combination of the properties of each system.

3.6 Understanding the Effect of Stiffness k_3

To better understand the effect that k_3 has on the coupled system, the two limits of k_3 being very small and very large are considered. To determine what happens when k_3 is small, the limit of k_3 in (3.6) and (3.7) is taken as k_3 goes to zero. This result is given by

$$\lim_{k_3 \to 0} \omega_p^2 = \frac{k_1}{m_1} = \omega_1^2 \tag{3.8}$$

$$\lim_{k_3 \to 0} \omega_m^2 = \frac{k_2}{m_2} = \omega_2^2 \tag{3.9}$$

Clearly in the limit, as k_3 approaches zero, there is no link between the two masses and the two natural frequencies should be those of the uncoupled system. This is indeed the case as can be seen in equations (3.8) and (3.9). To see what happens when k_3 is large, the limits of (3.6) and (3.7) are taken as k_3 it goes to infinity. This gives

$$\lim_{k_3 \to \infty} \omega_p^2 = \frac{k_1 + k_2}{m_1 + m_2} = \omega_s^2 \tag{3.10}$$

$$\lim_{k_3 \to \infty} \omega_m^2 = \infty \tag{3.11}$$

From the previous equations, it can be seen that when k_3 becomes very large, the system begins to act as a coupled system having only one natural frequency equivalent to a coupled system having a solid link.

Conversely, as k_3 becomes very small, the "plus" root natural frequency approaches that of uncoupled system 1 and the "minus" root natural frequency approaches that of uncoupled system 2. This result is to be expected from a system having such a small coupling stiffness that very little energy is transferred from one system to the other.

The above relationships can be further investigated by solving the natural frequencies using numerical values. This will allow investigation into the behaviour of the system as

the stiffness k_3 is changed. To determine appropriate stiffness and mass for each system, consider the properties of Sitka Spruce, the material of interest. Since Sitka Spruce, as well as any other wood, is an orthotropic material, property values in the longitudinal direction parallel to the grain will be used as described in section 1.7.

Table 3.1: Properties of Sitka Spruce (12% moisture) [14]

Density μ (kg/m^3)	Young's modulus E_L (MPa)	Poisson's ratio ν_{LR}
403.2	10890	0.372

These properties can be used along with the general dimensions of the test specimens to get a rough estimate for the mass and stiffness of each system. System 1 is represented by a thin square plate. System 2 is represented by a beam with a square cross section. The dimensions of the test specimens can be seen in table 3.2.

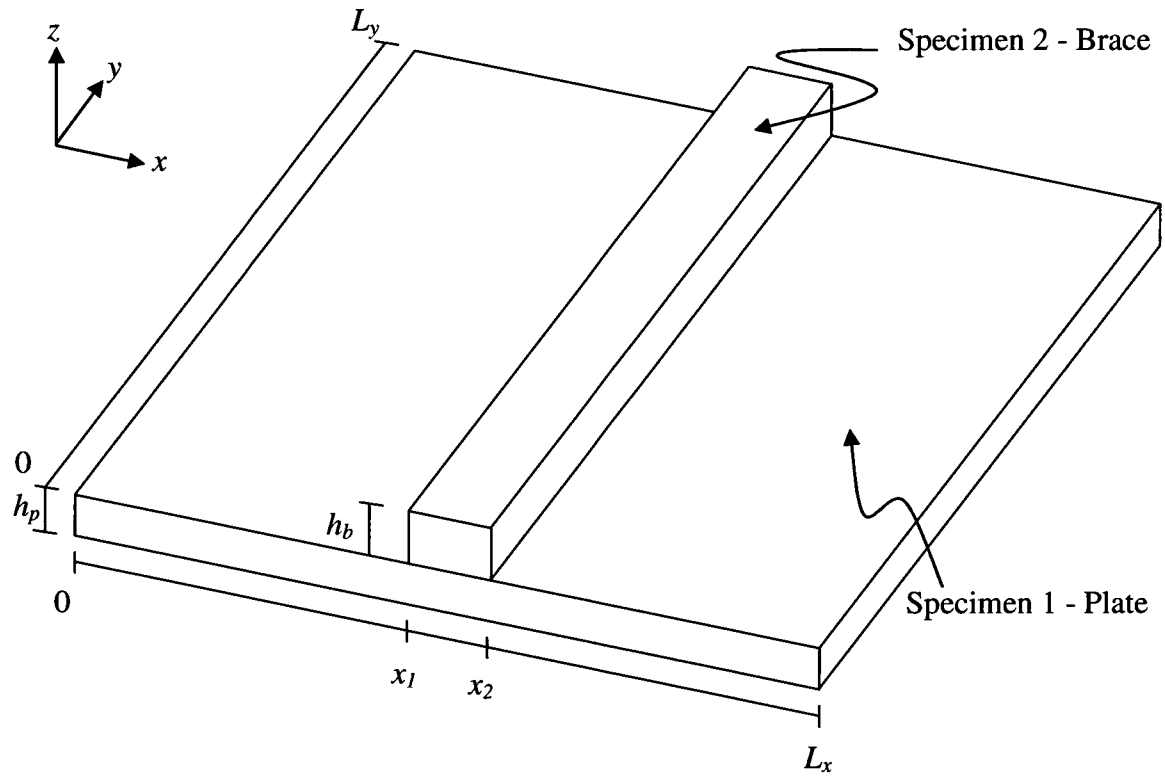

Figure 3.2: Test specimen

Table 3.2: Dimensions of the test specimens

Specimen	Length x - L_x (m)	Length y - L_y (m)	Thickness – h (m)
1	0.24	0.18	0.003
2	0.012	0.18	0.012

The calculation of the mass and stiffness for each system is detailed in appendix A. A summary of these values is found in table 3.3.

Table 3.3: Mass and stiffness of each system

m_1 (kg)	k_1 (N/m)	m_2 (kg)	k_2 (N/m)
0.05575	60569.74	0.01115	65340

The stiffness of the link k_3 is varied to see the effect it has on the system. The analysis is started by considering the natural frequencies of each individual system as calculated in equations (3.2). For the mass and stiffness stated in table 3.3, the natural frequencies are

$$\omega_1 = 1042.33\,rad/s \qquad \omega_2 = 2420.76\,rad/s$$

The natural frequency associated with the systems coupled by a solid link is given by equation (3.4)

$$\omega_s = 1371.88\,rad/s$$

As expected, this natural frequency falls between the natural frequencies associated with systems 1 and 2. Finally, from equations (3.6) and (3.7), the two natural frequencies associated with the coupled system having a link of stiffness k_3 are calculated. It can be seen from these equations that they are highly dependent on values of k_3. The values of the natural frequencies have been tabulated for various values of k_3 and are given in table 3.4.

Table 3.4: Natural frequencies for various values of k_3

k_3 *(N/m)*	ω_p *(rad/s)*	ω_m *(rad/s)*
1	1042.34	2420.78
10	1042.42	2420.95
100	1043.19	2422.61
1000	1050.74	2439.28
10000	1112.06	2605.01
100000	1287.90	4006.27
1000000	1361.43	10616.80
10000000	1370.81	32883.14
100000000	1371.77	103766.07
1000000000	1371.87	328067.65

The 1st natural frequency versus the stiffness k_3 is shown in figure 3.3, and it can be seen that within a range of stiffness of 1000 to 1000000 *N/m*, k_3 has a large effect on the coupled system's natural frequencies. However, below these values, the system acts as two separate systems with a 1st natural frequency of about 1042 *rad/s*, which coincides nicely with that of the natural frequency of system 1. Above these values, the system acts as a system with a solid link with a 1st natural frequency of about 1372 *rad/s*.

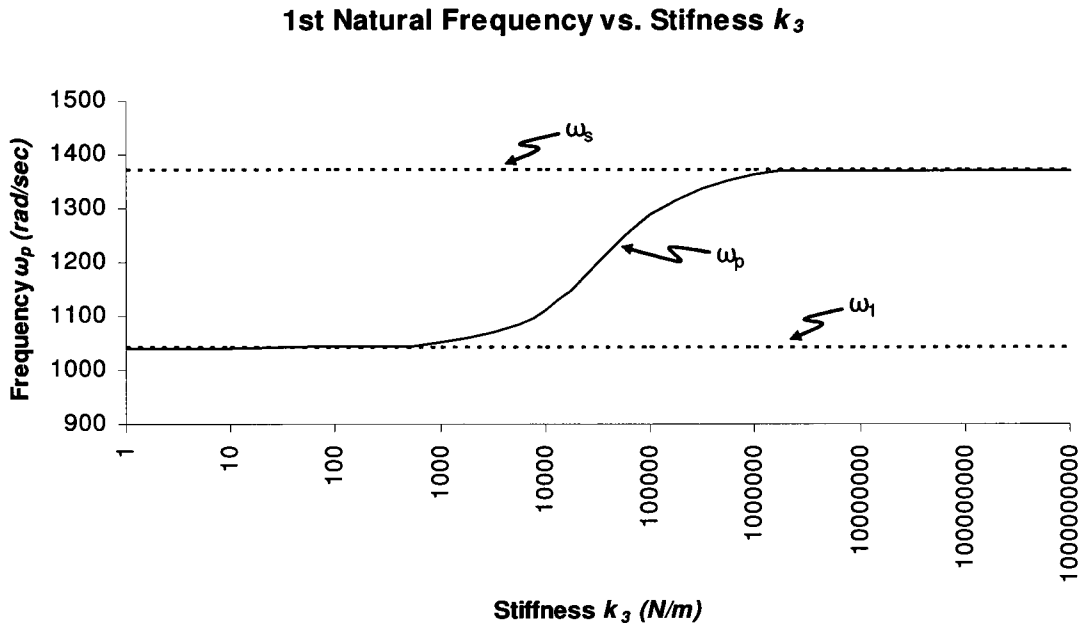

Figure 3.3: 1st natural frequency versus the stiffness k_3

The 2nd natural frequency, is considered in figure 3.4 and it can be observed that below 1000 *N/m*, the coupled system has a value of approximately 2421 *rad/s*. This coincides with the natural frequency of system 2. Above 1000000 *N/m* the link becomes so stiff that the system acts as though coupled by a solid link causing the 2nd natural frequency to increase to infinity.

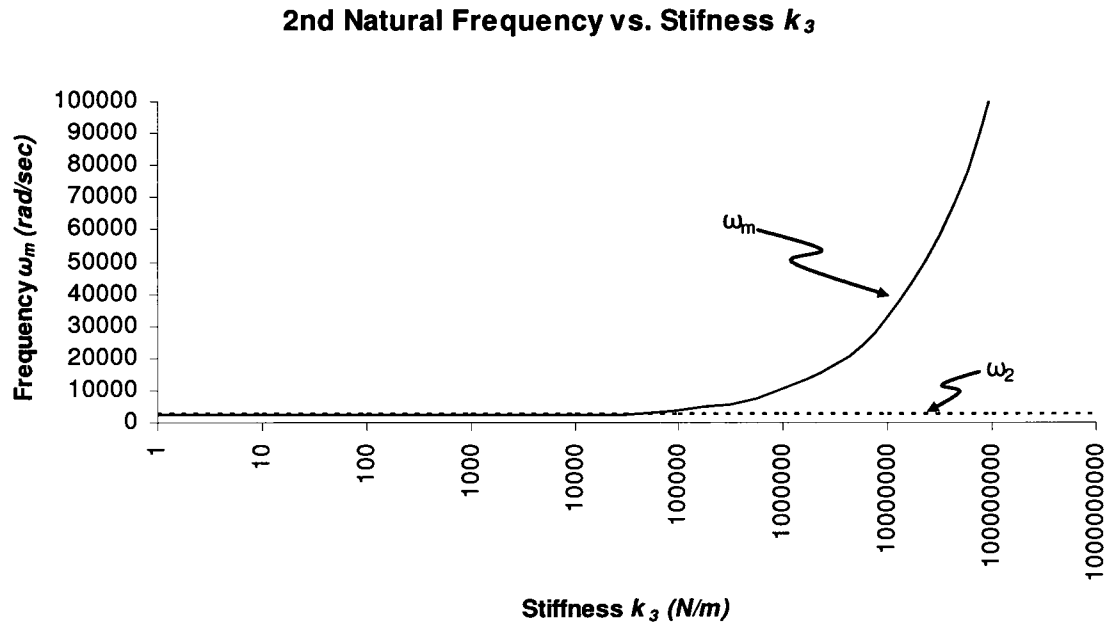

Figure 3.4: 2nd natural frequency versus the stiffness k_3

These observations indicate that if the coupling stiffness falls outside the range of 1000 to 1000000 *N/m*, a much simpler approach can be used to determine the systems natural frequencies. The coupled system can either be modeled as two separate systems if the stiffness is very small, or as a single system having a solid link if the stiffness is very large.

While this chapter presents an overly simplistic approach to the modeling of the system, it gives good insight into its behaviour. In the following chapters, better models for the system using beam and plate theory will be considered.

Chapter 4

Analysis of Continuous Models

The purpose of the following methods is to calculate the natural frequencies of the plate model with the attached cross-brace, as shown in figure 3.2 of chapter 3. It is also the purpose to visually demonstrate the mode shapes of the vibrating system. These mode shapes are the visual display of the manner in which the system vibrates and each shape or mode of vibration relates to a specific natural frequency. Certain simplifications were made in order to solve the system using the methods described herein. It has been assumed that the system is conservative in nature allowing us to neglect damping. Although there is a certain amount of damping found in wood, its effects on the lower natural frequencies is thought to be minimal and has been neglected. This is justified because the lower frequencies have a larger effect on the soundboard tuning than do the higher frequencies [6]. Finally, it is also important to note that the vibration studied herein is that of the free response and not that of the forced response.

The chapter begins by looking at the exact theory for both the plate and the beam which are later used when comparing the results from chapter 3. Higher order solutions for the plate are then given in order to see the effect that neglecting shear deformation and rotary inertia have on the analysis. The energies for an orthotropic plate are given in order to improve the model. This is followed by the explanation on how the simply supported modified plate will be modeled. Finally, the assumed shape method is described in detail, as well as an attempt at an alternate method which uses similar theory to the assumed shape method.

4.1 Beam Theory

As was done in the previous chapter, the analysis of the continuous system will be broken down into the analysis of the brace and of the plate separately and then together as a coupled system. The study begins by looking at the simpler of the two components, that of the brace. While the brace can be analysed using plate theory having two edges simply supported and two free edges, it can also be analysed using beam theory. In fact, because the ratio of its width to its length is so large, beam theory is better suited to this system.

Using beam theory, exact solutions for the vibration of the brace can be found. As with any exact solution, depending on the exact beam theory used, certain assumptions are made. The assumptions made are similar to those that are mentioned in section 4.2 on classical plate theory. Differences are due to the fact that only one planar axis is now present during analysis. Since beam theory is only used for comparative purposes, the results are given by Hamilton's principle for simply supported beams. These results are outlined in [16] and given by equation (4.1) below.

The natural frequencies for a simply supported beam are

$$\omega_{m_y} = \pi^2 \left(\frac{m_y}{L_y} \right)^2 \sqrt{\frac{EI}{\rho}} \quad for \ \ m_y = 1,2,... \tag{4.1}$$

where m is the mode number, L_y the length of the beam, E Young's modulus, I the area moment of inertia and ρ the beam's mass per unit area. The corresponding mass normalized modeshapes can be shown to be

$$w_{m_y}(y) = \sqrt{\frac{2}{\rho L_y}} \sin \frac{m_y \pi y}{L_y} \qquad for \ \ m_y = 1,2,... \tag{4.2}$$

The area moment of inertia of a beam with a rectangular cross section is given by equation (4.3).

$$I = \frac{L_b h_b^3}{12} \tag{4.3}$$

where L_b is the width of the beam and h_b is the thickness.

It is important to note that the results for this particular beam theory do not take into account shear deformation or rotary inertia. For such analysis, the results of the Timoshenko beam theory should be used.

4.2 Plate Theory

To set a benchmark for the study that is being performed on the plate, the extended Hamilton's principle is used to give an exact solution to the isotropic simply supported plate problem at hand, figure 4.1. The exact solution to the plate problem is used as a measure of comparison to validate the more complex problem later on.

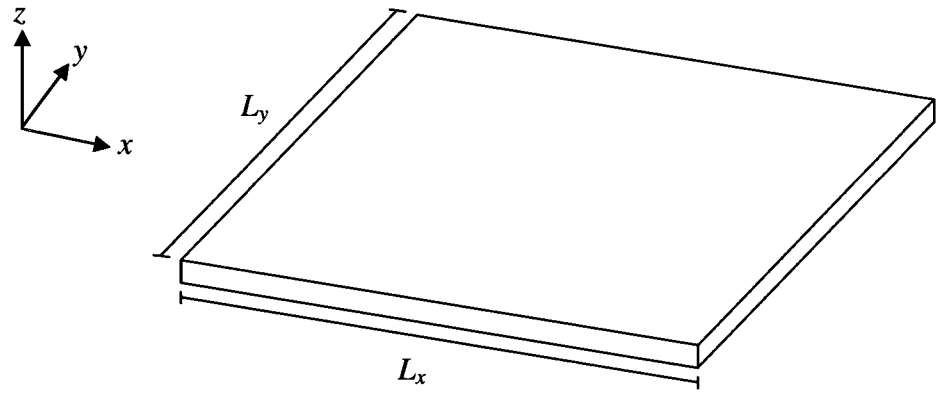

Figure 4.1: Plate problem

The extended Hamilton's principle is a variational energy method. As with any exact solution, a certain number of assumptions are made. For a thin plate, these assumptions are found within the classical plate theory developed by G. Kirchhoff. These assumptions are [17]:

1. When compared to the plate's thickness, deflections are small.
2. Transverse normal stresses are neglected.
3. Transverse shear stresses are neglected.
4. Straight lines normal to the plate's neutral plane before deformation remain normal to the neutral plane during deformation.

The displacement field used to develop the energy equations is bounded by these assumptions. It follows from the above assumptions that the displacement field has the following form [18]

$$\begin{aligned} u(x,y,z) &= -z\frac{\partial w_0}{\partial x} \\ v(x,y,z) &= -z\frac{\partial w_0}{\partial y} \\ w(x,y,z) &= w_0(x,y) \end{aligned} \tag{4.4}$$

where u and v are in-plane displacements, w is the transverse displacement and w_0 is the transverse displacement of the neutral plane. Equation (4.4) implies that w is the only independent variable and that u and v are dependent and bounded by the motion of w. From this displacement field, the non-zero linear strains can be shown to be [18]

$$\begin{aligned} \varepsilon_x &= \frac{\partial u}{\partial x} = -z\frac{\partial^2 w_0}{\partial x^2} \\ \varepsilon_y &= \frac{\partial v}{\partial y} = -z\frac{\partial^2 w_0}{\partial y^2} \\ \gamma_{xy} &= \frac{\partial u}{\partial y} + \frac{\partial v}{\partial x} = -2z\frac{\partial^2 w_0}{\partial x \partial y} \end{aligned} \tag{4.5}$$

where ε_x and ε_y are the in plane normal strains along the x and y axes respectively and γ_{xy} is the in-plane shear strain. For a vibrating plate, the stress-strain relationships are obtained from the generalized Hooke's law for a biaxial state of stress [19]. These stress-strain relationships are

$$\begin{aligned} \sigma_x &= \frac{E}{1-\nu^2}\varepsilon_x + \frac{\nu E}{1-\nu^2}\varepsilon_y \\ \sigma_y &= \frac{E}{1-\nu^2}\varepsilon_y + \frac{\nu E}{1-\nu^2}\varepsilon_x \\ \tau_{xy} &= G\gamma_{xy} \end{aligned} \tag{4.6}$$

where σ_x and σ_y are the in-plane normal stresses along the x and y axes respectively and τ_{xy} is the in-plane shear stress, E is Young's modulus, G is the shear modulus and finally, ν is Poisson's ratio.

It is these linear stresses and strains that are used to develop the strain energy equation U with all the implications of the assumptions made by Kirchhoff in developing the Classical Plate Theory.

Strain and kinetic energies of a plate are used to describe the motion of the plate. They can be easily developed for an isotropic plate [20].

4.2.1 Strain Energy

The plate's strain energy is given by [20]

$$U = \frac{1}{2} D \int_0^{L_x} \int_0^{L_y} \left[\left(w_{xx} + w_{yy} \right)^2 + 2(1-\nu)\left(w_{xy}^2 - w_{xx} w_{yy} \right) \right] dy dx \tag{4.7}$$

where each subscript on the displacement variable w represents a partial derivative along that axis (eg. $w_{xx} = \frac{\partial^2 w}{\partial x^2}$) and where D is the plate's stiffness defined as

$$D = \frac{E h^3}{12\left(1-\nu^2\right)} \tag{4.8}$$

and h is the thickness of the plate.

4.2.2 Kinetic Energy

The plate's kinetic energy is given by

$$T = \frac{1}{2} \int_0^{L_x} \int_0^{L_y} \dot{w}^2 \rho \, dy dx \tag{4.9}$$

where the dot above the displacement variable w represents the time derivative, ρ is the mass per unit area of the plate such that $\rho = \mu \cdot h$, μ is the material density and h the plate's thickness.

4.2.3 Hamilton's Principle

The equation of motion and the boundary conditions of a given system can be determined via the extended Hamilton's principle. It is generally expressed as [17]

$$\int_{t_1}^{t_2}(\delta T+\delta W)\,dt=0 \tag{4.10}$$

where the δT term is the variation in kinetic energy and δW is the variation in work of the given system. Equation (4.10) is based on the assumption that each end of the path is known, consequently the virtual displacement at times t_1 and t_2 are zero (eg. $\delta w(x,y,t_1)=\delta w(x,y,t_2)=0$). Hamilton's Principle for the plate seen in figure 4.1 has been developed in appendix B.

The kinetic energy term T comes from the kinetic energy of the plate as defined in equation (4.9). The work term W is composed of external forces due to potential energy V and internal forces due to strain energy U. Therefore the total work of the system is given by

$$W=-V-U \tag{4.11}$$

For the present system, only the strain energy of the plate applies, which is obtained from equation (4.7).

4.2.4 Hamilton's Principle Results for a Simply Supported Rectangular Plate

After developing Hamilton's principle (appendix B), we obtain the partial differential equation (PDE) of the rectangular plate as well as the plate's boundary conditions. The PDE representing the equation of motion of the plate and can be shown to be [17]

$$\rho\frac{\partial^2 w}{\partial t^2}+D\left(\frac{\partial^4 w}{\partial x^4}+2\frac{\partial^4 w}{\partial x^2\partial y^2}+\frac{\partial^4 w}{\partial y^4}\right)=0 \tag{4.12}$$

After some manipulation, the simply supported boundary conditions reduce to

$$w = 0 \qquad \frac{\partial^2 w}{\partial x^2} = 0 \qquad \text{at } x = 0, L_x \tag{4.13}$$

$$w = 0 \qquad \frac{\partial^2 w}{\partial y^2} = 0 \qquad \text{at } y = 0, L_y \tag{4.14}$$

Equations (4.13) are the boundary conditions for the edges running along the y-axis and equations (4.14) are the boundary conditions for the edges running along the x-axis.

Assuming a solution having a harmonic time dependence that depends on the frequency ω, equation (4.12) reduces to

$$D\left(\frac{\partial^4 w}{\partial x^4} + 2\frac{\partial^4 w}{\partial x^2 \partial y^2} + \frac{\partial^4 w}{\partial y^4}\right) = \omega^2 \rho w \tag{4.15}$$

Once a solution in w is found for equation (4.15) and the boundary equations have been applied as detailed in appendix B, it is possible to solve for the natural frequencies and modeshapes of the system. The natural frequencies for a simply supported isotropic rectangular plate are found to be [17]

$$\omega_{m_x m_y} = \pi^2 \left[\left(\frac{m_x}{L_x}\right)^2 + \left(\frac{m_y}{L_y}\right)^2\right]\sqrt{\frac{D}{\rho}} \qquad \text{for } m_x, m_y = 1, 2, \ldots \tag{4.16}$$

The corresponding mass normalized modeshapes can be shown to be

$$w_{m_x m_y}(x, y) = \frac{2}{\sqrt{\rho L_x L_y}} \sin\frac{m_x \pi x}{L_x} \sin\frac{m_y \pi y}{L_y} \qquad \text{for } m_x, m_y = 1, 2, \ldots \tag{4.17}$$

where m_x represents the mode number along the x-axis and m_y represents the mode number along the y-axis.

The values obtained in equations (4.16) and (4.17) for the natural frequencies and modeshapes are the exact solutions to the simply supported isotropic rectangular plate problem. They will be used to verify more complex approximate solution methods to plate problems for which no exact solutions are known.

4.3 Higher Order Solutions

While the plate problem, based on the Kirchhoff assumptions, admits an exact solution, it does not take into account shear deformation effects or rotary inertia, both of which reduce the natural frequency of the system by decreasing its overall stiffness and increasing its overall effective mass, respectively [21]. For this reason, the Kirchhoff theory applies only to thin plates, as these effects are negligible. As the plate's thickness increases, these effects become more prominent. To account for this, higher order solutions to the plate problem have been proposed. Notably, a first-order solution was developed by R.D. Mindlin which includes these two effects. This thesis does not develop this equation, however relationships that relate exact solutions between the Kirchoff model and the Mindlin model are presented in [18]. Knowing the natural frequency using the Kirchoff model, one can calculate the natural frequency of the Mindlin model using:

$$\left(\omega^2_{m_x m_y}\right)_M = \frac{6K_s G}{\rho h}\left\{\left[1+\frac{h^2}{12}\left(\omega_{m_x m_y}\right)_K\sqrt{\frac{\rho}{D}}\left(1+\frac{2}{K_s(1-\nu)}\right)\right]\right.$$
$$\left.-\sqrt{\left[1+\frac{h^2}{12}\left(\omega_{m_x m_y}\right)_K\sqrt{\frac{\rho}{D}}\left(1+\frac{2}{K_s(1-\nu)}\right)\right]^2-\frac{\rho h}{3K_s G}\left(\omega^2_{m_x m_y}\right)_K}\right\} \tag{4.18}$$

where the subscripts K and M on the natural frequencies represent the Kirchhoff and Mindlin models respectively and K_s is the shear correction factor suggested by Mindlin and for isotropic plates, is given by

$$K_s = \frac{5}{6-\nu} \tag{4.19}$$

Numerical results have shown that including shear deformation effects has a much larger impact on the natural frequency results then does including rotary inertia effects [18]. Neglecting rotary inertia, however, greatly simplifies the equations. By neglecting the rotary inertia effects, equation (4.18) becomes

$$\left(\omega^2_{m_x m_y}\right)_M = \frac{\left(\omega^2_{m_x m_y}\right)_K}{1+\frac{\left(\omega_{m_x m_y}\right)_K h^2}{6(1-\nu)K_s}\sqrt{\frac{\rho}{D}}} \tag{4.20}$$

Equations (4.18) and (4.20) are easily used to compare values between the Kirchhoff plate model and the Mindlin plate model. This allows for the observation of the effect the plate's thickness has on the natural frequencies of the system.

4.4 Orthotropic Plates

In order to improve the accuracy of the model, the orthotropic properties of wood are modeled. The difference between an isotropic plate and an orthotropic plate lies in its material properties. In developing the energies of a plate, the only material properties that need to be considered in evaluating the difference between an isotropic and orthotropic plate are Young's modulus E and Poisson's ratio ν. An isotropic plate has a uniform Young's modulus and Poisson's ratio acting in all directions as seen in equations (4.6). On the other hand, an orthotropic material has different values for these same material properties along all three of the orthotropic axes (eg. x, y, z). In wood, this occurs because grain runs longitudinally along the length of the wood. Also, since grain grows as a ring, properties are different both in the radial and tangential direction with regard to these rings as explained in section 1.7. While the displacement fields in equations (4.4) and the non-zero linear strains in equations (4.5) are unaffected by these differences in material properties, the same cannot be said about the stress-strain relationships. For an orthotropic plate the stress-strain relationships become [19]

$$\begin{aligned} \sigma_x &= S_{xx}\varepsilon_x + S_{xy}\varepsilon_y \\ \sigma_y &= S_{yx}\varepsilon_x + S_{yy}\varepsilon_y \\ \tau_{xy} &= G\gamma_{xy} \end{aligned} \tag{4.21}$$

where the S are stiffness components that are defined as

$$S_{xx} = \frac{E_x}{1-\nu_{xy}\nu_{yx}}$$
$$S_{yy} = \frac{E_y}{1-\nu_{xy}\nu_{yx}} \tag{4.22}$$
$$S_{xy} = S_{yx} = \frac{\nu_{yx}E_x}{1-\nu_{xy}\nu_{yx}} = \frac{\nu_{xy}E_y}{1-\nu_{xy}\nu_{yx}}$$

The subscripts represent the direction or the plane in which the material properties act. Therefore, E_x is the Young's modulus along the x-axis, E_y along the y-axis and ν_{xy} and ν_{yx} the major Poisson's ratios along the x-axis and y-axis respectively.

4.4.1 Strain Energy for an Orthotropic Plate

Using the modified stress-strain relationships of equations (4.21), the strain energy for an orthotropic plate is given by [20]

$$U = \frac{1}{2}\int_0^{L_x}\int_0^{L_y}\left[D_x w_{xx}^2 + 2D_{xy}w_{xx}w_{yy} + D_y w_{yy}^2 + 4D_k w_{xy}^2\right]dydx \tag{4.23}$$

Note that plate's stiffness D can no longer be taken out of the integral because it has different values in each direction and these are defined as

$$D_x = \frac{S_{xx}h^3}{12} \qquad D_y = \frac{S_{yy}h^3}{12}$$
$$D_{xy} = \frac{S_{xy}h^3}{12} \qquad D_k = \frac{G_{xy}h^3}{12} \tag{4.24}$$

4.4.2 Kinetic Energy for an Orthotropic Plate

Because the orthotropic properties of the plate only affect the plate's stiffness and not its density, the potential energy for an orthotropic plate remains the same as described for an isotropic plate in equation (4.9).

4.5 Modified Plate Energies

The problem that is of most interest in this thesis is not that of the simply supported rectangular plate as seen in figure 4.1, but rather that of a modified simply supported rectangular plate having a brace across its width as seen in figure 4.2.

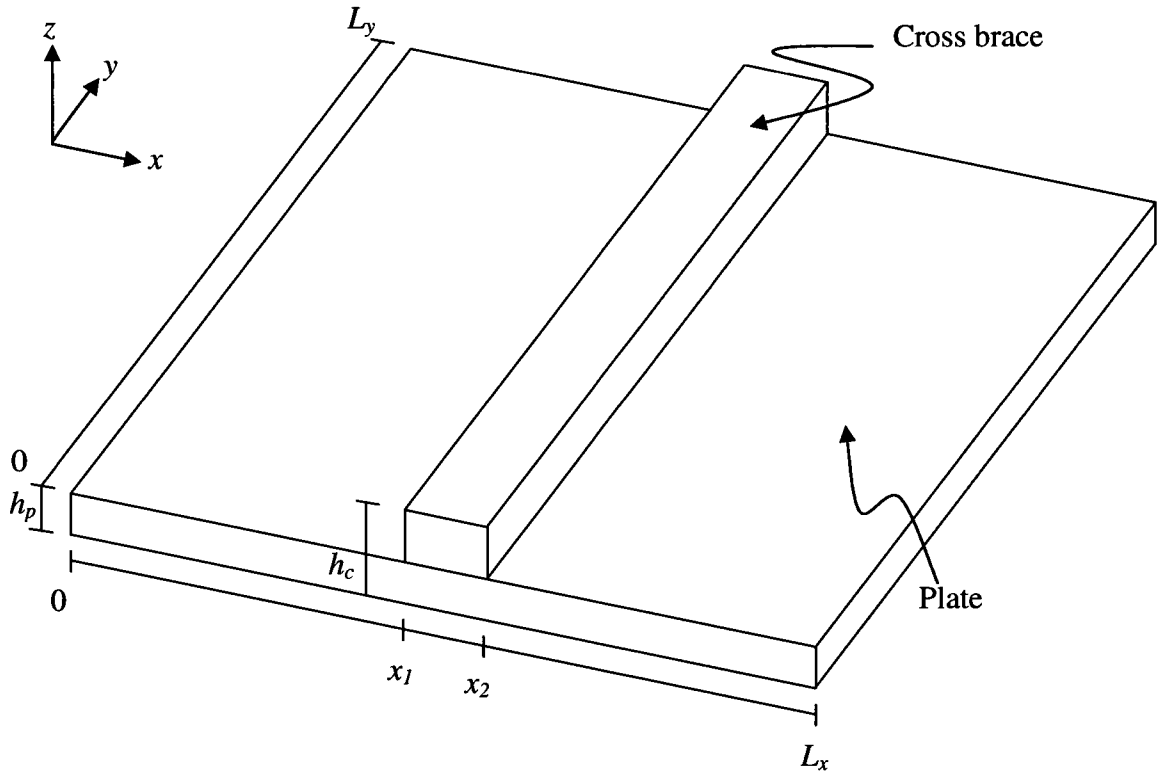

Figure 4.2: Modified simply supported rectangular plate with cross brace across its width

One way that can be used to solve such a problem is to modify the strain and kinetic energies directly in order to account for the change in thickness between x_1 and x_2. This modeling is based on the insight gained from chapter 3, where two systems, connected by a solid link, have a natural frequency composed of both the sum of stiffness and of mass from each system as seen in equation (3.4). Since the strain energy is a function of stiffness and the kinetic energy is a function of mass, the same principle can be applied. To do so, we look at both energies individually.

4.5.1 Strain Energy for a Modified Plate

Looking back at the strain energy for a rectangular plate in equation (4.7), it can be seen that the only term affected by the change in thickness between x_1 and x_2 is the stiffness D. This can be confirmed by looking at the stiffness equation (4.8), which contains the thickness term h. One way to overcome this change in thickness is to split the integral of equation (4.7) into three separate parts so that the strain energy becomes

$$\begin{aligned} U = &\frac{1}{2} D_p \int_0^{x_1} \int_0^{L_y} \left[\left(w_{xx} + w_{yy} \right)^2 + 2(1-\nu)\left(w_{xy}^2 - w_{xx} w_{yy} \right) \right] dydx \\ &+ \frac{1}{2} D_c \int_{x_1}^{x_2} \int_0^{L_y} \left[\left(w_{xx} + w_{yy} \right)^2 + 2(1-\nu)\left(w_{xy}^2 - w_{xx} w_{yy} \right) \right] dydx \\ &+ \frac{1}{2} D_p \int_{x_2}^{L_x} \int_0^{L_y} \left[\left(w_{xx} + w_{yy} \right)^2 + 2(1-\nu)\left(w_{xy}^2 - w_{xx} w_{yy} \right) \right] dydx \end{aligned} \tag{4.25}$$

Here, D_p and D_c are the stiffness for the sections having different thicknesses which can be seen in figure 4.2 and can be written as

$$D_p = \frac{E h_p^3}{12\left(1-\nu^2\right)} \qquad \text{and} \qquad D_c = \frac{E h_c^3}{12\left(1-\nu^2\right)} \tag{4.26}$$

The same can be done for a modified orthotropic plate, by splitting the integral of equation (4.23) into three parts

$$\begin{aligned} U = &\frac{1}{2} \int_0^{x_1} \int_0^{L_y} \left[D_{xp} w_{xx}^2 + 2D_{xyp} w_{xx} w_{yy} + D_{yp} w_{yy}^2 + 4D_{kp} w_{xy}^2 \right] dydx \\ &+ \frac{1}{2} \int_{x_1}^{x_2} \int_0^{L_y} \left[D_{xc} w_{xx}^2 + 2D_{xyc} w_{xx} w_{yy} + D_{yc} w_{yy}^2 + 4D_{kc} w_{xy}^2 \right] dydx \\ &+ \frac{1}{2} \int_{x_2}^{L_x} \int_0^{L_y} \left[D_{xp} w_{xx}^2 + 2D_{xyp} w_{xx} w_{yy} + D_{yp} w_{yy}^2 + 4D_{kp} w_{xy}^2 \right] dydx \end{aligned} \tag{4.27}$$

The stiffnesses D are now section specific because of the change in thickness h from x_1 to x_2:

$$D_{xp} = \frac{S_{xx} h_p^3}{12} \quad D_{yp} = \frac{S_{yy} h_p^3}{12} \quad D_{xyp} = \frac{S_{xy} h_p^3}{12} \quad D_{kp} = \frac{G_{xy} h_p^3}{12}$$

and

$$D_{xc} = \frac{S_{xx} h_c^3}{12} \quad D_{yc} = \frac{S_{yy} h_c^3}{12} \quad D_{xyc} = \frac{S_{xy} h_c^3}{12} \quad D_{kc} = \frac{G_{xy} h_c^3}{12} \tag{4.28}$$

4.5.2 Kinetic Energy for a Modified Plate

The change of thickness between x_1 and x_2 also affects the kinetic energy due to the mass per unit area term ρ in equation (4.9). The mass per unit area ρ is defined as $\rho = \mu \cdot h$ from which it is clear that it contains a thickness term h. Similar to the method used to modify the strain energy term, the kinetic energy can also be written to take into account the change in thickness from x_1 to x_2:

$$T = \frac{1}{2}\int_0^{x_1}\int_0^{L_y} \dot{w}^2 \rho_p \, dydx + \frac{1}{2}\int_{x_1}^{x_2}\int_0^{L_y} \dot{w}^2 \rho_c \, dydx + \frac{1}{2}\int_{x_2}^{L_x}\int_0^{L_y} \dot{w}^2 \rho_p \, dydx \tag{4.29}$$

where the density per unit area ρ is now calculated as:

$$\rho_p = \mu \cdot h_p \quad \text{and} \quad \rho_c = \mu \cdot h_c \tag{4.30}$$

As mentioned in section 4.4, since the orthotropic properties of the plate do not affect the plate's density, the orthotropic kinetic energy remains the same as given in equation (4.29).

4.6 The Assumed Shape Method

By using exact methods, it becomes extremely difficult to study anything other than simple models that have already been derived. Since this study goes beyond the analysis of a simply supported rectangular plate, a different method must be used.

The problem in question can be seen in figure 4.3, where a plate has been fitted with a brace across its width. No closed-form solution is expected.

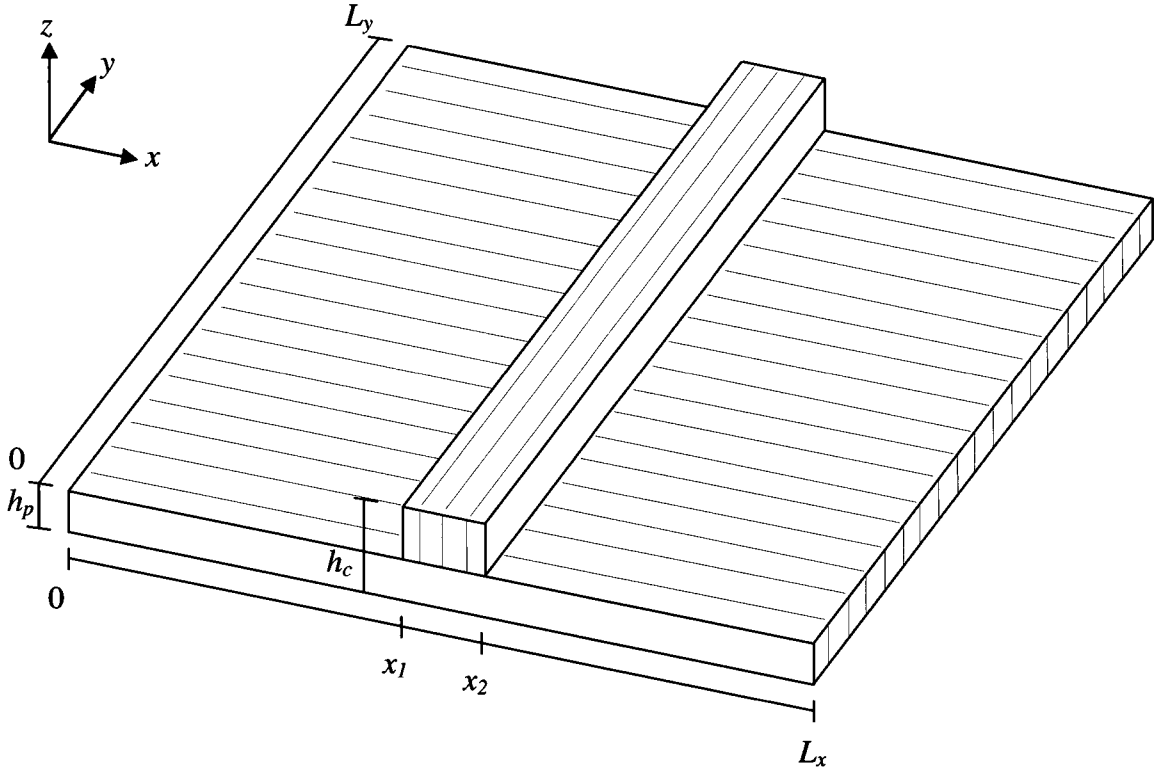

Figure 4.3: Orthotropic rectangular plate fitted with brace across its width

The addition of a brace across the width of the plate means that the properties of the overall system are not constant throughout. Notably, the plate becomes thicker between x_1 and x_2. The grain also changes direction in this area, meaning that Young's modulus and Poisson's ratio values also change direction with the grain.

To accommodate for these complexities in the system, an approximate method may be used. The approach chosen for the analysis here is the assumed shape method, which is also known as the assumed modes method or in some cases the Rayleigh-Ritz method

even though a similar but different method also takes this name. This method has been chosen because of its inherent ability to be both developed intuitively and to give clear physical results. Other approximate methods were considered, including global functions methods in which trial functions extend over the entire domain of the system. Such methods, which include the assumed shape method, also include the Rayleigh-Ritz method and the Galerkin method. The latter two methods are not used because they involve solving the harmonic free response before the application of the chosen trial functions to the problem, whereas the assumed shaped method solves for the harmonic free response after the chosen trial functions are applied. While all three methods lead to the same eigenvalue problem, which generally converges rapidly, the assumed shape method allows for the development of a more intuitive solution on which this work is based.

Also considered was the finite element method. While this method offers significant advantages over the other three methods, namely its ability to model complex systems and boundaries, its disadvantage for the purpose of this work, is its inability to be developed using the known mode shapes of the system without the brace and it also requires a large number of degrees of freedom in order for the solution to converge to accurate results. Contrary to the nature of the global functions approach, the finite element method uses local functions which extend over small subdomains of the system known as finite elements [22], thus expected global behaviour based on the exact solution of a simple plate problem cannot be incorporated into this solution approach. As a point of interest, any of the three mentioned global functions methods can be used to solve the eigenvalue problem of each individual finite element. The exact solution can also be used for elements that have shapes with known solutions. Nonetheless, the finite element method is used to compare results obtained from the assumed shape method.

All the methods mentioned use the superposition of a finite number of pre-assigned mode shapes on which the solution is built. In this manner, it is possible to discretize the system [15].

4.6.1 Procedure for Developing the Assumed Shape Method

The assumed shape method is a technique used to model a continuous system as a discrete one, thereby simplifying the solution. The assumed shape method is used to determine the equation of motion of a system from which an eigenvalue solution may be determined. The first step is to approximate the displacement $w(x, y, t)$ in the transverse z direction. To do so, a finite series for the displacement is chosen as [22]

$$w(x, y, t) = \sum_{n_x=1}^{m_x} \sum_{n_y=2}^{m_y} \phi_{n_x n_y}(x, y) \cdot q_{n_x n_y}(t) \tag{4.31}$$

The $\phi_{n_x n_y}$ are the chosen discrete spatial trial functions and $q_{n_x n_y}(t)$ are the generalized (time-dependent) coordinates. Also, m_x and n_x represent the mode number and trial function number in the x direction respectively and m_y and n_y represents the same in the y direction.

4.6.2 Trial Functions

The next step is to choose a suitable set of trial functions. The trial functions should satisfy the geometric boundary conditions and be complete in order to ensure convergence of the solution [22]. Because the trial functions satisfy the geometric boundary conditions from the beginning, no other considerations of the boundary conditions need to be taken into account while solving the problem.

A simply supported plate represents geometric boundary conditions on its perimeter such that the transverse displacement w of the perimeter of the plate is zero as seen in equations (4.32) and (4.33) [17].

$$w = 0 \qquad \text{at } x = 0, L_x \tag{4.32}$$

$$w = 0 \qquad \text{at } y = 0, L_y \tag{4.33}$$

When looking at the general solution to the rectangular plate problem, an exact solution having a displacement w as indicated in equation (4.17) is found. It is generally common in the assumed shape method to use the same modeshapes of a related simpler problem as the trial functions of the more complex problem in order to obtain good results [22]. Since in the case of this study, the modeshapes of the simply supported rectangular plate are known, these will be used as the trial functions in the finite series of equation (4.31), such that

$$\phi_{n_x n_y} = \sin\left(n_x \cdot \pi \cdot \frac{x}{L_x}\right) \cdot \sin\left(n_y \cdot \pi \cdot \frac{y}{L_y}\right) \tag{4.34}$$

where x represents the position along the x-axis and L_x the total length of the plate in the same direction and where y and L_y represent the same along the y-axis.

It is also possible to use other complete sets of trial functions. One such set that may be used is that of a polynomial series such that

$$\phi_{n_x n_y} = \left(\frac{x}{L_x}\right)^{(n_x-1)} \cdot \left(\frac{y}{L_y}\right)^{(n_y-1)} \tag{4.35}$$

Alternatively, a mix of a trigonometric and polynomial trial function can also be used over a two dimensional plate, as given by

$$\phi_{n_x n_y} = \left(\frac{x}{L_x}\right)^{(n_x-1)} \cdot \sin\left(n_y \cdot \pi \cdot \frac{y}{L_y}\right) \tag{4.36}.$$

The latter trial functions are used to verify the accuracy of the first set of trial functions in equation (4.34). While both sets of trial functions will produce slightly different results, they should all be within the same general range in order to validate the method. For plates, trigonometric functions usually produce more accurate results than do polynomial functions because they are the eigenfunctions of the simple plate problem and better match the dynamic characteristics of the plate than do polynomials [22]. For this reason, the trial functions as defined in equation (4.34) are used.

Applying the trial functions of equation (4.34) to the displacement equation (4.31), gives a discrete series

$$w(x,y,t)=\sum_{n_x=1}^{m_x}\sum_{n_y=2}^{m_y}\sin\left(n_x\cdot\pi\cdot\frac{x}{L_x}\right)\cdot\sin\left(n_y\cdot\pi\cdot\frac{y}{L_y}\right)\cdot q_{n_xn_y}(t) \tag{4.37}$$

Setting the mode number to 2, for example in both directions $\left(m_x \text{ and } m_y\right)$, gives a displacement for the plate of

$$\begin{aligned} w=&\sin\left(\frac{\pi x}{L_x}\right)\cdot\sin\left(\frac{\pi y}{L_y}\right)\cdot q_{11}(t)+\sin\left(\frac{\pi x}{L_x}\right)\cdot\sin\left(\frac{2\pi y}{L_y}\right)\cdot q_{12}(t)\\ &+\sin\left(\frac{2\pi x}{L_x}\right)\cdot\sin\left(\frac{\pi y}{L_y}\right)\cdot q_{21}(t)+\sin\left(\frac{2\pi x}{L_x}\right)\cdot\sin\left(\frac{2\pi y}{L_y}\right)\cdot q_{22}(t)\end{aligned} \tag{4.38}$$

It is this displacement that is then used in the strain and kinetic energy equations of sections 4.2, 4.4 and 4.5.

4.6.3 Strain and Kinetic Energies

Using the chosen trial functions, the next step is to develop the strain and kinetic energies for the system being considered. Since four cases are being considered, four separate strain and kinetic energies must be determined. These cases have already been developed in previous sections. Notably the case of a simply supported rectangular plate is developed in section 4.2, the orthotropic simply supported rectangular plate in section 4.4 and both the regular and orthotropic modified simply supported rectangular plates having a brace running across their width are developed in section 4.5.

Continuing the example using a mode number of 2 in both directions, the displacement, as calculated in equation (4.38), can be inserted into one of the previously developed strain energy equations by taking the displacement's second derivative in both directions such that

$$
\begin{aligned}
w_{xx} &= \frac{\partial^2 w}{\partial x^2} = -\frac{\pi^2}{L_x^2}\cdot\sin\left(\frac{\pi x}{L_x}\right)\cdot\sin\left(\frac{\pi y}{L_y}\right)\cdot q_{11}(t) - \frac{\pi^2}{L_x^2}\cdot\sin\left(\frac{\pi x}{L_x}\right)\cdot\sin\left(\frac{2\pi y}{L_y}\right)\cdot q_{12}(t) \\
&\quad -\frac{4\pi^2}{L_x^2}\cdot\sin\left(\frac{2\pi x}{L_x}\right)\cdot\sin\left(\frac{\pi y}{L_y}\right)\cdot q_{21}(t) - \frac{4\pi^2}{L_x^2}\cdot\sin\left(\frac{2\pi x}{L_x}\right)\cdot\sin\left(\frac{2\pi y}{L_y}\right)\cdot q_{22}(t) \\
w_{yy} &= \frac{\partial^2 w}{\partial y^2} = -\frac{\pi^2}{L_y^2}\cdot\sin\left(\frac{\pi x}{L_x}\right)\cdot\sin\left(\frac{\pi y}{L_y}\right)\cdot q_{11}(t) - \frac{4\pi^2}{L_y^2}\cdot\sin\left(\frac{\pi x}{L_x}\right)\cdot\sin\left(\frac{2\pi y}{L_y}\right)\cdot q_{12}(t) \\
&\quad -\frac{\pi^2}{L_y^2}\cdot\sin\left(\frac{2\pi x}{L_x}\right)\cdot\sin\left(\frac{\pi y}{L_y}\right)\cdot q_{21}(t) - \frac{4\pi^2}{L_y^2}\cdot\sin\left(\frac{2\pi x}{L_x}\right)\cdot\sin\left(\frac{2\pi y}{L_y}\right)\cdot q_{22}(t) \\
w_{xy} &= \frac{\partial^2 w}{\partial x\partial y} = \frac{\pi^2}{L_x L_y}\cdot\cos\left(\frac{\pi x}{L_x}\right)\cdot\cos\left(\frac{\pi y}{L_y}\right)\cdot q_{11}(t) + \frac{2\pi^2}{L_x L_y}\cdot\cos\left(\frac{\pi x}{L_x}\right)\cdot\cos\left(\frac{2\pi y}{L_y}\right)\cdot q_{12}(t) \\
&\quad +\frac{2\pi^2}{L_x L_y}\cdot\cos\left(\frac{2\pi x}{L_x}\right)\cdot\cos\left(\frac{\pi y}{L_y}\right)\cdot q_{21}(t) + \frac{4\pi^2}{L_x L_y}\cdot\cos\left(\frac{2\pi x}{L_x}\right)\cdot\cos\left(\frac{2\pi y}{L_y}\right)\cdot q_{22}(t)
\end{aligned}
\tag{4.39}
$$

Substituting equations (4.39) into, for example, the strain energy for a simply supported rectangular plate as developed in equation (4.7), after some simplification, the result becomes

$$
\begin{aligned}
U = \frac{D\pi^4}{8L_x^3 L_y^3}\Big[&\left(L_x^4 + 2L_x^2L_y^2 + L_y^4\right)q_{11}^2 + \left(16L_x^4 + 8L_x^2L_y^2 + L_y^4\right)q_{12}^2 \\
&+\left(L_x^4 + 8L_x^2L_y^2 + 16L_y^4\right)q_{21}^2 + \left(16L_x^4 + 32L_x^2L_y^2 + 16L_y^4\right)q_{22}^2\Big]
\end{aligned}
\tag{4.40}
$$

The same can be done for the kinetic energy of a simply supported rectangular plate as developed in equation (4.9), by taking the time derivative of the plate's displacement in equation (4.38) such that

$$
\begin{aligned}
\dot{w} = \frac{\partial w}{\partial t} &= \sin\left(\frac{\pi x}{L_x}\right)\cdot\sin\left(\frac{\pi y}{L_y}\right)\cdot\dot{q}_{11}(t) + \sin\left(\frac{\pi x}{L_x}\right)\cdot\sin\left(\frac{2\pi y}{L_y}\right)\cdot\dot{q}_{12}(t) \\
&\quad +\sin\left(\frac{2\pi x}{L_x}\right)\cdot\sin\left(\frac{\pi y}{L_y}\right)\cdot\dot{q}_{21}(t) + \sin\left(\frac{2\pi x}{L_x}\right)\cdot\sin\left(\frac{2\pi y}{L_y}\right)\cdot\dot{q}_{22}(t)
\end{aligned}
\tag{4.41}
$$

The time derived displacement is then substituted into the kinetic energy equation which leads to a simplified result given by

$$
T = \frac{\rho L_x L_y}{8}\left(\dot{q}_{11}^2 + \dot{q}_{12}^2 + \dot{q}_{21}^2 + \dot{q}_{22}^2\right) \tag{4.42}
$$

The same approach can be used to develop the strain and kinetic energies for an orthotropic and modified plate of sections 4.4 and 4.5.

4.6.4 Lagrange's Equations

To find the equation of motion, the potential and kinetic energies are used in Lagrange's equations. Lagrange's equations can be written as [22]

$$\frac{d}{dt}\left(\frac{\partial T}{\partial \dot{q}_{n_x n_y}}\right)-\frac{\partial T}{\partial q_{n_x n_y}}+\frac{\partial V}{\partial q_{n_x n_y}}=Q_{n_x n_y},\quad n_x=1,2,...,m_x \text{ and } n_y=1,2,...,m_y \tag{4.43}$$

where $Q_{n_x n_y}$ are the generalized non-conservative forces and where V is the potential energy. Since there are no other forces acting on the system, $Q_{n_x n_y}=0$. Also, since the potential energy V has not yet been defined, it is important to look at all the potential energies in the system. Given that the only potential energy in the plate system under consideration is that of the strain energy, then:

$$V=U \tag{4.44}$$

Continuing with the example by substituting in the strain and kinetic energies of equations (4.40) and (4.42) respectively into Lagrange's equations, equation (4.43), it is possible to determine the equation of motion of the system. First, some preliminary derivatives are calculated as

$$\frac{d}{dt}\left(\frac{\partial T}{\partial \dot{q}_{n_x n_y}}\right)=\begin{bmatrix}\frac{\rho L_x L_y}{4} & 0 & 0 & 0\\ 0 & \frac{\rho L_x L_y}{4} & 0 & 0\\ 0 & 0 & \frac{\rho L_x L_y}{4} & 0\\ 0 & 0 & 0 & \frac{\rho L_x L_y}{4}\end{bmatrix}\begin{bmatrix}\ddot{q}_{11}\\ \ddot{q}_{12}\\ \ddot{q}_{21}\\ \ddot{q}_{22}\end{bmatrix} \tag{4.45}$$

$$\frac{\partial T}{\partial q_{n_x n_y}}=0 \tag{4.46}$$

$$\frac{\partial V}{\partial q_{n_x n_y}} = \frac{D\pi^4}{4}\begin{bmatrix} \frac{\left(L_x^2+L_y^2\right)^2}{L_x^3 L_y^3} & 0 & 0 & 0 \\ 0 & \frac{\left(4L_x^2+L_y^2\right)^2}{L_x^3 L_y^3} & 0 & 0 \\ 0 & 0 & \frac{\left(L_x^2+4L_y^2\right)^2}{L_x^3 L_y^3} & 0 \\ 0 & 0 & 0 & 16\frac{\left(L_x^2+L_y^2\right)^2}{L_x^3 L_y^3} \end{bmatrix}\begin{bmatrix} q_{11} \\ q_{12} \\ q_{21} \\ q_{22} \end{bmatrix} \tag{4.47}$$

It then follows that the equation of motion is

$$M\ddot{\vec{q}} + K\vec{q} = \vec{0} \tag{4.48}$$

where M is the mass matrix

$$M = \frac{\rho L_x L_y}{4}\begin{bmatrix} 1 & 0 & 0 & 0 \\ 0 & 1 & 0 & 0 \\ 0 & 0 & 1 & 0 \\ 0 & 0 & 0 & 1 \end{bmatrix} \tag{4.49}$$

and K is the stiffness matrix given by

$$K = \frac{D\pi^4}{4}\begin{bmatrix} \frac{\left(L_x^2+L_y^2\right)^2}{L_x^3 L_y^3} & 0 & 0 & 0 \\ 0 & \frac{\left(4L_x^2+L_y^2\right)^2}{L_x^3 L_y^3} & 0 & 0 \\ 0 & 0 & \frac{\left(L_x^2+4L_y^2\right)^2}{L_x^3 L_y^3} & 0 \\ 0 & 0 & 0 & 16\frac{\left(L_x^2+L_y^2\right)^2}{L_x^3 L_y^3} \end{bmatrix} \tag{4.50}$$

Additionally, $\vec{q}$ is the generalized coordinate vector:

$$\vec{q} = \begin{bmatrix} q_{11} & q_{12} & q_{21} & q_{22} \end{bmatrix}^T \tag{4.51}$$

It is important to note that for any linear conservative system, the equation of motion will be the same as that presented in equation (4.48), however the mass matrix M and

stiffness matrix K will be system specific. Once again, the same can be done for orthotropic and modified plates of section 4.4 and 4.5.

4.6.5 Generalized Coordinate Solution

Letting the generalized coordinate system have a harmonic solution as in [17], then

$$\vec{q} = \vec{A}\cos(\omega t + \phi) \tag{4.52}$$

Here, ω is the system's natural frequencies, ϕ the phase shift and A is a magnitude vector of dimension $m_x \times m_y$ by 1. Then replacing the assumed harmonic solution into the equation of motion, equation (4.48) becomes

$$-M\omega^2\vec{A}\cos(\omega t + \phi) + K\vec{A}\cos(\omega t + \phi) = \vec{0} \tag{4.53}$$

Taking out the common factors

$$(K - \omega^2 M)\vec{A}\cos(\omega t + \phi) = \vec{0} \tag{4.54}$$

Finally, since $\cos(\omega t + \phi) \neq \vec{0}$, then it is clear that equation (4.54) leads to

$$(K - \omega^2 M)\vec{A} = \vec{0} \tag{4.55}$$

This equation is an algebraic eigenvalue problem which represents a set of simultaneous algebraic equations.

4.6.6 Eigenvalue Problem

The eigenvalue problem of equation (4.55) can be solved using the standard approach. While most computational software now available have built in eigensolvers, it is also possible to solve the eigenvalue problem by first equating its determinant to zero:

$$\det\left[(K - \omega^2 M)\vec{A}\right] = \vec{0} \tag{4.56}$$

Since nonzero solutions are sought, $\vec{A} \neq \vec{0}$ so then

$$\det\left[K-\omega^2 M\right]=\vec{0} \tag{4.57}$$

Calculating the determinant, a polynomial is obtained for the natural frequency ω. Solving this polynomial equation yields the total number of possible natural frequencies. The number of natural frequencies is due to the order of the polynomial and the order is directly based on the number of degrees of freedom of the system.

Once the natural frequencies have been found, they can be substituted back into equation (4.55) one by one. For each natural frequency, a nonzero vector $\vec{A}$ can then be found. Since equation (4.55) is made up of multiple independent equations with one dependent equation, it is necessary to set one of the values in vector $\vec{A}$. It is then possible to solve for the other values in the vector. Modeshapes (or plate displacements) associated with each natural frequency can be calculated by substituting each vector $\vec{A}$ into the generalized coordinate equation (4.52). The generalized coordinate $\vec{q}$ is then substituted into the displacement equation (4.31). In order to calculate the maximum amplitude of the displacement, the time function $\cos(\omega t+\phi)$ must be equal to 1. The result is a modeshape associated with each natural frequency obtained for the system.

To solve the example started previously, the mass matrix and stiffness matrix determined in equations (4.49) and (4.50) respectively are substituted into the eigenvalue problem, equation (4.55). The eigenvalue problem can then be solved using an eigensolver. This results in a set of natural frequencies given by

$$\begin{bmatrix}\omega_1\\ \omega_2\\ \omega_3\\ \omega_4\end{bmatrix}=\begin{bmatrix}\frac{D\pi^4}{\rho}\frac{\left(L_x^4+2L_x^2L_y^2+L_y^4\right)}{L_x^4L_y^4}\\ \frac{D\pi^4}{\rho}\frac{\left(16L_x^4+8L_x^2L_y^2+L_y^4\right)}{L_x^4L_y^4}\\ \frac{D\pi^4}{\rho}\frac{\left(L_x^4+8L_x^2L_y^2+16L_y^4\right)}{L_x^4L_y^4}\\ \frac{16D\pi^4}{\rho}\frac{\left(L_x^4+2L_x^2L_y^2+L_y^4\right)}{L_x^4L_y^4}\end{bmatrix} \tag{4.58}$$

and a set of magnitude vectors given by

$$\begin{bmatrix} A_{11} & A_{21} & A_{31} & A_{41} \\ A_{12} & A_{22} & A_{32} & A_{42} \\ A_{13} & A_{23} & A_{33} & A_{43} \\ A_{14} & A_{24} & A_{34} & A_{44} \end{bmatrix} = \begin{bmatrix} 1 & 0 & 0 & 0 \\ 0 & 1 & 0 & 0 \\ 0 & 0 & 1 & 0 \\ 0 & 0 & 0 & 1 \end{bmatrix} \tag{4.59}$$

where the magnitude column vector $\overrightarrow{A_1}$ is associated with the natural frequency ω_1 and so forth, that is $\overrightarrow{A_1} = [A_{11} \quad A_{12} \quad A_{13} \quad A_{14}]^T$. In this case, the magnitude matrix A is found to be the identity matrix because the solution is obtained for a rectangular plate. Since the trial functions used are the exact solutions for the plate, each trial function is individually the solution to one of the modes. Generally when the exact solution is unknown, the assumed shape method modal solutions would be built from a combination of trial functions having different magnitudes A. This would then increase the magnitude matrix's population.

The Maple codes used to solve all four cases, including the isotropic and orthotropic rectangular plates, as well as the isotropic and orthotropic rectangular modified plates, for a various number of trial functions can be found in appendix D. The simply supported rectangular plate using 2×2 trial functions used as an example herein was developed using one of these codes.

4.7 Alternate Method

For comparison purposes, an alternate method was considered where the brace and plate were separated along the x-axis at the location of thickness change, figure 4.4. This leads to a modification of the assumed shape method in which the boundary conditions of the first section of the plate are equal to those of its second section at x_1 and the boundary conditions of the second section are equal to those of the third section x_2.

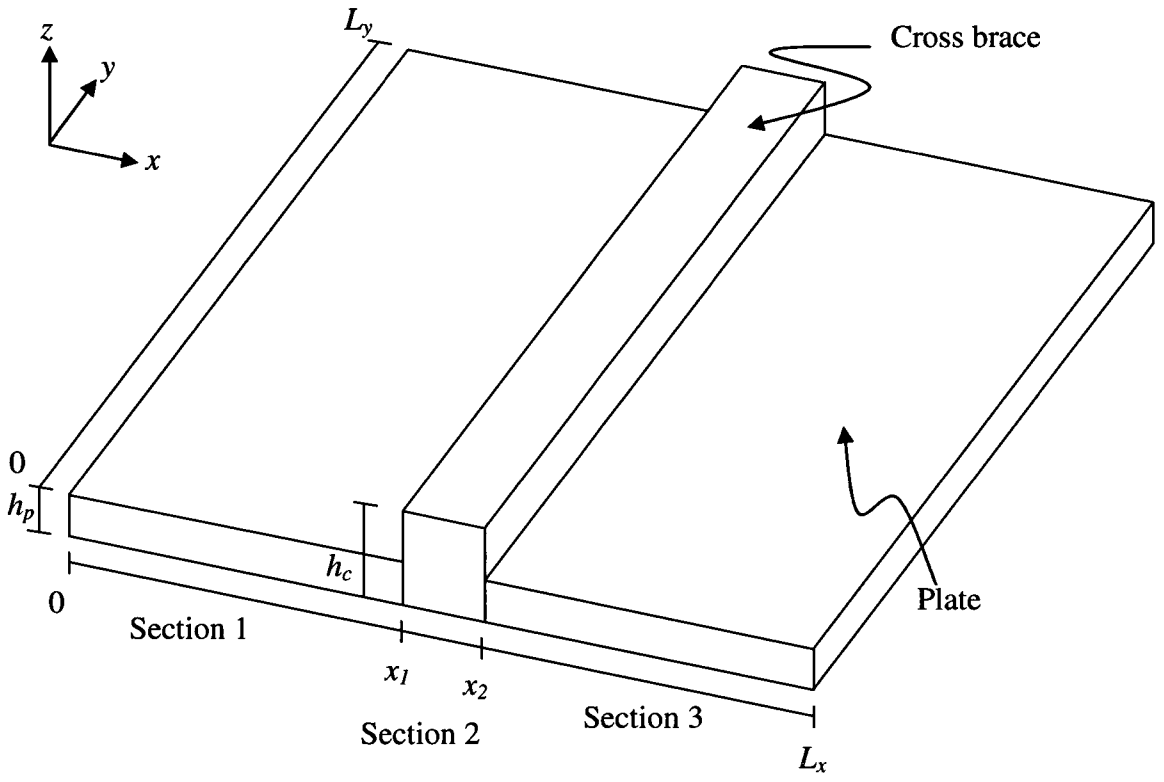

Figure 4.4: Modified plate divided into sections along the x-axis

If each section is considered to be an element with distinctive properties, then the method can be considered to be a form of the finite element method. This method was demonstrated to work for a two-section beam by Dr. Frank Vigneron in a set of unpublished notes given in appendix C [23], where a polynomial of the form found in equation (4.60) must be used in order to satisfy both the simply supported boundary conditions as well as the displacement and slope conditions found between the element boundaries.

$$\phi_n = \left(\frac{x}{L_x}\right)^{(n-1)} \tag{4.60}$$

Expanding this method to a three section beam has also been found to work well when compared to the exact solution of a single-section beam.

Problems with the method begin to occur when expanding it to a two dimensional plate. Degrees of freedom no longer seem to match the dependence of the available equations. Polynomials of the form seen in equations (4.61) and (4.62) have been tried with little success.

$$\phi_{n_x n_y} = \left(\frac{x}{L_x}\right)^{(n_x-1)} \cdot \left(\frac{y}{L_y}\right)^{(n_y-1)} \tag{4.61}$$

$$\phi_{n_x n_y} = \left(\frac{x}{L_x}\right)^{(n_x-1)} \cdot \sin\left(n_y \cdot \pi \cdot \frac{y}{L_y}\right) \tag{4.62}$$

Further investigation of this method is required in order to pinpoint the cause.

Analysis of all the methods described herein was done using Maple. Its symbolic computational abilities allowed the creation of algorithms which could symbolically solve the problem set forth using the various methods. Using Maple, a set of results were obtained and analysed.

Chapter 5

Results

The purpose of this analysis is to first validate a theoretical model that has not been used on a problem similar to that of the plate problem shown in chapter 4, and secondly, to verify if it is possible to frequency match a brace to a plate so as to obtain a desired set of natural frequencies from the coupled system knowing their respective properties before assembly. To do this, an in-depth analysis of all the theoretical models presented in chapter 4 will be performed. The results obtained herein are discussed in greater detail in chapter 6.

5.1 Software

5.1.1 Maple

In order to analyse the many cases described in chapter 4, it is necessary to formulate the problems using computational tools, which make it easier to change variables and update models. Maple is a symbolic algebra system produced by Waterloo Maple Inc which has the benefit of allowing a user to solve problems symbolically rather than numerically. This gives much greater insight into the internal workings of the theory as it is solved for various cases.

Once an algorithm is created satisfying the theory presented in chapter 4, Maple will create a symbolic solution to the eigenproblem. From there, various properties can be

given a value and the solution can be obtained analytically. By changing the property values, a new set of results can be obtained almost instantaneously. The advantage of solving such a complex set of equations symbolically is that once solved, it's a simple matter of solving the eigenproblem. Changing certain properties and seeing their effect on the system becomes a simple matter of entering the new values into the equation.

Three isotropic models are first analysed, notably that of the brace, the plate by itself and the plate with the brace across its width as seen in figure 4.2. Both the exact solutions (when available) and assumed shape method solutions are used in order to validate the accuracy of the latter method. These values are then compared to those of chapter 3 in order to verify if the same trends exist for both models. This will then help give insight as to what needs to be done in order to frequency match a cross-brace to a given plate in order to obtain the desired results from the coupled system.

Once the model has been validated, orthotropic properties of the wood will be taken into account in order to improve the model.

5.1.2 ANSYS

For the purpose of comparison and validation, a finite element model was also created. This helps verify the claims made about global versus finite element trial functions. While most of the analysis is done using global trial functions via the assumed shape method, the models have also been created using the finite element method. In order to do so, ANSYS was used to create these models. ANSYS is an engineering simulation software produced by ANSYS, Inc. It specializes in finite element analysis and more specifically for the purpose of this study, finite element modal analysis. The results obtained with finite element models are compared to those obtained using the assumed shape method.

5.2 System Properties and Dimensions

5.2.1 Materials Properties

The material used throughout the analysis is that of Sitka spruce. Material properties for Sitka spruce are obtained from the U.S. Department of Agriculture, Forest Products Laboratory [14]. Since properties between specimens of wood have a high degree of variability, the properties obtained from the Forest Products Laboratory are an average of specimen samplings. These properties are used in two ways. The first is by transforming the wood's orthotropic properties into an isotropic material for validation purposes. To do so, the properties longitudinal to the wood's grain are used as the materials overall properties. The properties of wood as an isotropic material are seen in table 5.1.

Table 5.1: Material properties for the isotropic plate and brace [14]

Material Properties	Values
Density – μ (kg/m^3)	403.2
Young's modulus – E (MPa)	10890
Poisson's ratio – v	0.372

The second way the material properties are used is as an orthotropic material. This is based on the naturally occurring properties of wood, which present different properties along each of its three main axes as seen in figure 1.5 of section 1.7. Values for Sitka spruce as an orthotropic material are seen in table 5.2. The subscripts 'R' and 'L' refer to the radial and longitudinal property directions of wood respectively. These property directions are adjusted accordingly for both the plate and the brace.

Table 5.2: Material properties for Sitka spruce as an orthotropic material [14]

Material Properties	Values
Density – μ (kg/m^3)	403.2
Young's modulus – E_R (MPa)	850
Young's modulus – E_L (MPa)	$E_R / 0.078$
Shear modulus – G_{LR} (MPa)	$E_L \times 0.064$
Poisson's ratio – ν_{LR}	0.372
Poisson's ratio – ν_{RL}	$\nu_{LR} \times E_R / E_L$

It is the orthotropic material properties that are used to verify the feasibility of frequency matching a brace to a plate.

5.2.2 Plate and Brace Dimensions

A control test specimen, having the same dimensions for every analysis, is used. The dimensions of the plate are based on a typical area of instrument soundboard for which a brace is used for structural reinforcement. The thickness of the plate is based on a typical soundboard thickness and the braces dimensions are also typical. The brace dimensions are defined as in figure 5.1.

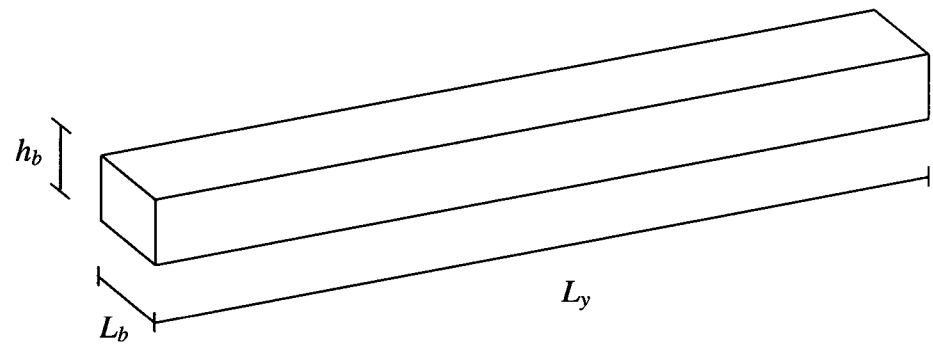

Figure 5.1: Brace showing pertinent dimensions

The plate dimensions are defined as in figure 5.2. Other important reference points are also indicated.

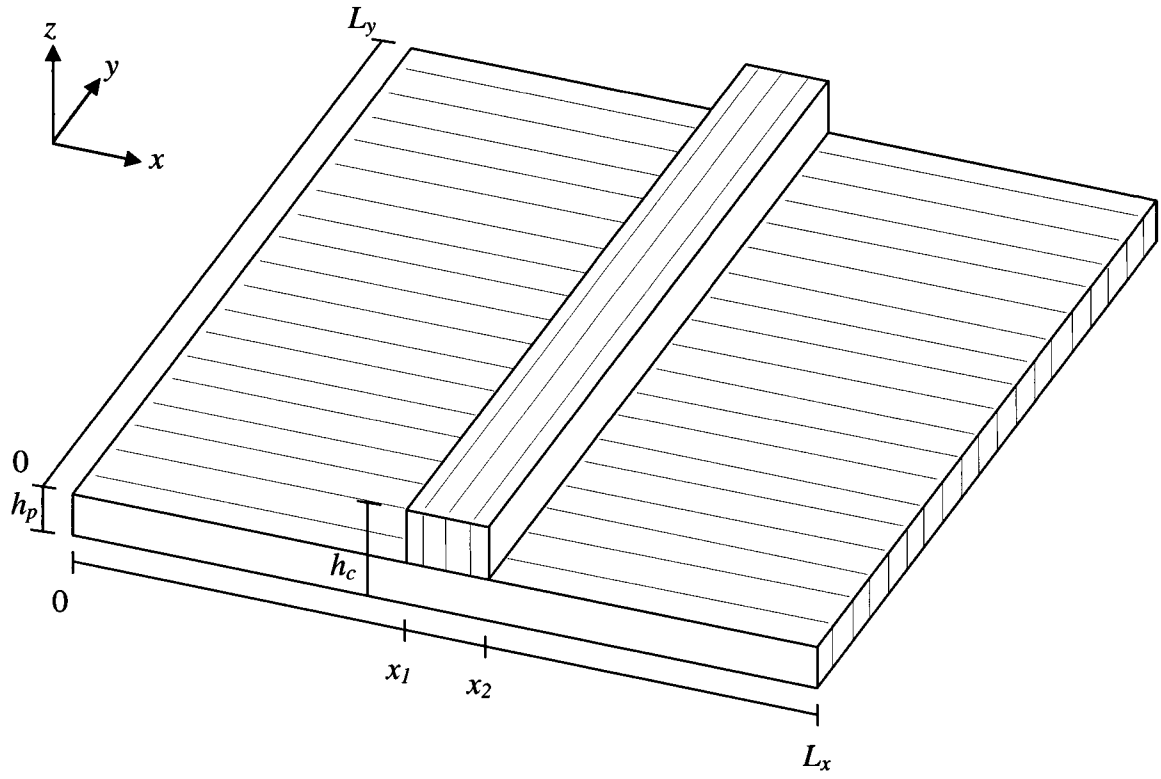

Figure 5.2: Plate and brace showing pertinent dimensions

All the dimensions used in this thesis for the brace and the plate as well as other pertinent reference points are listed in table 5.3. To avoid confusion, subscript '*p*' stands for plate, '*b*' for brace and '*c*' for combined plate and brace.

Table 5.3: Test specimen dimensions

Dimensions	Values
Length – L_x *(m)*	0.24
Length – L_y *(m)*	0.18
Length – L_b *(m)*	0.012
Reference – x_1 *(m)*	$L_x/2 - L_b/2$
Reference – x_2 *(m)*	$x_1 + L_b$
Thickness – h_p *(m)*	0.003
Thickness – h_b *(m)*	0.012
Thickness – h_c *(m)*	$h_p + h_b$

All the values presented herein are used throughout the various analyses. Specifics will be given for each case.

5.3 Exact Values of the Natural Frequencies

The exact values for the natural frequencies of the brace seen in figure 5.1 using beam theory are given by (4.1). For both the isotropic and orthotropic cases, the longitudinal properties of the wood are used in the beam equation. A list of the lowest frequencies calculated using beam theory can be seen in table 5.4.

Table 5.4: Natural frequencies of the exact solution to the isotropic and orthotropic brace

m_y	**Natural frequencies of Brace via Beam Theory (*rad/s*)**
1	5484.02
2	21936.08
3	49356.18
4	87744.32
5	137100.50

The exact values for the natural frequencies of the simply supported isotropic plate seen in figure 4.1 using the classical plate theory of (4.16), as well as Mindlin plate theory with and without rotary inertia as per (4.18) and (4.20) respectively can be seen in table 5.5.

Table 5.5: Natural frequencies of the exact solution to the simply supported isotropic plate

m_x	m_y	**Classical Plate Theory (*rad/s*)**	**Shear Plate Theory (*rad/s*)**	**Shear/Rotary Inertia (*rad/s*)**	**% Error Between Classical and Shear/Rotary Theory**
1	1	2307.82	2306.33	2305.92	0.08%
2	1	4800.27	4793.83	4792.09	0.17%
1	2	6738.84	6726.17	6722.75	0.24%
3	1	8954.35	8932.00	8926.02	0.32%
2	2	9231.29	9207.53	9201.19	0.33%

5.4 Number of Trial Functions Used

The number of trial functions used in the assumed shape method affects the value of the results. Since the interest lies within the lower natural frequencies, it is necessary to determine how many trial functions are needed. The lowest five natural frequencies are chosen for analysis and comparison. Although only the lowest five natural frequencies are analysed, because of the nature of the assumed shape method and its method of trial function superposition, it is necessary to determine how many trial functions are necessary for these five natural frequencies to converge to values which are sufficiently close to the exact values. A comparison is done for both the simply supported rectangular plate with and without the cross brace, as well as for both the isotropic and orthotropic cases. Since the number of natural frequencies is related to the number of trial functions used by the equation $m_x \times m_y$, a minimum of six trial function must be used to obtain five natural frequencies.

The simply supported isotropic rectangular plate's natural frequencies are found in table 5.6 using 6 trial functions (i.e. 3 in the x-direction and 2 in the y-direction).

Table 5.6: Natural frequencies of the isotropic plate using 6 trial functions

m_x	m_y	**Classical Plate Theory - Exact Solution** (*rad/s*)	**Assumed Shape Method** (*rad/s*)
1	1	2307.82	2307.82
2	1	4800.27	4800.27
1	2	6738.84	6738.84
3	1	8954.35	8954.35
2	2	9231.29	9231.29

As expected, since the trial functions used are the same as the exact modeshapes for this system, exact values are obtained no matter the number of trial functions used.

The simply supported orthotropic rectangular plate's natural frequencies are found in table 5.7 for various numbers of trial functions.

Table 5.7: Natural frequencies of the orthotropic plate using the assumed shape method

m_x	m_y	**Number of modes: $m_x = 2, m_y = 3$ (*rad/s*)**	**Number of modes: $m_x = 4, m_y = 4$ (*rad/s*)**
1	1	1040.61	1040.61
1	2	2075.18	2075.18
2	1	3332.59	3332.59
1	3	3951.13	3951.13
2	2	4162.45	4162.45

Once again the natural frequencies for the orthotropic plate go unchanged, as the trial solutions are the actual solutions to the system.

For the isotropic modified plate, the natural frequencies obtained for various numbers of trial functions are seen in table 5.8.

Table 5.8: Natural frequencies of the isotropic modified plate using the assumed shape method

m_x	m_y	**Number of modes: $m_x = 4, m_y = 4$ (*rad/s*)**	**Number of modes: $m_x = 5, m_y = 5$ (*rad/s*)**		**Number of modes: $m_x = 6, m_y = 6$ (*rad/s*)**	
			(*rad/s*)	**% change of previous**	(*rad/s*)	**% change of previous**
1	1	4262.90	4257.89	0.12%	4257.89	0.00%
2	1	7244.29	7244.29	0.00%	7132.40	1.57%
3	1	25442.48	11015.53	130.97%	11015.53	0.00%
2	2	11825.85	11825.85	0.00%	11611.43	1.85%
1	2	12821.82	11831.71	8.37%	11831.71	0.00%

For the isotropic modified plate, decent results are obtained from using a 6×6 number of trial functions since there is less than a 2% change from the previous number of trial functions. Although higher precision is possible using even more trial functions, this seems to be the computational limit of the current research setup. Using a higher number of trial functions causes Maple to become unresponsive during the analysis. It is unknown whether this is due to a hardware issue or an internal limit within Maple. Therefore, 6×6 trial functions will be used during the analysis.

It is interesting to note that for 4×4 trial functions, the order of the appearance of modeshapes changes. This makes this number of trial functions or lower inadequate for

modeling the system presented. In fact, the modeshape which shows up 3rd in table 5.8, falls to 8th behind the 2×3, 1×3 and 4×1 modes.

The number of trial functions required for the orthotropic modified plate is examined in table 5.9.

Table 5.9: Natural frequencies of the orthotropic modified plate using the assumed shape method

m_x	m_y	**Number of modes: $m_x = 4, m_y = 4$ (*rad/s*)**	**Number of modes: $m_x = 5, m_y = 5$ (*rad/s*)**		**Number of modes: $m_x = 6, m_y = 6$ (*rad/s*)**	
			(*rad/s*)	**% change of previous**	(*rad/s*)	**% change of previous**
1	1	3719.98	3717.52	0.07%	3717.52	0.00%
2	1	4567.43	4567.43	0.00%	4469.28	2.20%
2	2	6259.26	6259.26	0.00%	5969.38	4.86%
1	2	6798.69	6677.94	1.81%	6677.94	0.00%
2	3	7986.43	7986.43	0.00%	7609.13	4.96%

For the orthotropic modified plate, the order remains unchanged for all three sets of trial functions, however at 6×6 trial functions there is still just under a 5% change from the previous number of trial functions. While this may not be optimal convergence, due to computational limits, the natural frequencies obtained are decent for the purpose of this study. Therefore, as stated before, 6×6 trial function will be used during the analysis.

5.5 Validation

Using the assumed shape method for both the isotropic and orthotropic modified plates of figure 5.2 or similar has, to the best of the author's knowledge, never been done. In order to validate the method set forth, it is compared to a finite element model. Results of the natural frequencies obtained via the assumed shape method for the first five modes are compared to those obtained using the finite element model. Their associated modeshapes are also displayed. The finite element method uses over 21000 nodes for both models. Table 5.10 gives these results for the isotropic modified plate.

Table 5.10: Comparison of results for the assumed shape vs. the finite element method (isotropic)

m_x	m_y	Assumed Shape Method		Finite Element Method	
		Natural Frequency *(rad/s)*	Modeshape	Natural Frequency *(rad/s)*	Modeshape
1	1	4257.89	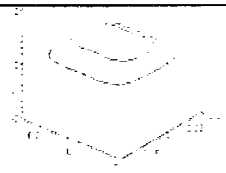	5394.9	
2	1	7132.40	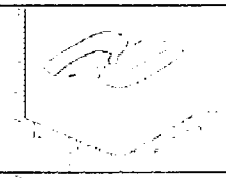	5826.8	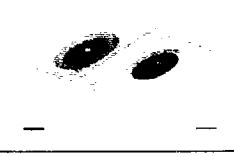
3	1	11015.53	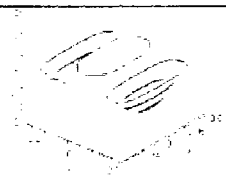	10017.9	
2	2	11611.43	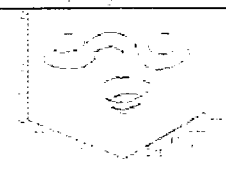	10340.9	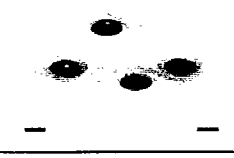
1	2	11831.71		10436.4	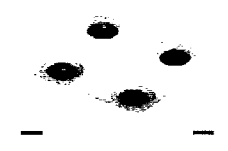

The dip in the center of the x-axis for the assumed shape method modeshapes is the location of the brace, which is clearly visible on the finite element method modeshapes. The brace stiffens this area and limits the amount of displacement that can occur. Similar results are also given for the orthotropic modified plate in table 5.11.

Table 5.11: Comparison of results for the assumed shape vs. the finite element method (orthotropic)

m_x	m_y	Assumed Shape Method		Finite Element Method	
		Natural Frequency *(rad/s)*	Modeshape	Natural Frequency *(rad/s)*	Modeshape
1	1	3717.52	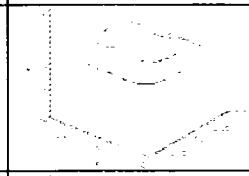	3489.3	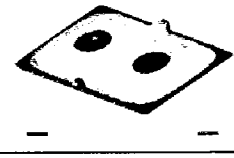
2	1	4469.28	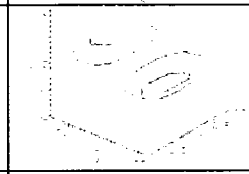	3528.5	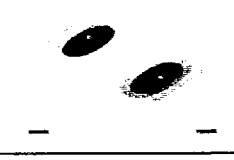
2	2	5969.38	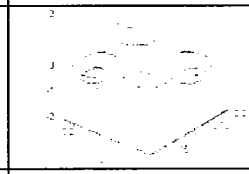	4679.0	
1	2	6677.94		5398.4	
2	3	7609.13	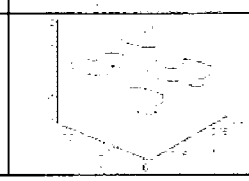	6287.0	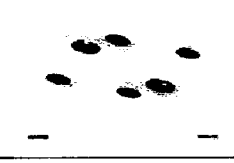

As seen in these two tables, lower estimates are obtained using the finite element method for all but the fundamental frequency of the isotropic modified plate. However, all the natural frequencies are within the same range. These interesting results are discussed in greater detail in chapter 6.

5.6 Simple Mass-Spring Model Comparison

The results from chapter 3 on the two degree of freedom simple mass-spring system with rigid link indicate that the combined system is the sum of the stiffness and of the mass components of each system. This leads to natural frequencies for the combined system which generally fall somewhere between the two separate system's original

5.7 Frequency Matching

The purpose of frequency matching is to adjust the natural frequencies of the brace so that when coupled to a soundboard having a given set of natural frequencies, the combined system's natural frequencies would have predetermined values.

In order to verify the feasibility of frequency matching braces to a plate having a predetermined cross-grain stiffness, it is necessary to look at effects of a change in both the Young's modulus in the radial direction E_R and the brace thickness h_b on the modified orthotropic plate of figure 5.2. Thus, it is the orthotropic simply supported modified plate model that is used during the analysis. Although the lowest five natural frequencies carry a certain importance in frequency matching, only two will be observed during the variation in structural properties. This is because frequencies that have a mode of vibration which contains a node at the location of the brace are not as affected by the brace as those which have a mode which passes through it. Therefore the two frequencies observed during this analysis are the first and fourth natural frequencies of the orthotropic modified plate. This is because the second and third modeshapes have a node at the location of the brace and are not as affected by the brace, contrary to the first and fourth modeshapes which do not have a node at this location. This can be observed in table 5.13, where the first and fourth modes use only one trial function along the x-axis such that $\omega_1 : m_x = 1,\ m_y = 1$ and $\omega_4 : m_x = 1,\ m_y = 2$.

Since it seems that the cross-grain stiffness of a soundboard has a large impact on its acoustical properties and since this stiffness is related to the soundboard's radial Young's modulus, the radial Young's modulus or E_R is varied to see its effect on the systems natural frequencies. The brace is kept to a constant thickness of $h_b = 0.012m$.

Table 5.14: Results of the 1st and 4th natural frequency when varying E_R (h_b = 0.012 m)

Young's Modulus E_R (MPa)	First Natural Frequency ω_1 (rad/s)	Fourth Natural Frequency ω_4 (rad/s)
750	3492.00	6272.83
800	3606.53	6478.56
850	3717.52	6677.94
900	3825.30	6871.55
950	3930.12	7059.84

It is clear from table 5.14 that as E_R increases, so do the 1st and 4th natural frequencies.

A similar analysis is again performed, but this time E_R is held constant at $850\,MPa$ and the thickness of the brace or h_b is varied.

Table 5.15: Results of the 1st and 4th natural frequency when varying h_b (E_R = 850 MPa)

Brace Thickness h_b (m)	First Natural Frequency ω_1 (rad/s)	Fourth Natural Frequency ω_4 (rad/s)
0.0110	3458.57	6481.33
0.0115	3587.91	6581.25
0.0120	3717.52	6677.94
0.0125	3847.25	6771.21
0.0130	3976.95	6860.91

In the same way as the previous case, from table 5.15, when h_b is increased so do the 1st and 4th natural frequencies.

Based on these results and in order to verify if it is possible to get consistency out of the natural frequencies, an analysis was performed in which an increase in the plate's radial stiffness was compensated by reducing the thickness of the brace, table 5.16. The plate's radial stiffness and the thickness of the brace were varied so as to keep the 1st natural frequency relatively constant while examining the effect this would have on the 4th natural frequency.

Table 5.16: The system is compensated so that the 1st natural frequency is held constant

Young's Modulus E_R (MPa)	Brace Thickness h_b (m)	1st Natural Frequency ω_1 (rad/s)	% Change of ω_1 From $E_R = 850$	4th Natural Frequency ω_4 (rad/s)	% Change of ω_4 From $E_R = 850$
750	0.0129	3711.34	0.17%	6428.13	3.74%
800	0.0124	3707.21	0.28%	6551.22	1.90%
850	0.0120	3717.52	0%	6677.94	0.00%
900	0.0116	3718.59	0.03%	6792.23	1.71%
950	0.0112	3711.02	0.17%	6894.64	3.25%

It is apparent from table 5.16 that although the first natural frequency has been held more or less constant, this also resulted in significant variation in the fourth natural frequency. This led to a further analysis in which the radial stiffness and brace thickness were varied so that the fourth natural frequency was held constant, table 5.17.

Table 5.17: The system is compensated so that the 4th natural frequency is held constant

Young's Modulus E_R (MPa)	Brace Thickness h_b (m)	1st Natural Frequency ω_1 (rad/s)	% Change of ω_1 From $E_R = 850$	4th Natural Frequency ω_4 (rad/s)	% Change of ω_4 From $E_R = 850$
750	0.0145	4099.29	10.27%	6676.50	0.02%
800	0.0131	3883.36	4.46%	6673.04	0.07%
850	0.0120	3717.52	0.00%	6677.94	0.00%
900	0.0110	3558.84	4.27%	6669.23	0.13%
950	0.0102	3438.51	7.51%	6676.37	0.02%

Once again, forcing the fourth natural frequency to be more or less constant causes the first natural frequency to vary considerably from its value at $E_R = 850\,MPa$.

While it is clear that it is possible to frequency match the brace to the plate so that the coupled system offers one desired frequency based on the analysis above, it remains inconclusive as to whether or not more than one match in frequencies can be obtained. A modification to the shape of the brace would undoubtedly be required.

Chapter 6

Discussion

Based on the results presented in the preceding chapter, it seems the analysis, while not entirely accurate from a natural frequency perspective, has demonstrated clear trends in the behaviour of a soundboard having a brace across its width. The results obtained throughout have been consistent with basic vibration theory, adding to its credibility. Detailed results are discussed herein.

6.1 Material Properties

The first thing to note during this analysis is the use of the statistical average values of spruce's material properties. It is obvious that these material properties vary on a specimen by specimen basis. However the assumption was made that there is a relationship between the radial stiffness E_R and the other properties. While this is definitely alluded to by the Forest Products Laboratory (US) [14], it is unclear how much variation is actually present in these relationships. Based on years of luthier experience in using the cross-grain stiffness as a measure of soundboard quality, it would appear that the relationship between this stiffness and other properties is more consistent than the properties themselves. It would however be quite interesting to further investigate this phenomenon, as this is has been found to be a great way of modeling the material properties of wood.

6.2 Dimensions

The dimensions used on the test specimen consisting of the simply supported rectangular plate and brace across the width, are based on typical dimensions of those used on guitar soundboards. The plate itself having only one brace is typical of the area on a soundboard around the lower bout where is positioned one of the legs of the typical x-brace pattern. This leads to a model which produces a set of the lowest frequencies within the acoustical range sought by a typical musical instrument (e.g. A0-C8 or $27.5-4186.01\,Hz$).

6.3 Exact Solutions

The natural frequency results using exact theory for the brace seen in table 5.4 show a rapid increase in the natural frequencies as the mode number is increased. This is primarily due to the thickness of the brace itself. When compared to the plate, the brace is much thicker and not as wide. This extra thickness of the brace significantly increases its stiffness while not drastically increasing its mass, thereby forcing higher natural frequencies across the entire spectrum.

Using exact theory for the plate, it is clear that including shear deformation and rotary inertia helps improve the model solution. As can be seen in table 5.5, as shear deformation and rotary inertia are included into the model the natural frequencies are lowered, improving the accuracy of the model. Shear deformation and rotary inertia act on the system by lowering its stiffness and increasing its effective inertia respectfully, both of which help reduce the natural frequencies. However, shear deformation and rotary inertia also complicate the problem enormously, which is why they are usually neglected.

Although this effect of frequency reduction is less than 1% for the plate, as seen in table 5.5, an increase in the plate's thickness would increase the frequency error. This is

because the plate is thin in comparison to its width, which leads to minimal shear and rotary effects and justifies the use of a thin-plate theory where these effects are typically neglected. This is not true for the brace since its width is similar to its thickness therefore shear and rotary effects become important. For increasingly accurate result using the assumed shape method, it would be necessary to take into account these effects when the brace is included in the system during analysis. However, taking into account these effects in the assumed shape method goes beyond the scope of this study, since the complexity increase involved is immense.

Although the assumed shape method is solved using ordinary differential equations, it follows similar theory to the Rayleigh-Ritz method which is based on minimisation principles. In fact the eigenproblems obtained at the end are the same. Since the Rayleigh-Ritz method is a minimisation method, this indicates that the solutions must be overestimates of the actual solution. Therefore a reduction in the natural frequencies is a great indication of an improved solution. This theory seemingly applies throughout the analysis, as a lower natural frequency indicates an improved solution over the previous one.

6.4 Trial Function Convergence

As seen in table 5.6 and table 5.7 for both the isotropic and orthotropic plates, because the exact modeshapes are used as trial functions for the plate, exact natural frequency solutions are obtained. This also helps validate the code used in Maple. Since the exact solutions are obtained from both the isotropic and orthotropic plate codes, it is reasonable to assume that the theory was applied correctly.

Trial function convergence becomes tricky when the plate is modified to include the brace. This is because the trial functions used are no longer the exact solutions, but rather solutions to a similar problem.

Another problem is that of the computational limit. This limit appears to be at 6×6 trial functions for the current setup. Since there is a lack of response that occurs during the analysis above this computational limit, it would be interesting to discover whether

this is a hardware issue or whether this is a computational limit within Maple itself. It is clear that the natural frequency solutions could be improved by increasing the number of trial functions. This is evident simply by looking at the percentage of change from the previous number of trial functions as seen in table 5.8 and table 5.9.

The reason for the higher number of trial functions necessary to model the lower frequencies is based on the fact that the assumed shape method is solved by superposition of the original trial functions. Since the brace of the modified plate now acts to stiffen the region of the plate to which the brace is attached, the nice dome shape seen on the regular plate for the 1×1 mode is now flattened. This can be seen in figure 6.1.

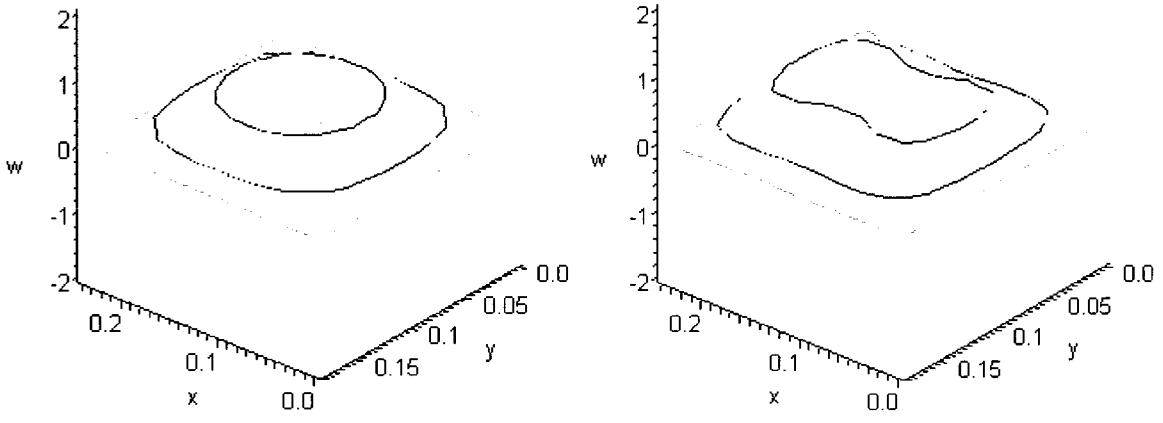

Simply supported rectangular plate without a brace

Simply supported modified plate with a brace

Figure 6.1: Comparison of the first mode for the simply supported plate with and without a brace

In order to obtain this local stiffening effect around the brace, a modeshape of $w(x)=A_1\cdot\sin(\pi\cdot x/L_x)$ along the x-axis is no longer sufficient to correctly model the first mode of the plate with the brace. Similarly, adding the second modeshape, $w(x)=A_1\cdot\sin(\pi\cdot)+A_2\cdot\sin(2\pi\cdot x/L_x)$, has little effect in modifying the results because the second modeshape contains a node at the location of the brace. Finally, by adding the third modeshape, $w(x)=A_1\cdot\sin(\pi\cdot)+A_2\cdot\sin(2\pi\cdot x/L_x)+A_3\cdot\sin(3\pi\cdot x/L_x)$ where $A_2=0$, the stiffening effect can finally be taken into account because the third shape can be used to diminish the peak of the first mode. This superposition of modes can be seen in figure 6.2.

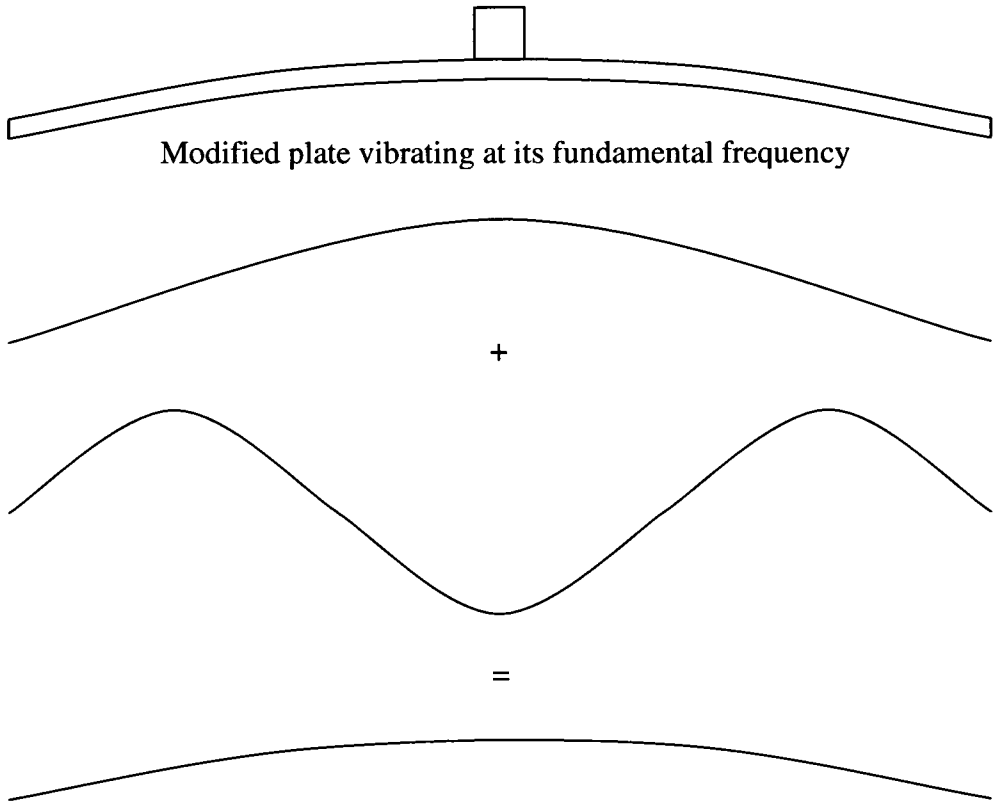

Figure 6.2: Modeshapes required in calculating the fundamental frequency of the modified plate

Clearly adding other odd modeshapes will help improve the accuracy of the modeled fundamental frequency by allowing the calculated shape to get closer and closer to the actual shape. As mentioned for the second mode, since even shapes have a node at the location of the brace, they do not affect odd calculated shapes. However, they are used for calculating even shapes as seen for the second modeshape of the modified plate in figure 6.3.

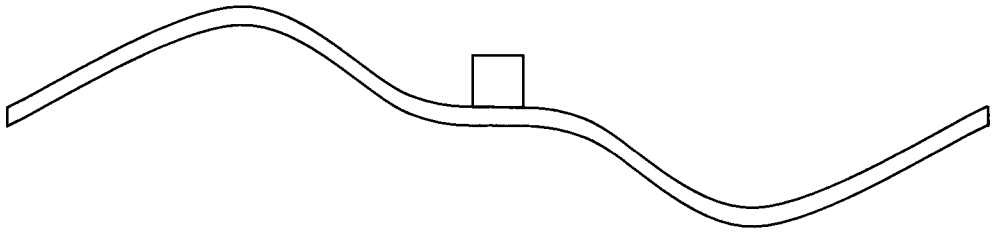

Modified plate vibrating at its second natural frequency

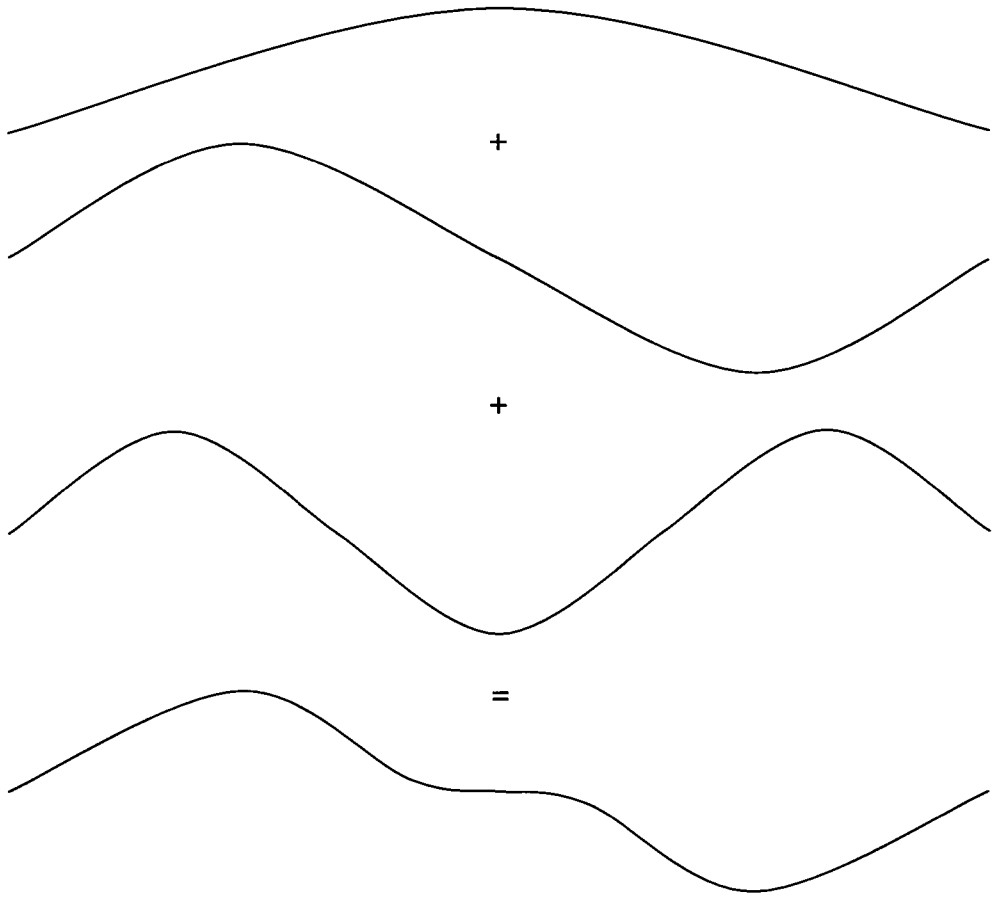

Figure 6.3: Modeshapes required in calculating the second natural frequency of the modified plate

Evidently, different magnitudes of each superimposed trial functions are required to create any given calculated modeshape, this is where the A_n's come in. While not perfect, 6×6 trial functions seem to produce decent results.

6.5 Assumed Shape versus Finite Element Method

The finite element method is used in this thesis for comparison purposes only. Since no experimental work has been done, another means of validation was necessary. Therefore, a simple finite element model was developed in ANSYS for both the isotropic and orthotropic modified plate systems. These finite element models are compared to their equivalent assumed shape method models. These comparisons are seen in table 5.10 for the isotropic modified plate and in table 5.11 for the orthotropic modified plate.

Looking at these results, the first thing that is apparent is how both sets of natural frequencies for each case fall within the same range. This helps justify the accuracy of the assumed shape method models. Differences in both models are primarily based on two factors. The first is the different assumptions made for each case, given that both methods are approximate ones. The second is the level of convergence attained by each model based on the computational limits of the current setup. However, even though these two models use completely different approaches in building the given systems, they both seem to be converging to similar frequencies.

It is also evident that the order of the modeshapes for both the isotropic and orthotropic cases has converged to the same result using both models. This convergence has occurred differently in both the isotropic and orthotropic case because of the large difference in the stiffness across the grain for each. The fact that both the assumed shape and finite element methods have converged to the same order of modeshapes indicates that a similar solution is obtained for both. This helps in validating the accuracy of the assumed shape method because it demonstrates a rigorous order in the natural frequencies of the system. Although the assumed shape method has not converged to the level of precision in the values of the natural frequencies obtained through the finite element method, both models indicate that they are vibrating in the same manner.

In acoustics, it is difficult to get extremely precise frequency results from theoretical calculations because of the number of assumptions necessary to create models that are computationally manageable. It is clear that this aspect needs to be improved in order to

produce models which can accurately predict the natural frequencies of a given system. This is ultimately necessary if the goal is to improve the manufacturing consistency of wooden musical instruments.

Future work involving precision of the natural frequencies should look to the finite element method. This is clear in the results presented in table 5.10 and table 5.11, since the natural frequencies obtained through the finite element method are lower than those obtained via the assumed shape method. Once again, this is true because both methods are based on minimisation theory which dictates that all solutions are over-approximations of the actual values.

It is interesting to note that the fundamental frequency of the isotropic modified plate is found to be lower when calculated using the assumed shape method. This indicates that, in this case the assumed shape method converges faster than does the finite element method. A mesh refinement of the finite element method should help it converge to a more accurate value.

6.6 Two Degree of Freedom versus Continuous

In chapter 3, a very simple two degree of freedom system was developed in order to understand exactly the effect of combining two mass-spring systems. While intuition and common sense may have led to the same results, it was important to get a good understanding of how such systems interact. Interestingly enough, very specific results were obtained.

The first thing that is observed from these simple systems and which helps form the fundamental understanding of vibration properties is that on their own, both systems have a natural frequency of $\omega^2 = k/m$. This form of the natural frequency, which may vary in magnitude depending on the theory used, always follows this stiffness over mass trend. Therefore if the stiffness of the system increases or the mass is reduced, the natural frequencies are also increased and vice-versa. Also, if both the stiffness and the mass are increased at the same time but the stiffness is increased by a larger amount than is the mass, the natural frequencies will go up. On the other hand if the increase in mass is more

significant, the natural frequencies will go down. While simple in nature, these facts form the basis on which frequency matching can be performed in order to improve the consistency of manufactured wooden musical instruments.

An example of this trend is the dimensions of the plate versus those of the brace. The plate's mass is distributed over a very large area making the plate thin. This thinness of the plate makes it more flexible in the direction normal to the plate's face but still allows for a large amount of material mass to be present. Meanwhile, the brace's mass is concentrated over a very small area, allowing it to be much stiffer along the brace without needing too much material mass. It is then clear that the brace will produce much higher frequencies by itself than would the plate.

The second interesting result is that when the two systems are combined with a solid link between them, forcing them to move in unison, the combined systems natural frequency becomes the ratio of the sum of both the stiffness and masses respectfully, $\omega^2 = (k_1 + k_2)/(m_1 + m_2)$. This, once again goes to show the simplicity in which the systems combine to form a new system when they are forced to move in unison. Since no previous energy model similar to the one developed in chapter 4 was found on which to base this work, it is this simple result for the sum of stiffness and mass that helped create the model used in the continuous model analysis. To do so, in the region from x_1 to x_2 as seen in figure 4.2, the material of the brace was simply added to that of the plate. This led to an increase in thickness in this region which affected both kinetic and strain energy of the plate. The mass and stiffness matrices are direct derivations of the kinetic and strain energy respectively and the results obtained from them for the modified plate represent a sum of both the original stiffness and masses but only in the region were the brace is directly attached to the plate.

Conversely, when results are compared between the plate and the plate with the brace as seen in table 5.12 and table 5.13, it is clear that the addition of the brace affects modes for which the location of the brace is not a node, such as $m_x = 1$, more than a mode having a node at the location of the brace, such as $m_x = 2$. This is also clear from the percentage increase in the natural frequencies for the $m_x = 1$ mode, which is much higher than for the $m_x = 2$ modes. This trend is even more obvious in the orthotropic plates

because there is a much higher increase in stiffness across the grain when the brace is added compared to the isotropic plate. It is also impossible to avoid a slight increase in the natural frequencies for the $m_x = 2$ modes or all other even modes because their nodes are along a line and the brace does in fact have a finite width. This finite brace width causes local stiffening to occur around it, affecting the curvature of the even modes and thereby also increasing their frequencies.

These tables also demonstrate that for modes directly affected by the brace, the natural frequencies in fact fall somewhere between those of the brace and plate alone. These are the same results obtained from the two degree of freedom system. For the modes not directly affected by the brace, a simple increase in the original plate's natural frequency is observed due to the forced changes in the mode's curvature.

Finally, as common sense would have indicated, the simple 2DOF model indicates that when the link between the brace and the plate is not solid, but rather has its own stiffness, the natural frequencies of the combined system are modified accordingly. In chapter 3 it is observed that as the link between the systems becomes more flexible, the combined system acts more and more like the individual systems. When the link becomes increasingly stiff, the combined system acts more and more like the system having a solid link. Since in practice, the link between the brace and the plate is wood glue, it would be important to know whether it acts as a solid link or rather has its own distinct flexible component. Background research has pointed to the former being the case, however this is a point that should be verified in the future.

6.7 Frequency Matching

The eventual purpose of this work is to create an optimisation system which helps improve the acoustical consistency of manufactured wooden stringed instruments. Since very little research has been done to this effect and in order to achieve this goal, it is crucial to start with the basics. The analysis begins by looking at the possibility of frequency matching a wooden brace to a wooden plate. This meaning that a brace could

be adjusted so that when combined to a plate of given stiffness, their coupled natural frequencies would be those as prescribed by a set standard. The orthotropic modified plate model is used for this analysis since it represents the closest model to reality. To do so, the effects of variations in the cross-grain stiffness of the plate, measured as E_R, are observed in table 5.14. It is clear that when the stiffness across the grain is reduced so too are the natural frequencies. This is exactly as expected and perfectly follows vibration theory.

Similarly, the effects of the brace's thickness, measured as h_b, are considered in table 5.15. Once again, it is noted that as the brace's thickness increases, so does its natural frequencies. This is entirely due to the fact that as the brace's thickness increases, its stiffness increases at a larger rate than its mass.

Luthiers use this phenomenon in order to adjust the braces to a given soundboard. This adjustment process is tested herein. In order to do so, the first natural frequency is held more or less constant by adjusting the brace inversely to the property values of the plate's cross-grain stiffness. These results can be seen in table 5.16. While the first natural frequency variation falls well below the 1% human hearing threshold for sound variation [11], the variation in the fourth natural frequency lies above it.

A second attempt was made to frequency match the fourth natural frequency. As can be see in table 5.17, a wider adjustment span is required for the brace in order to achieve consistency in the fourth natural frequency. This time, the frequency variation of the fourth natural frequency lies well below the 1% threshold. However, the variation in the first natural frequency is wider than the first attempt.

These results indicate that it is possible to produce an acoustically consistent set of brace-plate assemblies that have at least one matching natural frequency. Conversely, it does also indicate that a rectangular brace is not suitable for adjusting multiple frequencies.

After obtaining these results, it became clear that adjustments to the shape of the brace itself would be required. This led back to the debate on whether or not scalloped braces had in fact an acoustical role in producing more consistent instruments. This being an interesting topic on its own, further investigation of scalloped braces is found in chapter 7.

6.8 Interesting Insight

Interesting insight has been gained throughout this analysis. An overview of certain insight is discussed herein.

While this analysis describes a simple method in which a brace could be frequency matched to a soundboard, it demonstrates the possibility of developing a manufacturing process in which a brace could be modified according to the measured properties of the soundboard. It is suggested that after numerical measurement of the soundboard stiffness across the grain, braces could be custom-cut using computer numerical controlled (CNC) machinery during production to match a given soundboard. Since the stiffness across the grain is currently manually measured in industry, a numerical process would need to be implemented. Braces are currently already being cut using CNC machinery. However, these machines would need to be numerically linked to the soundboard measuring devices using software which would dictate the required dimension to the brace-cutting CNC machines. This would allow the braces to be frequency matched to specific soundboards before assembly, minimising overall cost increase of the process and limiting construction time.

This method does not need to be used exclusively on soundboards having only braces, but can also be used for graduated soundboards. To resist the immense tension of the strings, certain instruments such as the violin, mandolin and archtop guitars use arched soundboards instead of flat ones. Since these soundboards are generally thicker than their flat counterparts, their thickness is usually graduated. They are left thick at their peak for strength and are gradually thinned towards the edges to allow it to be flexible enough to produce beautiful musical tone. Graduating the thickness of the soundboard has the same effect as adjusting the thickness of the braces. In fact, a graduation method for the violin is described by Carleen Hutchins in [6]. Therefore, a similar process such as the one described earlier can also be used for graduated soundboard instruments.

Lloyd A. Loar was the acoustical engineer at the Gibson Mandolin-Guitar Company between 1920 and 1925. Under his supervision, Gibson Master Model instruments were

individually tap-tuned in order to optimise their sound and improve the consistency of their product [5]. Recently, a group of 25 Loar signed F5 mandolin owners gathered to compare instruments. The astounding result was the consistency in the sound of all the instruments present. When compared to other sets of dimensionally identical instruments, the difference in acoustical consistency is striking. For this reason, Loar signed instruments are highly sought after. While Lloyd Loar instruments were individually tap-tuned by hand, this would be unreasonable in today's economy. Therefore the process proposed herein represents a method in which similar results could one day be attained.

Another method people have used in attempting to overcome the acoustical inconsistencies of wood is to use composite materials instead. Composite structures can be designed to match the orthotropic structural properties of wood. Time and time again however, instruments built with composite soundboards have proven to have a different tone then those built of wood. Once again, this is due to the damping properties of wood which are quite different from those of composite. These different damping properties damp out specific frequency partials which help give the specific tone to a given instrument. In fact most people agree that a wooden instrument sounds warmer than a composite instrument. For this reason, wooden instruments are generally still preferred over those made of composite materials.

6.9 Sources of Error

While it has been previously mentioned that improved accuracy in the calculation of the natural frequencies of the modified plate could be obtained by incorporating shear deformation and rotary inertia theory into the model, other assumptions were also made which have an impact on the preciseness of the calculated values.

The first assumption was that the mass of air which would normally surround the soundboard of a musical instrument has been neglected. Including the mass of air surrounding the soundboard would in fact decrease the natural frequencies because the mass of air acts to increase the total inertia of the soundboard [21].

To simplify the model, the assumption was also made that the soundboard is simply supported when in fact it is probably somewhere between simply supported and clamped [1]. Since clamped edges prevent rotation at the edge, local stiffening occurs. This leads to an increase in the natural frequencies.

Damping was also neglected during the analysis, which allowed for a much simpler model. Although this assumption is justified due to the fact that a musical instrument is designed to sustain rather than to absorb vibration, it is the damping or decay time of specific partial frequencies, because of wood's distinct properties, which help give a wooden instrument its tone [11]. Therefore, to improve the acoustical preciseness of the model, damping would need to be included in the analysis.

Finally, in order to create the orthotropic modified plate model described in chapter 4, it was necessary to make an assumption about grain direction in the region between x_1 and x_2 as seen in figure 4.3. Because of the method in which the brace thickness is added to that of the plate in the kinetic and strain energy equations, it was necessary to change the direction of the grain of the plate, in this region only, to match that of the brace. This is a reasonable assumption because of how thin the plate is in comparison to the brace and the solid link of wood glue which bonds them together. Since the stiffness of the brace is much greater than that of the plate in this region, it is the brace which dominates the stiffness properties.

Chapter 7

Analysis of a Scalloped Brace

Based on the results obtained from the analysis of the modified plate in chapter 5, it is clear that a rectangular brace, while able to be modified to frequency match one of the lower frequencies of the system, is unable by itself to frequency match multiple frequencies at once. Based on these results, insight was obtained as to what needs to be done in order to frequency match at least two of the lower modes.

As previously mentioned in section 1.3 on soundboard optimisation, many times during the optimisation process, a brace will end up having a scalloped shape. While some believe this is the result of the optimisation process, speculation has led to the belief that this enables a luthier to control two modes at once [5]. This theory is based on the fact that because of a scalloped brace's peculiar shape, individual modifications of the two lowest modes running along its longitudinal direction, as seen in figure 7.1, are possible.

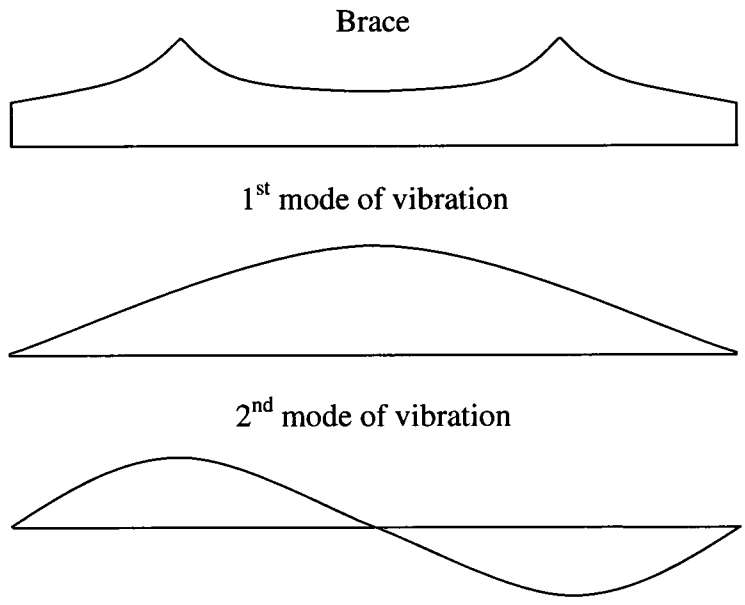

Figure 7.1: Scalloped brace with the modes of vibration it affects

7.1 Modeling of the Scalloped Brace

In order to model the scalloped brace, a second order piece-wise polynomial function was chosen to model the thickness of the brace. This polynomial function puts the peaks of the scallops at ¼ and ¾ of the way down the brace. The function can be seen in equation (7.1).

$$h_b = \begin{cases} y^2 + h_{bo} & \text{for} \quad y < \dfrac{L_y}{4} \\ \left(y - \dfrac{L_y}{2}\right)^2 + h_{bo} & \text{for} \quad \dfrac{L_y}{4} \le y \le \dfrac{3L_y}{4} \\ \left(y - L_y\right)^2 + h_{bo} & \text{for} \quad y > \dfrac{3L_y}{4} \end{cases} \tag{7.1}$$

where h_{bo} is the height of the brace at its ends and center. This h_b is then substituted into the kinetic and strain energy equations as used for the modified plate model in the assumed shape method.

7.2 Results

Since the equations of kinetic and strain energy now include a polynomial instead of a constant during the solution process, the computational power necessary for such a symbolic solution increases immensely. Therefore, due to computational limits, only 2×2 trial functions on the isotropic modified plate will be considered for analysis. Also, for the same reasons, only the lowest four natural frequencies are examined in table 7.1. In order to compare results, the rectangular brace is given a thickness of $h_b = 0.012m$, as before. The original thickness of the scalloped brace is also marked as $h_{bo} = 0.012m$.

Table 7.1: Comparison of brace geometry on a simply supported isotropic modified plate

m_x	m_y	**Rectangular Brace Natural Frequencies** (*rad/s*)	**Scalloped Brace Natural Frequencies** (*rad/s*)	**% Change in Frequencies**
1	1	6108.00	6448.31	5.57%
2	1	10012.40	10565.2	5.52%
1	2	19485.21	21238.89	9.00%
2	2	19833.26	20286.20	2.28%

7.3 Discussion

Although the natural frequencies have a clear increase in value throughout for the scalloped brace compared to the rectangular brace, there is a marked difference for the 1×2 mode, where the increase is almost double that of the others. The reason for the increase is that the original thickness of the scalloped brace is equal to that of the rectangular brace. Since the scalloping of the brace only serves to add additional material (mass) to the system, it is only logical for all of the natural frequencies to increase.

Since the peaks of the scalloped brace occur at the maximum displacement locations of the 3rd mode of vibration in the direction of the brace, it limits the amount of displacement possible through this mode by increasing the stiffness locally. This is the reason for the higher increase in the natural frequency observed for the 3rd modeshape.

These peaks also minimise the effect of extra stiffness on the other modes of vibration, because their maximum displacement is found to be either at the center of the brace where the brace's thickness goes unchanged or the brace is in fact at a location of one of their nodes.

These discoveries lead to the theory that what a luthier is in fact doing when scalloping a brace, is adjusting two or more modes at once, or at least controlling which modes are affected the most by the bracing since not all modes are equally affected. It is evident that the exact shape chosen based on the polynomial of equation (7.1) may not be the optimal solution. Further investigation into the scallop shape itself is necessary to further grasp the magnitude of its effect on the frequency spectrum of the soundboard.

Chapter 8

Summary, Conclusions and Future Work

8.1 Summary

In this thesis, the problem of increasing the acoustical consistency in wooden manufactured musical instruments has been considered. This was approached by looking at the feasibility of adjusting the soundboard's braces before assembly in order to compensate for the variability in the soundboard's stiffness so that the coupled system's natural frequencies would match those of a set standard. In order to accomplish this, the problem was turned into a vibration problem. Chapter 3 introduced the problem as a simple mass-spring system used to model the plate and brace. Chapter 4 gave the theory for the continuous system model by developing the exact solution for both the brace and the plate. It also described the kinetic and strain energy of a plate for both isotropic and orthotropic materials. Higher order solutions were also discussed. Finally the assumed shape method is explained. Chapter 5 gave the results of the analysis for the exact solutions of the brace and plate along with a comparison of the solutions from the assumed shape and finite element methods for the modified plate and brace system. The ability to frequency match a brace to a plate was also investigated. Chapter 6 discussed the results obtained through the analysis and also discussed the insight gained throughout the research. Chapter 7 developed and discussed the possibility of using a brace having a scalloped shape in order to frequency match more than one natural frequency in the combined system.

8.2 Conclusions

This analysis set forth has proven insightful for the manner in which a brace affects the natural frequencies of a soundboard. Although the frequency accuracy of the model has been shown to be less than perfect when compared to a finite element model because of minimisation theory, insight gained by using the assumed shape method has demonstrated to be tremendous.

First, the analysis has shown that the acoustic properties of a soundboard can be modified by adjusting the thickness of a brace. In fact, it has shown that specific natural frequencies can be targeted to be made consistent within a set standard. However, the rectangular brace used for most of the analysis has been found to have the ability to only frequency match one frequency at a time.

Scalloped braces have been shown to be a solution for which multiple natural frequencies of a soundboard can be adjusted. This not only helps to clarify the purpose of using scalloped braces, as has been done for hundreds of years, but also gives hope that it is possible for a wooden musical instrument manufacturing process to include acoustical consistency.

While much work still needs to be done in order to implement a frequency matching process. Overall, the study shows promising results which could lead to a mechanized process in which braces could be frequency matched to a soundboard in order to improve the acoustical consistency of manufactured wooden musical instruments.

8.3 Recommendations for Future Work

In order to increase the accuracy of the model with the assumed shape method, things that have otherwise been neglected during this analysis should be included. These include shear deformation and rotary inertia effects, the mass of air surrounding the soundboard,

the flexibility of the soundboard's edge support (simply supported versus clamped), as well as the damping properties of wood and its effect on various partials of the natural frequency spectrum.

For a more complex system involving multiple braces and an irregular soundboard shape which is better representative of an actual soundboard, a finite element model should be developed.

Experimental results of a test specimen having the same dimensions as those used during this analysis would be an asset in determining the validity of the work performed herein.

Finally, more time needs to be spent looking at the material properties themselves. This includes investigating the relationship between the Young's modulus in the radial direction and other wood properties, as well as the flexibility of the wood glue used in the assembly of the braces to the soundboard.

Appendix A

Derivation of a Simple Mass – Spring System

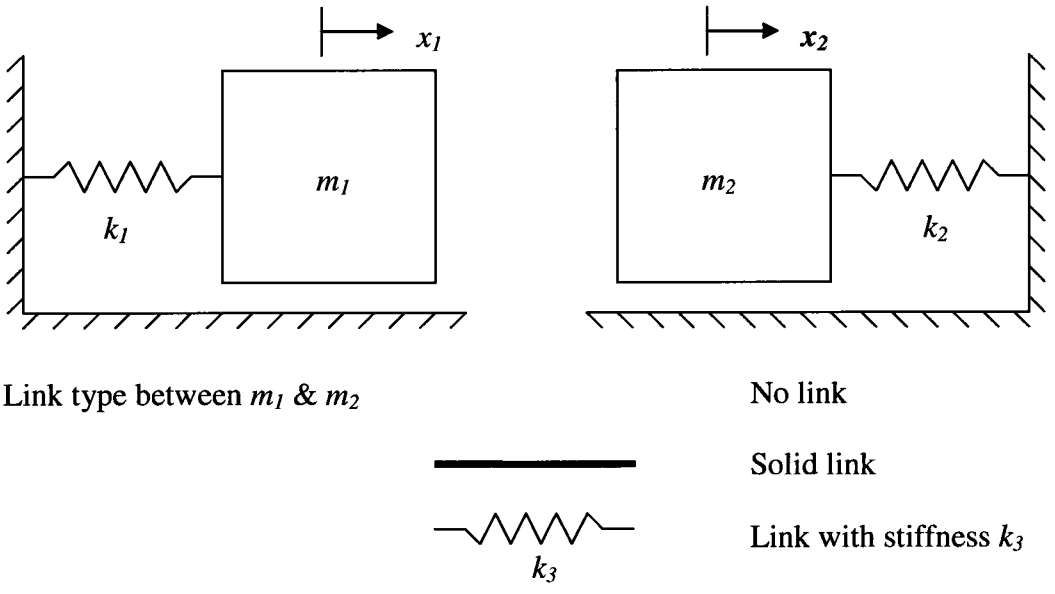

Figure A.1: Mass - spring system

A.1 Calculation of the System's Natural Frequencies

Lagrange's Equations

$$\frac{d}{dt}\left(\frac{\partial L}{\partial \dot{q}_i}\right)+\frac{\partial D}{\partial \dot{q}_i}-\frac{\partial L}{\partial q_i}=Q_i \qquad \text{for } i=1,2,...,n \tag{A.1}$$

where
T : Kinetic Energy
V : Potential Energy
D : Power Dissipation
Q : External Forces
$L=T-V$
$D=0$
$Q=0$
$\lambda=\sigma\pm i\omega$

A.1.1 Two Masses With No Link Between Them

System 1	System 2
$T_1=\frac{1}{2}m_1\dot{x}_1^{\,2}$	$T_2=\frac{1}{2}m_2\dot{x}_2^{\,2}$
$V_1=\frac{1}{2}k_1x_1^{\,2}$	$V_2=\frac{1}{2}k_2x_2^{\,2}$
$L_1=\frac{1}{2}m_1\dot{x}_1^{\,2}-\frac{1}{2}k_1x_1^{\,2}$	$L_2=\frac{1}{2}m_2\dot{x}_2^{\,2}-\frac{1}{2}k_2x_2^{\,2}$
$\frac{d}{dt}\left(\frac{\partial L}{\partial \dot{x}_1}\right)=m_1\ddot{x}_1$	$\frac{d}{dt}\left(\frac{\partial L}{\partial \dot{x}_2}\right)=m_2\ddot{x}_2$
$\frac{\partial L}{\partial x_1}=-k_1x_1$	$\frac{\partial L}{\partial x_2}=-k_2x_2$
$m_1\ddot{x}_1+k_1x_1=0$	$m_2\ddot{x}_2+k_2x_2=0$
$m_1\lambda_1^{\,2}+k_1=0$	$m_2\lambda_2^{\,2}+k_2=0$

(A.2)

Solving we get:

$$\lambda = \pm\sqrt{\frac{-k_1}{m_1}} \qquad \lambda = \pm\sqrt{\frac{-k_2}{m_2}} \tag{A.3}$$

$$\boxed{\omega_1 = \sqrt{\frac{k_1}{m_1}}} \tag{A.4}$$

$$\boxed{\omega_2 = \sqrt{\frac{k_2}{m_2}}} \tag{A.5}$$

A.1.2 Two Masses With a Solid Link Between Them

$$\begin{aligned} T &= \frac{1}{2}(m_1 + m_2)\dot{x}_1^2 \\ V &= \frac{1}{2}(k_1 + k_2)x_1^2 \\ L &= \frac{1}{2}(m_1 + m_2)\dot{x}_1^2 - \frac{1}{2}(k_1 + k_2)x_1^2 \end{aligned} \tag{A.6}$$

$$\begin{aligned} &\frac{d}{dt}\left(\frac{\partial L}{\partial \dot{x}_1}\right) = (m_1 + m_2)\ddot{x}_1 \\ &\frac{\partial L}{\partial x_1} = -(k_1 + k_2)x_1 \\ &(m_1 + m_2)\ddot{x}_1 + (k_1 + k_2)x_1 = 0 \\ &(m_1 + m_2)\lambda_1^2 + (k_1 + k_2) = 0 \end{aligned} \tag{A.7}$$

Solving we get:

$$\lambda = \pm\sqrt{\frac{-(k_1 + k_2)}{(m_1 + m_2)}} \tag{A.8}$$

$$\boxed{\omega_s = \sqrt{\frac{(k_1 + k_2)}{(m_1 + m_2)}}} \tag{A.9}$$

A.1.3 Two Masses With a Link of Stiffness k_3 Between Them

$$
\begin{aligned}
T &= \frac{1}{2}m_1\dot{x}_1^{\,2} + \frac{1}{2}m_2\dot{x}_2^{\,2} \\
V &= \frac{1}{2}k_1x_1^{\,2} + \frac{1}{2}k_2x_2^{\,2} + \frac{1}{2}k_3\left(x_2 - x_1\right)^2 \\
L &= \frac{1}{2}m_1\dot{x}_1^{\,2} + \frac{1}{2}m_2\dot{x}_2^{\,2} - \frac{1}{2}k_1x_1^{\,2} - \frac{1}{2}k_2x_2^{\,2} - \frac{1}{2}k_3\left(x_2 - x_1\right)^2
\end{aligned}
\tag{A.10}
$$

$$
\begin{aligned}
&\frac{d}{dt}\left(\frac{\partial L}{\partial \dot{x}_1}\right) = m_1\ddot{x}_1 && \frac{d}{dt}\left(\frac{\partial L}{\partial \dot{x}_2}\right) = m_2\ddot{x}_2 \\
&\frac{\partial L}{\partial x_1} = -k_1x_1 + k_3\left(x_2 - x_1\right) && \frac{\partial L}{\partial x_2} = -k_2x_2 - k_3\left(x_2 - x_1\right) \\
&m_1\ddot{x}_1 + k_1x_1 - k_3\left(x_2 - x_1\right) = 0 && m_2\ddot{x}_2 + k_2x_2 + k_3\left(x_2 - x_1\right) = 0 \\
&m_1\ddot{x}_1 + \left(k_1 + k_3\right)x_1 - k_3x_2 = 0 && m_2\ddot{x}_2 + \left(k_2 + k_3\right)x_2 - k_3x_1 = 0
\end{aligned}
\tag{A.11}
$$

In matrix form:

$$
\underbrace{\begin{bmatrix} m_1 & 0 \\ 0 & m_2 \end{bmatrix}}_{M}\begin{bmatrix} \ddot{x}_1 \\ \ddot{x}_2 \end{bmatrix} + \underbrace{\begin{bmatrix} k_1 + k_3 & -k_3 \\ -k_3 & k_2 + k_3 \end{bmatrix}}_{K}\begin{bmatrix} x_1 \\ x_2 \end{bmatrix} = \begin{bmatrix} 0 \\ 0 \end{bmatrix}
\tag{A.12}
$$

$$
M\vec{\ddot{x}} + K\vec{x} = 0
$$

$$
\begin{aligned}
&\det\left(M\lambda^2 + K\right) = 0 \\
&\det\begin{bmatrix} \lambda^2m_1 + k_1 + k_3 & -k_3 \\ -k_3 & \lambda^2m_2 + k_2 + k_3 \end{bmatrix} = 0 \\
&\lambda^4m_1m_2 + \left(\left(m_1 + m_2\right)k_3 + m_1k_2 + m_2k_1\right)\lambda^2 + \left(k_1 + k_2\right)k_3 + k_1k_2 = 0
\end{aligned}
\tag{A.13}
$$

Solving we get:

$$
\begin{aligned}
\lambda^2 = \frac{1}{2m_1m_2}&\left(-m_1\left(k_3 + k_2\right) - m_2\left(k_3 + k_1\right)\right. \\
&\left.\pm\sqrt{m_1^2\left(k_3^2 + k_2^2 + 2k_2k_3\right) + m_2^2\left(k_3^2 + k_1^2 + 2k_1k_3\right) + 2m_1m_2\left(k_3^2 - k_1k_3 - k_2k_3 - k_1k_2\right)}\right)
\end{aligned}
\tag{A.14}
$$

$$\omega_p = \left(-\frac{1}{2m_1 m_2}\left(-m_1\left(k_3+k_2\right)-m_2\left(k_3+k_1\right) + \sqrt{m_1^2\left(k_3^2+k_2^2+2k_2k_3\right)+m_2^2\left(k_3^2+k_1^2+2k_1k_3\right)+2m_1m_2\left(k_3^2-k_1k_3-k_2k_3-k_1k_2\right)}\right)\right)^{\frac{1}{2}} \tag{A.15}$$

and

$$\omega_m = \left(-\frac{1}{2m_1 m_2}\left(-m_1\left(k_3+k_2\right)-m_2\left(k_3+k_1\right) - \sqrt{m_1^2\left(k_3^2+k_2^2+2k_2k_3\right)+m_2^2\left(k_3^2+k_1^2+2k_1k_3\right)+2m_1m_2\left(k_3^2-k_1k_3-k_2k_3-k_1k_2\right)}\right)\right)^{\frac{1}{2}} \tag{A.16}$$

A.2 Calculation of the System's Mass

Volume:

$$V = L_x \cdot L_y \cdot h \tag{A.17}$$

Masse:

$$m = \rho \cdot V \tag{A.18}$$

System 1	System 2	
$V_1 = 0.24m \cdot 0.18m \cdot 0.003m$	$V_2 = 0.012m \cdot 0.18m \cdot 0.012m$	
$V_1 = 0.0001296m^3$	$V_2 = 0.00002592m^3$	(A.19)
$m_1 = 430.2kg/m^3 \cdot 0.0001296m^3$	$m_2 = 430.2kg/m^3 \cdot 0.00002592m^3$	
$m_1 = 0.05575kg$	$m_2 = 0.01115kg$	

A.3 Calculation of the Beam's Stiffness

To calculate the beam's stiffness, we use the beam equation for a simply supported beam loaded at its center.

Stiffness:

$$k = \frac{P}{w} \tag{A.20}$$

where P is a point load and w the displacement

Area moment of inertia:

$$I = \frac{L_x h^3}{12} \tag{A.21}$$

$$w = \frac{PL_y^{\,3}}{48EI} = \frac{PL_y^{\,3}}{4L_x h^3 E} \tag{A.22}$$

$$\boxed{k = \frac{4L_x h^3 E}{L_y^{\,3}}} \tag{A.23}$$

System 2

$$k_2 = \frac{4 \cdot 0.012m \cdot (0.012m)^3 \cdot 10.89 \times 10^9 Pa}{(0.24m)^3} \tag{A.24}$$

$$\boxed{k_2 = 65340 N/m}$$

A.4 Calculation of the Plate's Stiffness

To calculate the plate's stiffness, we use the Navier solution for a simply supported plate loaded at its center.

Stiffness:

$$k = \frac{P}{w} \tag{A.25}$$

Plate's stiffness:

$$D = \frac{Eh^3}{12(1-\nu^2)} \tag{A.26}$$

Plate loaded at its center:

$$a = x = \frac{L_x}{2}, \; b = y = \frac{L_y}{2} \tag{A.27}$$

$$w=\frac{4P}{\pi^4 DL_xL_y}\sum_{m=1}^{\infty}\sum_{n=1}^{\infty}\frac{\sin\left(\frac{m\pi a}{L_x}\right)\sin\left(\frac{n\pi b}{L_y}\right)\sin\left(\frac{m\pi x}{L_x}\right)\sin\left(\frac{n\pi y}{L_y}\right)}{\left(\left(\frac{m}{L_x}\right)^2+\left(\frac{n}{L_y}\right)^2\right)^2} \tag{A.28}$$

$$\boxed{k=\frac{\pi^4 DL_xL_y}{4\sum_{m=1}^{\infty}\sum_{n=1}^{\infty}\frac{\sin\left(\frac{m\pi a}{L_x}\right)\sin\left(\frac{n\pi b}{L_y}\right)\sin\left(\frac{m\pi x}{L_x}\right)\sin\left(\frac{n\pi y}{L_y}\right)}{\left(\left(\frac{m}{L_x}\right)^2+\left(\frac{n}{L_y}\right)^2\right)^2}}} \tag{A.29}$$

System1

$$D=\frac{10.89\times10^9\ Pa\cdot(0.003\,m)^3}{12\left(1-0.372^2\right)}=28.44\,Nm \tag{A.30}$$

$$k_1=\frac{\pi^4\cdot 28.44\,Nm\cdot 0.24\,m\cdot 0.18\,m}{4\sum_{m=1}^{\infty}\sum_{n=1}^{\infty}\frac{\sin\left(\frac{m\pi\cdot 0.12\,m}{0.24\,m}\right)\sin\left(\frac{n\pi\cdot 0.09\,m}{0.18m}\right)\sin\left(\frac{m\pi\cdot 0.12m}{0.24\,m}\right)\sin\left(\frac{n\pi\cdot 0.09\,m}{0.18m}\right)}{\left(\left(\frac{m}{0.24\,m}\right)^2+\left(\frac{n}{0.18\,m}\right)^2\right)^2}}$$

$$\boxed{k_1=60569.74\,N/m}$$

A.5 Maple Code for Calculating the Stiffness of the Plate

$$E := 10.89e9$$
$$Lx := 0.24$$
$$Ly := 0.18$$
$$a := \frac{Lx}{2}$$
$$b := \frac{\mathrm{Ly}}{2}$$
$$h := 0.003$$
$$\nu := 0.372$$
$$x := a$$
$$y := b$$
$$d := \frac{E \cdot h^3}{12\left(1 - \nu^2\right)}$$
$$k := \frac{1}{\frac{4}{\pi^4 \cdot d \cdot Lx \cdot Ly} \sum_{m=1}^{150} \sum_{n=1}^{150} \frac{\sin\left(\frac{m \cdot \pi \cdot a}{Lx}\right) \sin\left(\frac{n \cdot \pi \cdot b}{Ly}\right) \sin\left(\frac{m \cdot \pi \cdot x}{Lx}\right) \sin\left(\frac{n \cdot \pi \cdot y}{Ly}\right)}{\left(\left(\frac{m}{Lx}\right)^2 + \left(\frac{n}{Ly}\right)^2\right)^2}}$$

A.6 Maple Code for Calculating Natural Frequencies

Block 1 is a 0.24 x 0.18 m plate that is 3 mm thick
Block 2 is a 0.012 x 0.012 m bar that is 0.18 m long
Stiffness 3 is that due to the glue holding the two blocks together

$m_1 := 0.05575$
$m_2 := 0.01115$
$k_1 := 60569.75$
$k_2 := 65340$
$k_3 := 1000$

Two Masses with no link between them

$$\omega 1 := \sqrt{\frac{k_1}{m_1}}$$
$$\omega 2 := \sqrt{\frac{k_2}{m_2}}$$

Two Masses with a solid link between them

$$\omega s := \sqrt{\frac{k_1 + k_2}{m_1 + m_2}}$$

Two Masses with a spring of stiffness k3 between them

$$\omega p := \left(-\frac{1}{2}\frac{1}{m_1 m_2}\left(-m_1 k_3 - m_1 k_2 - k_3 m_2 - k_1 m_2 \right.\right.$$
$$\left. + \left(m_1^2 k_3^2 + 2\, m_1^2 k_3 k_2 + 2\, m_1 k_3^2 m_2 - 2\, m_1 k_3 k_1 m_2 + m_1^2 k_2^2 \right.\right.$$
$$\left.\left. - 2\, m_1 k_2 k_3 m_2 - 2\, m_1 k_2 k_1 m_2 + k_3^2 m_2^2 + 2\, k_3 m_2^2 k_1 + k_1^2 m_2^2 \right)^{\frac{1}{2}} \right)\Bigg)^{\frac{1}{2}}$$

$$\omega m := \left(-\frac{1}{2}\frac{1}{m_1 m_2}\left(-m_1 k_3 - m_1 k_2 - k_3 m_2 - k_1 m_2 \right.\right.$$
$$\left. - \left(m_1^2 k_3^2 + 2\, m_1^2 k_3 k_2 + 2\, m_1 k_3^2 m_2 - 2\, m_1 k_3 k_1 m_2 + m_1^2 k_2^2 \right.\right.$$
$$\left.\left. - 2\, m_1 k_2 k_3 m_2 - 2\, m_1 k_2 k_1 m_2 + k_3^2 m_2^2 + 2\, k_3 m_2^2 k_1 + k_1^2 m_2^2 \right)^{\frac{1}{2}} \right)\Bigg)^{\frac{1}{2}}$$

Appendix B

Hamilton's Principle for a Simply Supported Plate

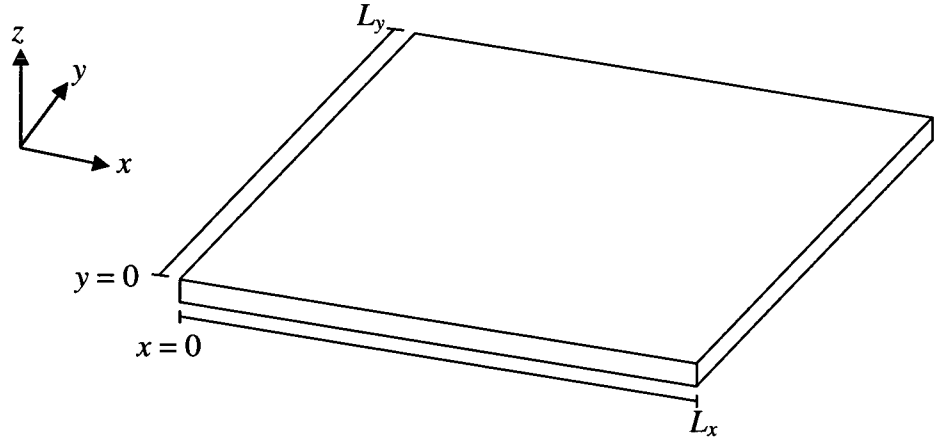

Figure B.1: Simply supported rectangular plate

In order to solve Hamilton's principle for the case of the simply supported vibrating rectangular plate, the displacement variable is $w(x,y,t)$.

Hamilton's principle is stated as

$$\int_{t_1}^{t_2}(\delta T+\delta W)\,dt=0 \tag{B.1}$$

$$\delta w(x,y,t_1)=\delta w(x,y,t_2)=0 \tag{B.2}$$

Geometric boundary conditions of the problem:

@ $x=0$

$$w(0,y,t)=0 \;\Rightarrow\; \delta w(0,y,t)=0 \tag{B.3}$$

@ $x = L_x$

$$w(L_x,y,t)=0 \;\Rightarrow\; \delta w(L_x,y,t)=0 \tag{B.4}$$

@ $y = 0$

$$w(x,0,t)=0 \;\Rightarrow\; \delta w(x,0,t)=0 \tag{B.5}$$

@ $y = L_y$

$$w(0,L_y,t)=0 \;\Rightarrow\; \delta w(0,L_y,t)=0 \tag{B.6}$$

B.1 Kinetic Energy

$$\begin{aligned} T &= \frac{1}{2}\int_0^{L_x}\int_0^{L_y} \dot{w}^2 \rho \, dydx \\ \delta T &= \delta\left[\frac{1}{2}\int_0^{L_x}\int_0^{L_y} \dot{w}^2 \rho \, dydx\right] = \frac{1}{2}\int_0^{L_x}\int_0^{L_y} 2\dot{w}\delta\dot{w}\rho \, dydx \end{aligned} \tag{B.7}$$

$$\boxed{\delta T = \int_0^{L_x}\int_0^{L_y} \dot{w}\delta\dot{w}\rho \, dydx} \tag{B.8}$$

B.2 Strain Energy

$$U = \frac{1}{2}D\int_0^{L_x}\int_0^{L_y}\left[\left(w_{xx}+w_{yy}\right)^2 + 2(1-\nu)\left(w_{xy}^2 - w_{xx}w_{yy}\right)\right]dydx \tag{B.9}$$

where

$$D = \frac{E h^3}{12\left(1-\nu^2\right)} \tag{B.10}$$

$$W = -U = -\frac{1}{2}D\int_0^{L_x}\int_0^{L_y}\left[\left(w_{xx}+w_{yy}\right)^2 + 2(1-\nu)\left(w_{xy}^2 - w_{xx}w_{yy}\right)\right]dydx$$

$$\delta W = \delta\left[-\frac{1}{2}D\int_0^{L_x}\int_0^{L_y}\left[w_{xx}^2 + 2w_{xx}w_{yy} + w_{yy}^2 + 2(1-\nu)\left(w_{xy}^2 - w_{xx}w_{yy}\right)\right]dydx\right] \tag{B.11}$$

$$\delta W = -\frac{1}{2}D\int_0^{L_x}\int_0^{L_y}\left[2\left(w_{xx}\delta w_{xx} + w_{yy}\delta w_{yy} + w_{xx}\delta w_{yy} + w_{yy}\delta w_{xx}\right)\right.$$
$$\left.+2(1-\nu)\left(2w_{xy}\delta w_{xy} - w_{xx}\delta w_{yy} - w_{yy}\delta w_{xx}\right)\right]dydx$$

$$\boxed{\begin{aligned}\delta W = -D\int_0^{L_x}\int_0^{L_y}\Big[&w_{xx}\delta w_{xx} + w_{yy}\delta w_{yy} + w_{xx}\delta w_{yy} + w_{yy}\delta w_{xx}\\ &+(1-\nu)\left(2w_{xy}\delta w_{xy} - w_{xx}\delta w_{yy} - w_{yy}\delta w_{xx}\right)\Big]dydx\end{aligned}} \tag{B.12}$$

B.3 Hamilton's Principle

Substitute δT and δW into (B.1).

$$\int_{t_1}^{t_2}\int_0^{L_x}\int_0^{L_y}\dot{w}\delta\dot{w}\rho\,dydxdt - \int_{t_1}^{t_2}D\int_0^{L_x}\int_0^{L_y}\Big[w_{xx}\delta w_{xx} + w_{yy}\delta w_{yy} + w_{xx}\delta w_{yy} + w_{yy}\delta w_{xx}$$
$$+(1-\nu)\left(2w_{xy}\delta w_{xy} - w_{xx}\delta w_{yy} - w_{yy}\delta w_{xx}\right)\Big]dydxdt = 0 \tag{B.13}$$

$$\int_0^{L_x}\int_0^{L_y}\underbrace{\left[\int_{t_1}^{t_2}\dot{w}\delta\dot{w}dt\right]}_{\{1\}}\rho\,dydx - \int_{t_1}^{t_2}\underbrace{\left[\begin{aligned}&D\int_0^{L_x}\int_0^{L_y}\Big[w_{xx}\delta w_{xx} + w_{yy}\delta w_{yy} + w_{xx}\delta w_{yy} + w_{yy}\delta w_{xx}\\ &+(1-\nu)\left(2w_{xy}\delta w_{xy} - w_{xx}\delta w_{yy} - w_{yy}\delta w_{xx}\right)\Big]dydx\end{aligned}\right]}_{\{2\}}dt = 0 \tag{B.14}$$

Each term is considered separately.

Consider $\{1\}$.

$$\begin{aligned}\int_{t_1}^{t_2}\dot{w}\frac{\partial}{\partial t}\delta w dt &= \dot{w}\delta w\Big|_{t_1}^{t_2} - \int_{t_1}^{t_2}\ddot{w}\delta w dt\\ &= \dot{w}(t_2)\,\cancel{\delta w(t_2)} - \dot{w}(t_1)\,\cancel{\delta w(t_1)} - \int_{t_1}^{t_2}\ddot{w}\delta w dt\end{aligned} \tag{B.15}$$

$$\boxed{\int_{t_1}^{t_2} \dot{w} \frac{\partial}{\partial t} \delta w dt = -\int_{t_1}^{t_2} \ddot{w} \delta w dt} \tag{B.16}$$

Consider $\{2\}$.

$$D \int_0^{L_x} \int_0^{L_y} \Big[\underbrace{w_{xx}\delta w_{xx}}_{3} + \underbrace{w_{yy}\delta w_{yy}}_{4} + \underbrace{w_{xx}\delta w_{yy}}_{5} + \underbrace{w_{yy}\delta w_{xx}}_{6} + (1-\nu)\Big(\underbrace{2w_{xy}\delta w_{xy}}_{7} - \underbrace{w_{xx}\delta w_{yy}}_{8} - \underbrace{w_{yy}\delta w_{xx}}_{9} \Big) \Big] dydx \tag{B.17}$$

Using the Green- Gauss theorem [24]

$$\begin{aligned} \int_A u \frac{\partial v}{\partial x} dA &= \int_c uvn_x dc - \int_A \frac{\partial u}{\partial x} v dA \\ \int_A u \frac{\partial v}{\partial y} dA &= \int_c uvn_y dc - \int_A \frac{\partial u}{\partial y} v dA \end{aligned} \tag{B.18}$$

where for the plane case, $n_x dc = dy$ and $n_y dc = -dx$.

Consider $\{3\}$.

$$\int_0^{L_x} \int_0^{L_y} w_{xx}\delta w_{xx} dydx = \int_c w_{xx}\delta w_x n_x dc - \underbrace{\int_0^{L_x} \int_0^{L_y} w_{xxx}\delta w_x dydx}_{10} \tag{B.19}$$

Consider $\{10\}$.

$$-\int_0^{L_x} \int_0^{L_y} w_{xxx}\delta w_x dydx = -\int_c w_{xxx}\delta w n_x dc + \int_0^{L_x} \int_0^{L_y} w_{xxxx}\delta w dydx \tag{B.20}$$

$$\boxed{\therefore \int_0^{L_x} \int_0^{L_y} w_{xx}\delta w_{xx} dydx = \int_c w_{xx}\delta w_x n_x dc - \int_c w_{xxx}\delta w n_x dc + \int_0^{L_x} \int_0^{L_y} w_{xxxx}\delta w dydx} \tag{B.21}$$

Consider $\{4\}$.

In the same way as $\{3\}$, it can be shown that

$$\boxed{\int_0^{L_x} \int_0^{L_y} w_{yy}\delta w_{yy} dydx = \int_c w_{yy}\delta w_y n_y dc - \int_c w_{yyy}\delta w n_y dc + \int_0^{L_x} \int_0^{L_y} w_{yyyy}\delta w dydx} \tag{B.22}$$

Consider $\{5\}$.

$$\int_0^{L_x}\int_0^{L_y} w_{xx}\delta w_{yy}dydx = \int_c w_{xx}\delta w_y n_y dc - \underbrace{\int_0^{L_x}\int_0^{L_y} w_{xxy}\delta w_y dydx}_{11} \tag{B.23}$$

Consider $\{11\}$.

$$-\int_0^{L_x}\int_0^{L_y} w_{xxy}\delta w_y dydx = -\int_c w_{xxy}\delta w n_y dc + \int_0^{L_x}\int_0^{L_y} w_{xxyy}\delta w dydx \tag{B.24}$$

$$\therefore \int_0^{L_x}\int_0^{L_y} w_{xx}\delta w_{yy}dydx = \int_c w_{xx}\delta w_y n_y dc - \int_c w_{xxy}\delta w n_y dc + \int_0^{L_x}\int_0^{L_y} w_{xxyy}\delta w dydx \tag{B.25}$$

Consider $\{6\}$.

In the same way as $\{5\}$, it can be shown that

$$\int_0^{L_x}\int_0^{L_y} w_{yy}\delta w_{xx}dydx = \int_c w_{yy}\delta w_x n_x dc - \int_c w_{xyy}\delta w n_x dc + \int_0^{L_x}\int_0^{L_y} w_{xxyy}\delta w dydx \tag{B.26}$$

Consider $\{7\}$.

We can expand as follow

$$\int_0^{L_x}\int_0^{L_y} 2w_{xy}\delta w_{xy}dydx = \underbrace{\int_0^{L_x}\int_0^{L_y} w_{xy}\delta w_{xy}dydx}_{12} + \underbrace{\int_0^{L_x}\int_0^{L_y} w_{yx}\delta w_{yx}dydx}_{13} \tag{B.27}$$

Consider $\{12\}$.

$$\int_0^{L_x}\int_0^{L_y} w_{xy}\delta w_{xy}dydx = \int_c w_{xy}\delta w_y n_x dc - \underbrace{\int_0^{L_x}\int_0^{L_y} w_{xxy}\delta w_y dydx}_{14} \tag{B.28}$$

Consider $\{14\}$.

$$-\int_0^{L_x}\int_0^{L_y} w_{xxy}\delta w_y dydx = -\int_c w_{xxy}\delta w n_y dc + \int_0^{L_x}\int_0^{L_y} w_{xxyy}\delta w dydx \tag{B.29}$$

$$\therefore \int_0^{L_x}\int_0^{L_y} w_{xy}\delta w_{xy}dydx = \int_c w_{xy}\delta w_y n_x dc - \int_c w_{xxy}\delta w n_y dc + \int_0^{L_x}\int_0^{L_y} w_{xxyy}\delta w dydx \tag{B.30}$$

Consider $\{13\}$.

In the same way as $\{12\}$, it can be shown that

$$\int_0^{L_x}\int_0^{L_y} w_{yx}\delta w_{yx}dydx = \int_c w_{yx}\delta w_x n_y dc - \int_c w_{xyy}\delta w n_x dc + \int_0^{L_x}\int_0^{L_y} w_{xxyy}\delta w dydx \tag{B.31}$$

Consider $\{8\}$.

In the same way as $\{5\}$, it can be shown that

$$-\int_0^{L_x}\int_0^{L_y} w_{xx}\delta w_{yy}dydx = -\int_c w_{xx}\delta w_y n_y dc + \int_c w_{xxy}\delta w n_y dc - \int_0^{L_x}\int_0^{L_y} w_{xxyy}\delta w dydx \tag{B.32}$$

Consider $\{9\}$.

In the same way as $\{6\}$, it can be shown that

$$-\int_0^{L_x}\int_0^{L_y} w_{yy}\delta w_{xx}dydx = -\int_c w_{yy}\delta w_x n_x dc + \int_c w_{xyy}\delta w n_x dc - \int_0^{L_x}\int_0^{L_y} w_{xxyy}\delta w dydx \tag{B.33}$$

Gathering all the terms back together as in (B.17),

$$\begin{aligned}
&D\int_0^{L_x}\int_0^{L_y}\Big[w_{xxxx}+w_{yyyy}+2w_{xxyy}+(1-\nu)\cancel{\left(2w_{xxyy}-2w_{xxyy}\right)}\Big]\delta w dydx \\
&\quad +D\int_c\Big[\Big(w_{xx}n_x+w_{yy}n_x+(1-\nu)\left(-w_{yy}n_x+w_{yx}n_y\right)\Big)\delta w_x \\
&\qquad +\Big(w_{yy}n_y+w_{xx}n_y+(1-\nu)\left(-w_{xx}n_y+w_{xy}n_x\right)\Big)\delta w_y \\
&\qquad +\left(-w_{xxx}n_x-w_{yyy}n_y-w_{xxy}n_y-w_{xyy}n_x\right) \\
&\qquad +(1-\nu)\left(w_{xxy}n_y+w_{xyy}n_x-w_{xxy}n_y-w_{xyy}n_x\right)\delta w\Big]dc
\end{aligned} \tag{B.34}$$

$$\begin{aligned}
&D\int_0^{L_x}\int_0^{L_y}\Big[w_{xxxx}+2w_{xxyy}+w_{yyyy}\Big]\delta w dydx \\
&\quad +D\int_c\Big[\Big(w_{xx}n_x+\nu w_{yy}n_x+(1-\nu)\left(w_{yx}n_y\right)\Big)\delta w_x \\
&\qquad +\Big(w_{yy}n_y+\nu w_{xx}n_y+(1-\nu)\left(w_{xy}n_x\right)\Big)\delta w_y \\
&\qquad +\left(-w_{xxx}n_x-w_{yyy}n_y-\nu w_{xxy}n_y-\nu w_{xyy}n_x\right) \\
&\qquad -(1-\nu)\left(w_{xxy}n_y+w_{xyy}n_x\right)\delta w\Big]dc
\end{aligned} \tag{B.35}$$

where $n_x dc = dy$ and $n_y dc = -dx$ [24].

$$
\begin{aligned}
D\int_0^{L_x}\int_0^{L_y}&\left[w_{xxxx}+2w_{xxyy}+w_{yyyy}\right]\delta w dy dx \\
&+D\int_c\Big[\left(w_{xx}+\nu w_{yy}\right)\delta w_x dy-(1-\nu)w_{yx}\delta w_x dx \\
&-\left(w_{yy}+\nu w_{xx}\right)\delta w_y dx+(1-\nu)w_{xy}\delta w_y dy \\
&-\left(w_{xxx}+\nu w_{xyy}\right)\delta w dy+\left(w_{yyy}+\nu w_{xxy}\right)\delta w dx \\
&+(1-\nu)w_{xxy}\delta w dx-(1-\nu)w_{xyy}\delta w dy\Big]
\end{aligned}
\tag{B.36}
$$

Reorganising,

$$
\begin{aligned}
D\int_0^{L_x}\int_0^{L_y}&\left[w_{xxxx}+2w_{xxyy}+w_{yyyy}\right]\delta w dy dx \\
&+D\int_c\Big\{\Big[\left(w_{yyy}+\nu w_{xxy}\right)+(1-\nu)w_{xxy}\Big]\delta w dx \\
&-\Big[\left(w_{yy}+\nu w_{xx}\right)\delta w_y+\underbrace{(1-\nu)w_{yx}\delta w_x}_{\{15\}}\Big]dx \\
&-\Big[\left(w_{xxx}+\nu w_{xyy}\right)+(1-\nu)w_{xyy}\Big]\delta w dy \\
&+\Big[\left(w_{xx}+\nu w_{yy}\right)\delta w_x+\underbrace{(1-\nu)w_{xy}\delta w_y}_{\{16\}}\Big]dy\Big\}
\end{aligned}
\tag{B.37}
$$

Consider $\{15\}$.

$$
\begin{aligned}
\int_c(1-\nu)w_{yx}\frac{\partial}{\partial x}\delta w dx &= (1-\nu)w_{yx}\,\delta w\big|_0^{L_x}-\int_c(1-\nu)w_{yxx}\delta w dx \\
&= (1-\nu)w_{yx}(L_x)\cancelto{B.C.s}{\delta w(L_x)}-(1-\nu)w_{yx}(0)\cancelto{B.C.s}{\delta w(0)} \\
&\quad -\int_c(1-\nu)w_{yxx}\delta w dx \\
\int_c(1-\nu)w_{yx}\frac{\partial}{\partial x}\delta w dx &= -\int_c(1-\nu)w_{yxx}\delta w dx
\end{aligned}
\tag{B.38}
$$

Consider $\{16\}$.

$$\begin{aligned}\int_c (1-\nu) w_{xy} \frac{\partial}{\partial y} \delta w dy &= (1-\nu) w_{xy} \delta w \Big|_0^{L_y} - \int_c (1-\nu) w_{xyy} \delta w dy \\ &= (1-\nu) w_{xy}(L_y) \cancel{\delta w(L_y)}^{B.C.s} - (1-\nu) w_{xy}(0) \cancel{\delta w(0)}^{B.C.s} \\ &\quad - \int_c (1-\nu) w_{xyy} \delta w dy \\ \int_c (1-\nu) w_{xy} \frac{\partial}{\partial y} \delta w dy &= - \int_c (1-\nu) w_{xyy} \delta w dy\end{aligned} \tag{B.39}$$

Finally,

$$\begin{aligned} & D \int_0^{L_x} \int_0^{L_y} \left[w_{xxxx} + 2w_{xxyy} + w_{yyyy} \right] \delta w dy dx \\ & \quad + D \int_c \Big\{ \Big[\left(w_{yyy} + \nu w_{xxy} \right) + (1-\nu) w_{xxy} \\ & \quad + (1-\nu) w_{yx} \Big] \delta w dx \\ & \quad - \left[\left(w_{yy} + \nu w_{xx} \right) \delta w_y \right] dx \\ & \quad - \Big[\left(w_{xxx} + \nu w_{xyy} \right) + (1-\nu) w_{xyy} \\ & \quad + (1-\nu) w_{xy} \Big] \delta w dy \\ & \quad + \left[\left(w_{xx} + \nu w_{yy} \right) \delta w_x \right] dy \Big\} \end{aligned} \tag{B.40}$$

Put equations (B.16) and (B.40) back into equation (B.14),

$$-\int_0^{L_x} \int_0^{L_y} \left[\int_{t_1}^{t_2} \ddot{w} \delta w dt \right] \rho dy dx - \int_{t_1}^{t_2} \left[\begin{array}{l} D \int_0^{L_x} \int_0^{L_y} \left[w_{xxxx} + 2w_{xxyy} + w_{yyyy} \right] \delta w dy dx \\ + D \int_c \Big\{ \Big[\left(w_{yyy} + \nu w_{xxy} \right) + (1-\nu) w_{xxy} \\ + (1-\nu) w_{yx} \Big] \delta w dx \\ - \left[\left(w_{yy} + \nu w_{xx} \right) \delta w_y \right] dx \\ - \Big[\left(w_{xxx} + \nu w_{xyy} \right) + (1-\nu) w_{xyy} \\ + (1-\nu) w_{xy} \Big] \delta w dy \\ + \left[\left(w_{xx} + \nu w_{yy} \right) \delta w_x \right] dy \Big\} \end{array} \right] dt = 0 \tag{B.41}$$

Regrouping

$$-\int_{t_1}^{t_2}\int_0^{L_x}\int_0^{L_y}\underbrace{\begin{bmatrix}\rho\ddot{w}\\ +w_{xxxx}\\ +2w_{xxyy}\\ +w_{yyyy}\end{bmatrix}}_{1^{st}\text{ term}}\delta w dy dx dt - D\int_{t_1}^{t_2}\underbrace{\begin{bmatrix}\left[\left(w_{yyy}+\nu w_{xxy}\right)+(1-\nu)w_{xxy}\right.\\ \left.+(1-\nu)w_{yx}\right]\delta w dx\\ -\left[\left(w_{yy}+\nu w_{xx}\right)\delta w_y\right]dx\\ -\left[\left(w_{xxx}+\nu w_{xyy}\right)+(1-\nu)w_{xyy}\right.\\ \left.+(1-\nu)w_{xy}\right]\delta w dy\\ +\left[\left(w_{xx}+\nu w_{yy}\right)\delta w_x\right]dy\end{bmatrix}}_{2^{nd}\text{ term}}dt=0 \qquad \text{(B.42)}$$

The two terms are independent since δw is arbitrary, therefore

1st term:

Since $\delta w=\delta w(x,y,t)\neq 0$, therefore

$$\rho\ddot{w}+w_{xxxx}+2w_{xxyy}+w_{yyyy}=0 \qquad \text{(B.43)}$$

which can be rewriting in the form

$$\boxed{\rho\frac{\partial^2 w}{\partial t^2}+D\left(\frac{\partial^4 w}{\partial x^4}+2\frac{\partial^4 w}{\partial x^2\partial y^2}+\frac{\partial^4 w}{\partial y^4}\right)=0} \qquad \text{(B.44)}$$

Equation (B.44) represents the equation of motion of the rectangular plate

2nd term:

Since $\delta w=\delta w(x,y,t)\neq 0$, $\delta w_x=\delta w_x(x,y,t)\neq 0$ and $\delta w_y=\delta w_y(x,y,t)\neq 0$, therefore

Along x:

$$\cancel{\left(w_{yyy}+\nu w_{xxy}\right)+(1-\nu)w_{xxy}}+(1-\nu)w_{yx}=0 \qquad \text{(B.45)}$$

and

$$w_{yy} + \nu w_{xx} = 0 \tag{B.46}$$

$$\frac{\partial^2 w}{\partial x^2} 0 \tag{B.47}$$

Along y:

$$\left(w_{xxx} + \nu w_{xyy}\right) + (1-\nu) w_{xyy} + (1-\nu) w_{xy} = 0 \tag{B.48}$$

and

$$w_{xx} + \nu w_{yy} \tag{B.49}$$

$$\frac{\partial^2 w}{\partial y^2} 0 \tag{B.50}$$

Therefore it follows that the boundary conditions are,

$$\begin{array}{lll} w = 0 & \dfrac{\partial^2 w}{\partial x^2} = 0 & \text{at } x = 0, L_x \\ w = 0 & \dfrac{\partial^2 w}{\partial y^2} = 0 & \text{at } y = 0, L_y \end{array} \tag{B.51}$$

These boundary conditions are those of a simply supported rectangular plate.

B.4 Solving the Plate's Equation of Motion

From the equation of motion, equation (B.44), a harmonic solution is applied such as,

$$\begin{aligned} w(x,y,t) &= w(x,t) \cdot \cos(\omega t + \phi) \\ \ddot{w}(x,y,t) &= -\omega^2 w(x,t) \cdot \cos(\omega t + \phi) \end{aligned} \tag{B.52}$$

Substituting equation (B.52) into the equation of motion,

$$D\left(\frac{\partial^4}{\partial x^4} + 2\frac{\partial^4}{\partial x^2 \partial y^2} + \frac{\partial^4}{\partial y^4}\right) w(x,y) \cos(\omega t + \phi) = \omega^2 \rho\, w(x,y) \cos(\omega t + \phi) \tag{B.53}$$

$$D\left(\frac{\partial^4 w}{\partial x^4} + 2\frac{\partial^4 w}{\partial x^2 \partial y^2} + \frac{\partial^4 w}{\partial y^4}\right) = \omega^2 \rho\, w \tag{B.54}$$

the solution in $w(x,y)$ is found to be [17],

$$\begin{aligned} w(x,y) = {} & A_1 \sin\alpha x \sin\gamma y + A_2 \sin\alpha x \cos\gamma y + A_3 \cos\alpha x \sin\gamma y \\ & + A_4 \cos\alpha x \cos\gamma y + A_5 \sinh\beta x \sinh\eta y \\ & + A_6 \sinh\beta x \cosh\eta y + A_7 \cosh\beta x \sinh\eta y \\ & + A_8 \cosh\beta x \cosh\eta y \end{aligned} \tag{B.55}$$

where $\alpha, \beta, \gamma, \eta$ are arbitrary constants represented by,

$$\alpha^2 + \gamma^2 = \beta^2 + \eta^2 = \sqrt{\frac{\omega^2 \rho}{D}} \tag{B.56}$$

Applying the simply supported boundary conditions of equations (B.51), all A's with the exception of A_1 are found to be zero. Therefore,

$$\sin\alpha L_x = 0 \quad \text{and} \quad \sin\gamma L_y = 0 \tag{B.57}$$

Their solutions are,

$$\begin{aligned} \alpha_{m_x} &= \frac{m_x \pi}{L_x}, & m_x &= 1,2,... \\ \gamma_{m_y} &= \frac{m_y \pi}{L_y}, & m_y &= 1,2,... \end{aligned} \tag{B.58}$$

Substituting back into equation (B.56), the natural frequencies are obtained,

$$\omega_{m_x m_y} = \pi^2 \left[\left(\frac{m_x}{L_x} \right)^2 + \left(\frac{m_y}{L_y} \right)^2 \right] \sqrt{\frac{D}{\rho}} \qquad \text{for } m_x, m_y = 1,2,... \tag{B.59}$$

Solving the mass normalized modes so that $\int_0^{L_x} \int_0^{L_y} \rho w^2 dy dx = 1$, results in following modeshapes,

$$w_{m_x m_y}(x,y) = \frac{2}{\sqrt{\rho L_x L_y}} \sin\frac{m_x \pi x}{L_x} \sin\frac{m_y \pi y}{L_y} \qquad \text{for } m_x, m_y = 1,2,... \tag{B.60}$$

The solution to the simply supported isotropic rectangular plate is thus obtained.

Appendix C

Assumed Shape Method for a Beam Divided into Two Equal Sections [23]

F. Vigneron
April 6, 2009

APR - 6 2009

Assumed Shape Method for Beam divided into Two Equal Sections

Consider a beam of length $2L$, which is simply supported as shown below

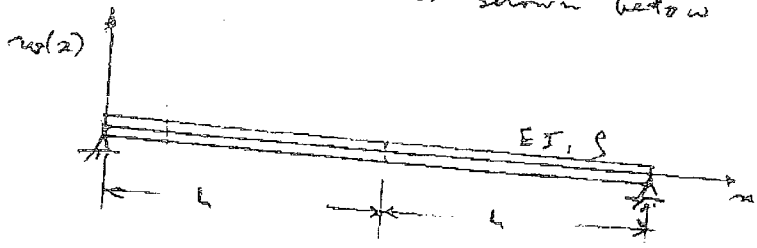

Divide it into two sections. Use Assumed Shape Method for each section, to obtain a model for vibration.

Assumed shapes/kinematics

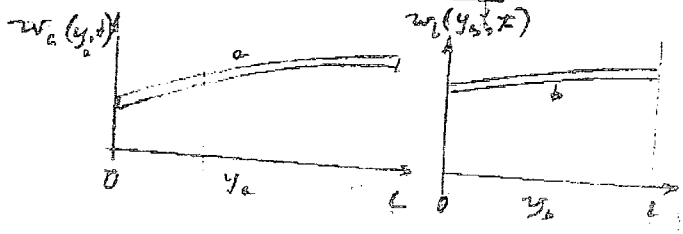

In the above figure
- each section, 'a' and 'b' are assigned a local coordinate axis. $[y_a, w_a(\cdot,t)]$ and $[y_b, w_b(\cdot,t)]$ respectively
- each section is shown schematically in displaced state

For section "a", assume a displacement of the form

$$w_a(y_a,t) = q_1(t) + \left(\frac{y_a}{L}\right) q_2(t) + \left(\frac{y_a}{L}\right)^2 q_3(t) \qquad (1a)$$

Convert to dimensionless variable ξ:

$$\boxed{w_a(\xi,t) = q_1 + \xi q_2 + \xi^2 q_3} \qquad (1b)$$

where ξ is a dummy variable

$$\xi = y_a/L \qquad (2)$$

Likewise, for section (b)

$$w_b(y_b,t) = q_4(t) + \left(\frac{y_b}{L}\right) q_5(t) + \left(\frac{y_b}{L}\right)^2 q_6(t) \qquad (3a)$$

Convert to dimensionless variable η

$$\boxed{w_b(\eta,t) = q_4 + \eta q_5 + \eta^2 q_6} \qquad (3b)$$

where

$$\eta = y_b/L \qquad (4)$$

The geometric boundary conditions follow

$$w_a(0,t) = 0 \qquad (5a)$$

$$w_b(L,t) = 0 \qquad (5b)$$

$$w_a(L,t) = w_b(0,t) \qquad (5c)$$

$$\frac{\partial w}{\partial y_a}(L,t) = \frac{\partial w}{\partial y_b}(0,t) \qquad (5d)$$

Convert to dimensionless variables

$$w_a(0,t) = 0 \qquad -(6a)$$

$$w_b(1,t) = 0 \qquad -(6b)$$

$$w_a(1,t) = w_b(0,t) \qquad -(6c)$$

$$\frac{\partial w_a(1,t)}{\partial \xi} = \frac{\partial w_b(0,t)}{\partial \eta} \qquad -(6d)$$

Substitute Eq (1b) into (6a) and reduce to

$$q_1 = 0 \qquad -(7a)$$

Substitute Eq (8b) into (6b):

$$q_4 + q_5 + q_6 = 0 \qquad -(7b)$$

Substitute Eqs (4b) and (5b) into Eq (6c):

$$q_1 + q_2 + q_3 = q_4 \qquad -(7c)$$

Substitute Eqs (8b) and (3b) into Eq (6d):

$$\left[0 + q_2 + 2\xi q_3\right]_{\xi=1} = \left[0 + q_5 + 2\eta q_6\right]_{\eta=0}$$

$$q_2 + 2q_3 = q_5 \qquad -(7d)$$

4

Equations (7a – d) are four algebraic relationships amongst the six variables (q_1 q_2 q_3 q_4 q_5 q_6).
Thus we can choose two of them as independent, and the remaining four will be dependent on them.

– Don't choose q_1 (=0) because it is not an active variable

– Instead choose q_5 and q_6 to be the independent variables.

We will work in matrix format, in order to present the technique in a format that can be easily extended to higher-order unequal-length and/or more-than-two elements. Reconfigure Equations (7) to put the independent variables on the right, and the active (non-zero) dependent ones on the left

$$q_1 = 0 \quad \text{– (non-active)} \quad \text{– (8a)}$$

$$q_4 = -q_5 - q_6 \quad \text{– (8b)}$$

$$q_1 + q_2 + q_3 - q_4 = 0 \quad \text{– (8c)}$$

$$q_2 + 2q_3 = q_5 \quad \text{– (8d)}$$

dependent — independent

5

Rearrange (8 b - d) into matrix format

$$\begin{bmatrix} 0 & 0 & 1 \\ 1 & 1 & -1 \\ 1 & 2 & 0 \end{bmatrix} \begin{bmatrix} q_2 \\ q_3 \\ q_4 \end{bmatrix} = \begin{bmatrix} -1 & -1 \\ 0 & 0 \\ 1 & 0 \end{bmatrix} \begin{bmatrix} q_5 \\ q_6 \end{bmatrix} \quad (9)$$

$[B]$ $\underline{b}$ $= [A]$ $\underline{a}$

$[B]\ \underline{b} = [A]\ \underline{a}$

$\underline{b} = [B]^{-1}[A]\ \underline{a}$

Solve the above using MATLAB.

```
EDU» cd a:
EDU» dumond

B =

     0     0     1
     1     1    -1
     1     2     0

A =

    -1    -1
     0     0
     1     0

invB =

     2     2    -1
    -1    -1     1
     1     0     0

inBstA =

    -3    -2
     2     1
    -1    -1

EDU»
```

```
% M-file for 2-piece beam (Dumond)
% dumond.m
B=[0 0 1;1 1 -1;1 2 0]
A=[-1 -1;0 0;1 0]
invB=inv(B)
inBstA=invB*A
```

6

Thus

$$\begin{bmatrix} q_2 \\ q_3 \\ q_4 \end{bmatrix} = \begin{bmatrix} -3 & -2 \\ 2 & 1 \\ -1 & -1 \end{bmatrix} \begin{bmatrix} q_5 \\ q_6 \end{bmatrix}$$

Use this to construct the following

$$\begin{bmatrix} q_1 \\ q_2 \\ q_3 \\ q_4 \\ q_5 \\ q_6 \end{bmatrix} = \begin{bmatrix} 0 & 0 \\ -3 & -2 \\ 2 & 1 \\ -1 & -1 \\ 1 & 0 \\ 0 & 1 \end{bmatrix} \begin{bmatrix} q_5 \\ q_6 \end{bmatrix} \qquad (10a)$$

$$\underline{Q} = \underline{\Pi}\ \underline{q} \qquad (10b)$$

$\underline{Q}$: all q's; $\underline{q}$: independent q's

Check on kinematics and JT

Before going further, let's verify that the above Eq (10b) and the shapes are error-free. To do this, work a trial case where

$q_5 = 1$ and $q_6 = 1$

Then, from Eq (10a)

$$\left.\begin{aligned} q_1 &= 0 \\ q_2 &= -3(1) - 2(1) = -5 \\ q_3 &= 2(1) + 1(1) = +3 \\ q_4 &= -1(1) - 1(1) = -2 \\ q_5 &= 1(1) + 0(1) = 1 \\ q_6 &= 0(1) + 1(1) = 1 \end{aligned}\right\}$$

Then from Eqs (11) and (3b)

$w_a(\xi,1) = 0 + \xi(-5) + \xi^2(+3$

$$w_a(\xi) = -5\xi + 3\xi^2 \qquad (\alpha)$$

$w_b(\eta,1) = -2 + \eta(1) + \eta^2(1)$

$$w_b(\eta) = -2 + \eta + \eta^2 \qquad (\beta)$$

Eqs. (α) and (β) are plotted with Excel in my TI-89 calculator. Check that they satisfy the B.C.s and also Eqs (6a to d).

Eq (6a): $w_a(0,t) = 0 + 0 = 0$ ✓

Eq (6b): $w_1(1,t) = -2 + 1 + 1 = 0$ ✓

Eq (6c): $w_a(1,t) = w_b(0,t)$?

$-5(1) + 3(1^2) = -2 + 0$

$-2 = -2$ ✓

Eq (6d): $\left.\frac{\partial w}{\partial \xi}\right|_{\xi=1} = \left.\frac{\partial w}{\partial \eta}\right|_{\eta=0}$?

$\left[-5 + 6\xi\right|_{\xi=1} = \left[0 + 1 + 2\eta\right|_{\eta=0}$ (?)

$1 = 1$ ✓

Then the B.C.s are satisfied.

Equations (10) seem ok.

9

EXCEL

Check on kinematics

$q_5 = 1$
$q_6 = 1$

id	wa	wb
0	0	-2
0.1	-0.47	-1.89
0.2	-0.88	-1.76
0.3	-1.23	-1.61
0.4	-1.52	-1.44
0.5	-1.75	-1.25
0.6	-1.92	-1.04
0.7	-2.03	-0.81
0.8	-2.08	-0.56
0.9	-2.07	-0.29
1	-2	0

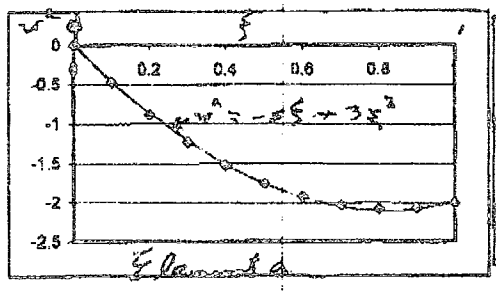

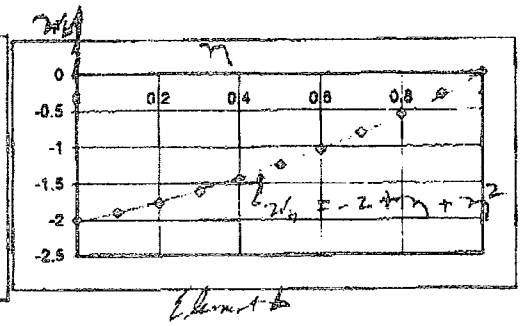

0 0 0 0.3333 0.2500 0.2000

Kinetic Energy

Work out for element a first. write Eq(16) as

$$w_a = q_1 + \xi q_2 + \xi^2 q_3$$

$$= \begin{bmatrix} 1 & \xi & \xi^2 \end{bmatrix} \begin{Bmatrix} q_1 \\ q_2 \\ q_3 \end{Bmatrix}$$

10

Thus

$$w_a = \underline{\psi}_a^T \underline{q}_a \qquad \text{— (11)}$$

where

$$\underline{\psi}_a = \begin{bmatrix} 1 \\ \xi \\ \xi^2 \end{bmatrix} \quad \text{and} \quad \underline{q}_a = \begin{bmatrix} q_1 \\ q_2 \\ q_3 \end{bmatrix} \qquad (12)$$

$$T_a = \frac{1}{2}\int_0^L \dot{w}_a^2 \rho \, dy_a = \frac{1}{2}\int_0^1 (\dot{\underline{q}}^T \underline{\psi})(\underline{\psi}^T \dot{\underline{q}}) \rho L \, d(1-\xi)$$

$$= \frac{1}{2}\dot{\underline{q}}_a^T \underbrace{\left[\rho L \int_0^1 \underline{\psi}_a \underline{\psi}_a^T d\xi\right]}_{m} \dot{\underline{q}}_a$$

Write as

$$T_a = \frac{1}{2}\dot{\underline{q}}_a^T m \dot{\underline{q}}_a \qquad (13)$$

---

where

$$m = \rho L \int_0^1 \underline{\psi}_a \underline{\psi}_a^T d\xi \qquad \text{—(14)}$$

Work out m:

$$m = \rho L \int_0^1 \begin{bmatrix} 1 \\ \xi \\ \xi^2 \end{bmatrix} \begin{bmatrix} 1 & \xi & \xi^2 \end{bmatrix} d\xi$$

11

$$Im = \rho L \int_0^1 \begin{bmatrix} 1 & \xi & \xi^2 \\ \xi & \xi^2 & \xi^3 \\ \xi^2 & \xi^3 & \xi^4 \end{bmatrix} d\xi$$

$$= \rho L \begin{bmatrix} \xi & \xi^2/2 & \xi^3/3 \\ \xi^2/2 & \xi^3/3 & \xi^4/4 \\ \xi^3/3 & \xi^4/4 & \xi^5/5 \end{bmatrix}$$

$$\boxed{Im = \rho L \begin{bmatrix} 1 & 1/2 & 1/3 \\ 1/2 & 1/3 & 1/4 \\ 1/3 & 1/4 & 1/5 \end{bmatrix}} \quad (15)$$

Likewise work out T_b for element 'b'

$$w_b = \begin{bmatrix} 1 & \eta & \eta^2 \end{bmatrix} \begin{bmatrix} q_4 \\ q_5 \\ q_6 \end{bmatrix} = \underline{\Psi}^T \underline{q}_b$$

$$w_b = \underline{\Psi}_b^T \underline{q}_b \quad (16)$$

Recognize that η is a dummy integration variable in the context of evaluating T and V, and thus ξ can be substituted for η

12

Change η to ξ for convenience.

$$y_b = L\eta \rightarrow L\xi$$

$$\bar{\Psi}_b = \begin{bmatrix} \eta \\ \eta^2 \end{bmatrix} \rightarrow \begin{bmatrix} \xi \\ \xi^2 \end{bmatrix} \qquad (17)$$

Then

$$T_b = \frac{1}{2}\int_0^L \dot{w}_b^2 \rho \, dy_b = \frac{1}{2}\int_0^L (\dot{q}_b^T \bar{\Psi}_b)(\bar{\Psi}_b^T \dot{q}_b)\, d(L\xi)$$

$$T_b = \frac{1}{2}\dot{\underline{q}}_b^T \underbrace{\left[\rho L \int_0^1 \bar{\Psi}_b \bar{\Psi}_b^T \, d\xi\right]}_{\text{IRM}} \dot{\underline{q}}_b$$

Since $\bar{\Psi}_b = \bar{\Psi}_a$, the center matrix is IRM (see Eqn (14)). Thus

$$T_b = \frac{1}{2}\dot{\underline{q}}_b^T \text{IRM}\, \dot{\underline{q}}_b \qquad (18)$$

The total kinetic energy, T, is

$$T = T_a + T_b = \frac{1}{2}\dot{\underline{q}}_a^T \text{IRM}\, \dot{\underline{q}}_a + \frac{1}{2}\dot{\underline{q}}_b^T \text{IRM}\, \dot{\underline{q}}_b$$

13

Write the above as

$$T = \frac{1}{2}\begin{bmatrix}\dot{\underline{q}}_a & \dot{\underline{q}}_b\end{bmatrix}^T \begin{bmatrix} m & 0 \\ 0 & m \end{bmatrix} \begin{bmatrix}\dot{\underline{q}}_a \\ \dot{\underline{q}}_b\end{bmatrix}$$

Define

$$\underline{Q} = \begin{bmatrix}\underline{q}_a \\ \underline{q}_b\end{bmatrix} = \begin{bmatrix} q_1 \\ q_2 \\ q_3 \\ q_4 \\ q_5 \\ q_6 \end{bmatrix} \quad \text{—— (19)}$$

$$\boxed{M_u = \begin{bmatrix} m & 0 \\ 0 & m \end{bmatrix} \text{ (symmetric)}} \quad \text{—— (20)}$$

where M_u is the mass matrix of the system with the q_i's unrestrained by boundary conditions. Thus

$$T = \frac{1}{2}\dot{\underline{Q}}^T M_u \dot{\underline{Q}} \quad \text{—— (21)}$$

Next impose the B.C.s on $\underline{Q}$. From

14

Eq (10b)

$$q = \Pi \underline{\xi}$$

↑ independent $q_i = \begin{bmatrix} q_5 \\ q_6 \end{bmatrix}$

Substitute the above into Eq (2).

$$T = \frac{1}{2} (\Pi \dot{\xi})^T M_u (\Pi \xi)$$

$$T = \frac{1}{2} \dot{\xi}^T \Pi^T M_u \Pi \xi$$

define

$$M = \Pi^T M_u \Pi \qquad (27)$$

$2\times 6 \quad 6\times 6 \quad 6\times 2$

where M is the mass matrix of the system with B.C.'s imposed.

- M is of order 2×2
- Also M_u is symmetric, and so is M.

Proof: $M^T = (\Pi^T M_u \Pi)^T = (M_u \Pi)^T \Pi$

then $= \Pi^T M_u^T \Pi = \Pi^T M_u \Pi$

$M^T = M$, because M_u is symmetric

15

Thus

$$T = \frac{1}{2}\dot{q}^T M \dot{q} \qquad (24)$$

Strain Energy

Element (a)

$$U_a = \frac{1}{2} EI \int_0^L \left[\frac{\partial^2 w_a}{\partial y_a^2}\right]^2 dy_a$$

$$U_a = \frac{1}{2} EI \int_0^1 \left[\frac{\partial^2 w_a}{\partial (L\xi)^2}\right]^2 d(L\xi)$$

$$U_a = \frac{1}{2} \frac{EI}{L^3} \int_0^1 \left(\frac{\partial^2 w}{\partial \xi^2}\right)^2 d\xi$$

Substitute in

$$w = \psi^T q_a$$

$$U_a = \frac{1}{2} \frac{EI}{L^3} \int_0^1 \left[q_a^T \frac{\partial^2 \psi}{\partial \xi^2}\right]\left[\frac{\partial^2 \psi^T}{\partial \xi^2} q_a\right] d\xi$$

$$U_a = \frac{1}{2} q_a^T \left[\frac{EI}{L^3} \int_0^1 \left(\frac{\partial^2 \psi}{\partial \xi^2} \frac{\partial^2 \psi^T}{\partial \xi^2}\right) d\xi\right] q_a$$

Define K_a as

16

$$k_R = \frac{EI}{L^3}\int_0^1 \psi_{ss}\,\psi_{ss}^T\,d\xi$$

then

$$U_a = \frac{1}{2}\,q_a^T\,k_R\,q_a \qquad \text{——— (25a)}$$

the strain energy of element b is the same as element a except $q_a \Rightarrow q_b$. Then

$$U_b = \frac{1}{2}\,q_b^T\,k_R\,q_b \qquad \text{——— (25b)}$$

work out k_R at this point

$$\psi = \begin{bmatrix} 1 \\ \xi \\ \xi^2 \end{bmatrix} \;;\; \psi_\xi = \begin{bmatrix} 0 \\ 1 \\ 2\xi \end{bmatrix} \;;$$

$$\psi_{\xi\xi} = \begin{bmatrix} 0 \\ 0 \\ 2 \end{bmatrix} \qquad \text{——— (26)}$$

$$k = \frac{EI}{L^3}\int_0^1 \begin{bmatrix} 0 \\ 0 \\ 2 \end{bmatrix}\begin{bmatrix} 0 & 0 & 2 \end{bmatrix} d\xi = \frac{EI}{L^3}\int_0^1 \begin{bmatrix} 0 & 0 & 0 \\ 0 & 0 & 0 \\ 0 & 0 & 4 \end{bmatrix} d\xi$$

$$= \frac{EI}{L^3}\begin{bmatrix} 0 & 0 & 0 \\ 0 & 0 & 0 \\ 0 & 0 & 4\xi \end{bmatrix}_0^1$$

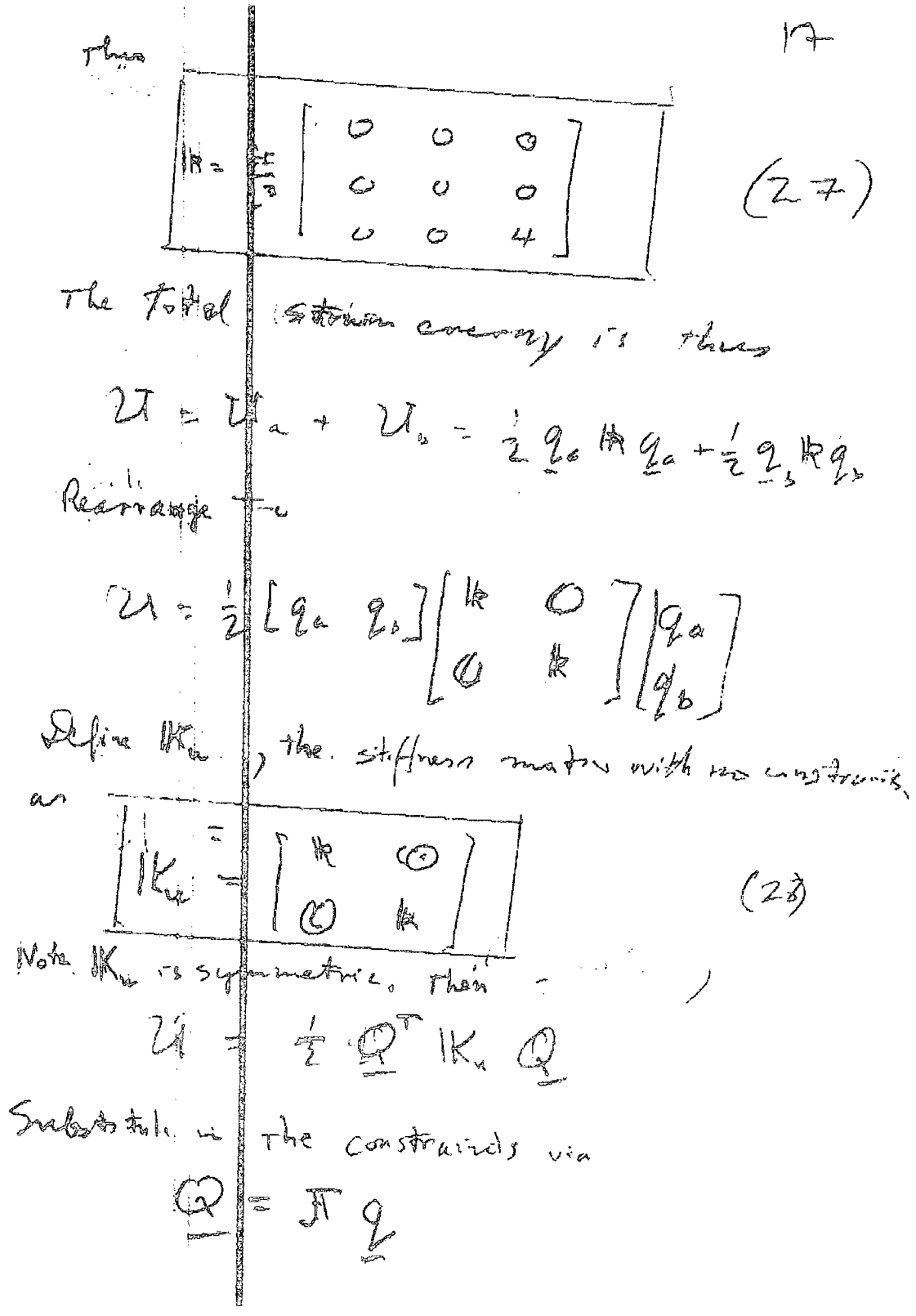
17
Thus
$[K] = \frac{EI}{L^3}\begin{bmatrix} 0 & 0 & 0 \\ 0 & 0 & 0 \\ 0 & 0 & 4 \end{bmatrix}$ (27)
The Total strain energy is thus
$U = U_a + U_b = \frac{1}{2} q_a^T k q_a + \frac{1}{2} q_b^T k q_b$
Rearrange to
$U = \frac{1}{2}\begin{bmatrix} q_a & q_b \end{bmatrix}\begin{bmatrix} k & 0 \\ 0 & k \end{bmatrix}\begin{bmatrix} q_a \\ q_b \end{bmatrix}$
Define $[K_u]$, the stiffness matrix with no constraints, as
$[K_u] = \begin{bmatrix} k & 0 \\ 0 & k \end{bmatrix}$ (28)
Note $[K_u]$ is symmetric, then
$U = \frac{1}{2} Q^T [K_u] Q$
Substitute in the constraints via
$Q = T q$

18

Get

$$U = \frac{1}{2} q^T (\Pi^T K_e \Pi) q$$

Define the stiffness matrix of the combined joined two elements as,

$$K = \Pi^T K_e \Pi \qquad (29)$$

As with the main matrix, K is order 2n and can be shown to be symmetric

Then

$$U = \frac{1}{2} q^T K q \qquad (30)$$

Model of the System via Lagrange Equations

Lagrange's equations, with the above simple quadratic forms for T and U. results in (See Mech 5808 Notes, chapter 8).

$$M \ddot{q} + K q = Q \qquad (31)$$

19

Natural Frequencies and Mode Shapes

As an example, solve the eigen problem of Eq (31) for a specific set of parameters, i.e.

$\rho = 1$

$L = 1$

$EI = 1$.

The eigen problem is then (Mech 5Tvo)

$$(K - \omega^2 M)\,\Phi = 0 \qquad \text{— (32)}$$

The MATLAB code and solution are given fully on a data page; the results are summarized and analyzed below

$$K = \begin{bmatrix} 16 & 8 \\ 8 & 8 \end{bmatrix} \qquad M = \begin{bmatrix} 1.1333 & 1.0667 \\ 1.0667 & 1.0667 \end{bmatrix}$$

1st Eigenvalue: From MATLAB

$\omega_1 = 2.73$ rad/s $\qquad \Phi_1 = \begin{bmatrix} q_{10} \\ q_{20} \end{bmatrix} = \begin{bmatrix} 0. \\ 1. \end{bmatrix}$

Calculate the other q_{ik}'s using Eq (10a).

$q_{10} = 0$

$q_{20} = -3(0) - 2(1) = -2$

$q_{30} = 2(0) - 1(1) = 1$

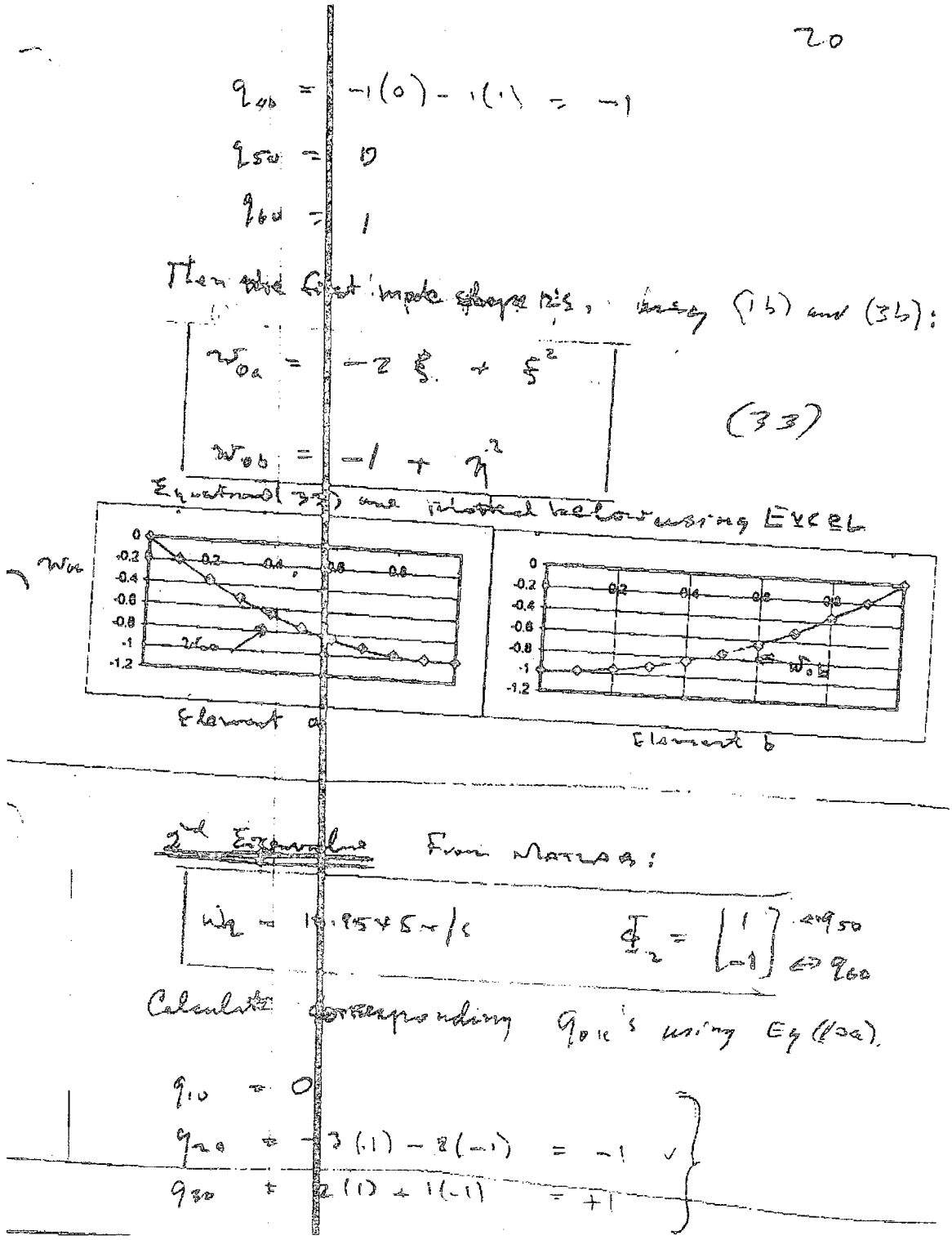
2.0
$q_{40} = -1(0) - 1(1) = -1$
$q_{50} = 0$
$q_{60} = 1$
Then the first two shape functions, using (1b) and (3b):
$w_{0a} = -2\xi + \xi^2$
$w_{0b} = -1 + \eta^2$
(33)
Equations (33) are plotted below using Excel
w_{0a}
w_{0b}
Element a
Element b
2nd Example From Maple:
$\omega_2 = 10.954 \text{ rad/s}$
$\Phi_2 = \begin{bmatrix} 1 \\ -1 \end{bmatrix} \Leftrightarrow q_{50} \Leftrightarrow q_{60}$
Calculate corresponding q_{10}'s using Eq (12a).
$q_{10} = 0$
$q_{20} = -3(1) - 2(-1) = -1$ ✓
$q_{30} = 2(1) + 1(-1) = +1$

21

$$q_{40} = -1(1) - 1(-1) = 0$$

$$q_{50} = 1$$

$$q_{60} = -1$$

Then the second mode shapes is, from Eq (33) and (34)

$$w_{0a} = -\xi + \xi^2$$

$$w_{0b} = +\eta - \eta^2 \qquad (34)$$

Eqs (34) are plotted below

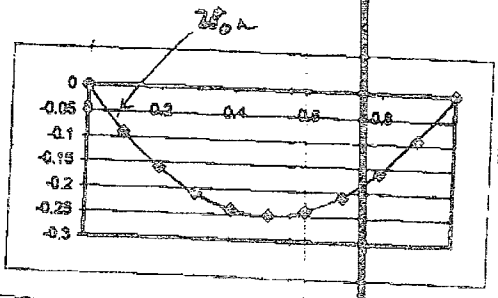

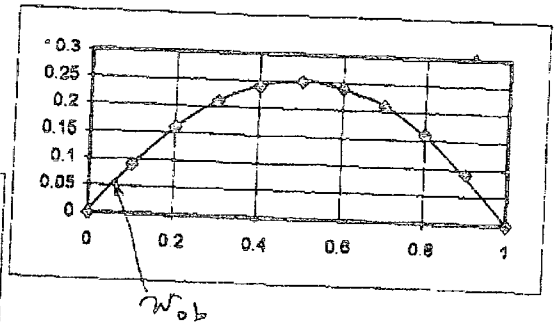

23

Comparison of frequencies by Exact (PDE) solution

Den Hartog gives the following exact formula:

$$\omega_1 = \pi^2 \sqrt{\frac{EI}{\rho l^3}} \qquad \omega_2 = 4\pi^2 \sqrt{\frac{EI}{\rho l^3}}$$

In our case $l = 2L$. Put into the above to get

$$\omega_1 = 2.4675 \sqrt{\frac{EI}{\rho L^4}}$$

$$\omega_2 = 9.87 \sqrt{\frac{EI}{\rho L^4}}$$

Comparison for $EI : \rho = L : 1$:

	Exact	Assumed Shape	% error
ω_1	2.4675	2.73886	+11%
ω_2	9.87	10.96	+11%

The above is typical for an assumed-shape that is essentially a second-order polynomial

24

Observations & Concluding Remarks

1. The above obviously works
2. It is straight forward to extend the method:
   - to shapes that have a higher order polynomial in ξ. ie to
     $w = q_1 + \xi^2 q_2 + \xi^3 q_3 + \xi^4 q_4 + \ldots$
   - from two elements to a higher number (3 or 4 seems practical)
3. For some applications of the assumed shape method, it isn't obvious from inspection what an orderly higher order polynomial sequence would be. E.g. the following:

The technique of this note can be used to determine a sequence (for the beam as a single element) to any degree of polynomial desired.

Appendix D

Maple Code for the Assumed Shape Method Plate Models

D.1 Maple Code for the Simply Supported Isotropic Rectangular Plate

Isotropic Rectangular Plate

$with(LinearAlgebra)$:

Assumed Shape

Direction 1 = x

$m_1 := 6$

Direction 2 = y

$m_2 := 6$

$$\phi_{n_1, n_2} := \sin\left(n_1 \cdot \pi \cdot \frac{x}{Lx}\right) \cdot \sin\left(n_2 \cdot \pi \cdot \frac{y}{Ly}\right)$$

$$w_o := \sum_{n_1=1}^{m_1} \sum_{n_2=1}^{m_2} \phi_{n_1, n_2} \cdot q_{n_1, n_2}(t)$$

$$w_d := \dot{w}_o$$

$$w_x := \frac{\partial}{\partial x} w_o$$

$$w_y := \frac{\partial}{\partial y} w_o$$

$$w_{xx} := \frac{\partial^2}{\partial x^2} w_o$$

$$w_{yy} := \frac{\partial^2}{\partial y^2} w_o$$

$$w_{xy} := \frac{\partial}{\partial x} \frac{\partial}{\partial y} w_o$$

Kinetic Energy

$$T := \frac{1}{2} \int_0^{Lx} \int_0^{Ly} w_d^2 \cdot \rho \, dy dx$$

Mass Matrix

$Q_d := Vector(1..m_1 \cdot m_2)$:

$k := 0$:;
for i **from** 1 **by** 1 **to** m_1 **do**
for j **from** 1 **by** 1 **to** m_2 **do**
$k := k + 1$;
$Q_d[k] := \dot{q}_{i,j}(t)$;
$T := subs(Q_d[k] = p_k, T)$;
end do;
end do;

$k := 0$:;
for i **from** 1 **by** 1 **to** m_1 **do**
for j **from** 1 **by** 1 **to** m_2 **do**
$k := k + 1$;
$g_k := \frac{\partial}{\partial p_k} T$;
end do;
end do;

$G := [seq(g_k, k = 1..m_1 \cdot m_2)]$
$P := [seq(p_k, k = 1..m_1 \cdot m_2)]$

$M, Z := GenerateMatrix(G, P)$

Potential Energy

$$V := \frac{1}{2} d \int_0^{Lx} \int_0^{Ly} \left(\left(w_{xx} + w_{yy} \right)^2 + 2(1 - \nu) \cdot \left(w_{xy}^2 - w_{xx} \cdot w_{yy} \right) \right) \mathrm{dydx}$$

Stiffness Matrix

$Q_o := Vector(1..m_1 \cdot m_2)$:

$k := 0$:;
for i **from** 1 **by** 1 **to** m_1 **do**
for j **from** 1 **by** 1 **to** m_2 **do**
$k := k + 1$;
$Q_o[k] := q_{i,j}(t)$;
$V := subs(Q_o[k] = p_k, V)$;
end do;
end do;

$k := 0$:;
for i **from** 1 **by** 1 **to** m_1 **do**
for j **from** 1 **by** 1 **to** m_2 **do**
$k := k + 1$;
$g_k := \frac{\partial}{\partial p_k} V$;
end do;
end do;

$G := [seq(g_k\ k = 1..m_1 \cdot m_2)]$
$P := [seq(p_k\ k = 1..m_1 \cdot m_2)]$

$K, Z := GenerateMatrix(G, P)$

Numerical Solutions

Properties

$Ly := 0.18$
$Lx := 0.24$
$h := 0.003$
$\mu := 403.2$
$\rho := \mu \cdot h$
$E := 10.89e9$

$$\nu := 0.372$$

$$d := \frac{E \cdot h^3}{12\left(1 - \nu^2\right)}$$

Natural Frequencies

$$M2 := evalf(M)$$
$$K2 := evalf(K)$$
$$\lambda, A := Eigenvectors(K2, M2) :$$
$$\lambda := \Re(\lambda)$$
$$A := \Re(A)$$
$$\omega := map(\mathrm{sqrt}, \lambda)$$

Plots

$$\Phi := Vector\left(1..m_1 \cdot m_2\right) :$$
$$U := Vector\left(1..m_1 \cdot m_2\right) :$$
$$w2 := Vector\left(1..m_1 \cdot m_2\right) :$$

for l **from** 1 **by** 1 **to** $m_1 \cdot m_2$ **do**
$k := 0;$
for n_1 **from** 1 **by** 1 **to** m_1 **do**
for n_2 **from** 1 **by** 1 **to** m_2 **do**
$k := k + 1;$
$$\Phi[k] := \sin\left(n_1 \cdot \pi \cdot \frac{x}{Lx}\right) \cdot \sin\left(n_2 \cdot \pi \cdot \frac{y}{Ly}\right);$$
$U[k] := A[k, l];$
end do;
end do;
$w2[l] := w1[l] = U^{+}.\Phi;$
end do:;

$with(plots) :$

```
for l from 1 by 1 to m1·m2 do
implicitplot3d(w2[l], x=0..Lx, y=0..Ly, w1[l]=-2..2, title
    =convert(Natural Frequency=ω[l], string), titlefont=[TIMES, 12], axes
    =boxed, orientation=[134, 45])
end do;
```

D.2 Maple Code for the Simply Supported Orthotropic Rectangular Plate

Orthotropic Rectangular Plate

$with(LinearAlgebra)$:

Assumed Shape

Direction 1 = x

$m_1 := 6$

Direction 2 = y

$m_2 := 6$

$$\phi_{n_1, n_2} := \sin\left(n_1 \cdot \pi \cdot \frac{x}{Lx}\right) \cdot \sin\left(n_2 \cdot \pi \cdot \frac{y}{Ly}\right)$$

$$w_o := \sum_{n_1=1}^{m_1} \sum_{n_2=1}^{m_2} \phi_{n_1, n_2} \cdot q_{n_1, n_2}(t)$$

$$w_d := \dot{w}_o$$

$$w_x := \frac{\partial}{\partial x} w_o$$

$$w_y := \frac{\partial}{\partial y} w_o$$

$$w_{xx} := \frac{\partial^2}{\partial x^2} w_o$$

$$w_{yy} := \frac{\partial^2}{\partial y^2} w_o$$

$$w_{xy} := \frac{\partial}{\partial x} \frac{\partial}{\partial y} w_o$$

Kinetic Energy

$$T := \frac{1}{2} \int_0^{Lx} \int_0^{Ly} w_d^2 \cdot \rho \, dy dx$$

Mass Matrix

$Q_d := Vector(1..m_1 \cdot m_2)$:

$k := 0$:;
for i **from** 1 **by** 1 **to** m_1 **do**
for j **from** 1 **by** 1 **to** m_2 **do**
$k := k + 1$;
$Q_d[k] := \dot{q}_{i,j}(t)$;
$T := subs(Q_d[k] = p_k, T)$;
end do;
end do;

$k := 0$:;
for i **from** 1 **by** 1 **to** m_1 **do**
for j **from** 1 **by** 1 **to** m_2 **do**
$k := k + 1$;
$g_k := \frac{\partial}{\partial p_k} T$;
end do;
end do;

$G := [seq(g_k, k = 1..m_1 \cdot m_2)]$
$P := [seq(p_k, k = 1..m_1 \cdot m_2)]$

$M, Z := GenerateMatrix(G, P)$

Potential Energy

$$V := \frac{1}{2}\int_0^{Lx}\int_0^{Ly} \left(dx \cdot w_{xx}^2 + dy \cdot w_{yy}^2 + 4 \cdot dxy \cdot w_{xy}^2 + 2 \cdot dl \cdot w_{xx} \cdot w_{yy}\right) dy dx$$

Stiffness Matrix

$Q_o := Vector(1..m_1 \cdot m_2)$:

$k := 0$:;
for i **from** 1 **by** 1 **to** m_1 **do**
for j **from** 1 **by** 1 **to** m_2 **do**
$k := k + 1$;
$Q_o[k] := q_{i,j}(t)$;
$V := subs(Q_o[k] = p_k, V)$;
end do;
end do;

$k := 0$:;
for i **from** 1 **by** 1 **to** m_1 **do**
for j **from** 1 **by** 1 **to** m_2 **do**
$k := k + 1$;
$g_k := \frac{\partial}{\partial p_k} V$;
end do;
end do;

$G := [seq(g_k, k = 1..m_1 \cdot m_2)]$
$P := [seq(p_k, k = 1..m_1 \cdot m_2)]$

$K, Z := GenerateMatrix(G, P)$

Numerical Solutions

Properties

$Ly := 0.18$
$Lx := 0.24$
$h := 0.003$
$\mu := 403.2$
$\rho := \mu \cdot h$
$Ey := 850e6$

$$Ex := \frac{Ey}{0.078}$$
$$Gxy := Ex \cdot 0.064$$
$$\nu xy := 0.372$$
$$\nu yx := \frac{\nu xy \cdot Ey}{Ex}$$
$$Sxx := \frac{Ex}{1 - \nu xy \cdot \nu yx}$$
$$Syy := \frac{Ey}{1 - \nu xy \cdot \nu yx}$$
$$Sxy := \frac{\nu yx \cdot Ex}{1 - \nu xy \cdot \nu yx}$$
$$dx := \frac{Sxx \cdot h^3}{12}$$
$$dy := \frac{Syy \cdot h^3}{12}$$
$$d1 := \frac{Sxy \cdot h^3}{12}$$
$$dxy := \frac{Gxy \cdot h^3}{12}$$

Natural Frequencies

$$M2 := evalf(M)$$
$$K2 := evalf(K)$$
$$\lambda, A := Eigenvectors(K2, M2) :$$
$$\lambda := \Re(\lambda)$$
$$A := \Re(A)$$
$$\omega := map(\mathrm{sqrt}, \lambda)$$

Plots

$$\Phi := Vector(1..m_1 \cdot m_2) :$$
$$U := Vector(1..m_1 \cdot m_2) :$$

$w2 := Vector(1..m_1 \cdot m_2)$:

for l **from** 1 **by** 1 **to** $m_1 \cdot m_2$ **do**
$k := 0$;
for n_1 **from** 1 **by** 1 **to** m_1 **do**
for n_2 **from** 1 **by** 1 **to** m_2 **do**
$k := k + 1$;
$\Phi[k] := \sin\left(n_1 \cdot \pi \cdot \frac{x}{Lx}\right) \cdot \sin\left(n_2 \cdot \pi \cdot \frac{y}{Ly}\right)$;
$U[k] := A[k, l]$;
end do;
end do;
$w2[l] := w1[l] = U^{+} . \Phi$;
end do:;

with(*plots*) :
for l **from** 1 **by** 1 **to** $m_1 \cdot m_2$ **do**
implicitplot3d($w2[l]$, $x = 0..Lx$, $y = 0..Ly$, $w1[l] = -2..2$, *title*
= *convert*(*Natural Frequency* = $\omega[l]$, *string*), *titlefont* = [*TIMES*, 12], *axes*
= *boxed*, *orientation* = [134, 45])
end do;

D.3 Maple Code for the Simply Supported Isotropic Modified Plate

Isotropic Modified Plate

$with(LinearAlgebra)$:

Assumed Shape

Direction 1 = x

$m_1 := 6$

Direction 2 = y

$m_2 := 6$

$$\phi_{n_1,n_2} := \sin\left(n_1 \cdot \pi \cdot \frac{x}{Lx}\right) \cdot \sin\left(n_2 \cdot \pi \cdot \frac{y}{Ly}\right)$$

$$w_o := \sum_{n_1=1}^{m_1} \sum_{n_2=1}^{m_2} \phi_{n_1,n_2} \cdot q_{n_1,n_2}(t)$$

$$w_d := \dot{w}_o$$

$$w_x := \frac{\partial}{\partial x} w_o$$

$$w_y := \frac{\partial}{\partial y} w_o$$

$$w_{xx} := \frac{\partial^2}{\partial x^2} w_o$$

$$w_{yy} := \frac{\partial^2}{\partial y^2} w_o$$

$$w_{xy} := \frac{\partial}{\partial x} \frac{\partial}{\partial y} w_o$$

Kinetic Energy

$$T := \frac{1}{2}\int_0^{x_1}\int_0^{Ly} w_d^2 \cdot \rho_p \, dy dx + \frac{1}{2}\int_{x_1}^{x_2}\int_0^{Ly} w_d^2 \cdot \rho_c \, dy dx + \frac{1}{2}\int_{x_2}^{Lx}\int_0^{Ly} w_d^2 \cdot \rho_p \, dy dx$$

Mass Matrix

$Q_d := Vector(1..m_1 \cdot m_2)$:

$k := 0$:;
for i **from** 1 **by** 1 **to** m_1 **do**
for j **from** 1 **by** 1 **to** m_2 **do**
$k := k + 1$;
$Q_d[k] := \dot{q}_{i,j}(t)$;
$T := subs(Q_d[k] = p_k, T)$;
end do;
end do;

$k := 0$:;
for i **from** 1 **by** 1 **to** m_1 **do**
for j **from** 1 **by** 1 **to** m_2 **do**
$k := k + 1$;
$g_k := \frac{\partial}{\partial p_k} T$;
end do;
end do;

$G := [seq(g_k, k = 1..m_1 \cdot m_2)]$
$P := [seq(p_k, k = 1..m_1 \cdot m_2)]$

$M, Z := GenerateMatrix(G, P)$

Potential Energy

$$V := \frac{1}{2} d_p \int_0^x \int_0^{Ly} \left(\left(w_{xx} + w_{yy} \right)^2 + 2(1 - \nu) \cdot \left(w_{xy}^2 - w_{xx} \cdot w_{yy} \right) \right) dy dx$$

$$+\frac{1}{2}d_c\int_{x_1}^{x_2}\int_{0}^{Ly}\left(\left(w_{xx}+w_{yy}\right)^2+2\left(1-\nu\right)\cdot\left(w_{xy}^2-w_{xx}\cdot w_{yy}\right)\right)\,dydx$$

$$+\frac{1}{2}d_p\int_{x_2}^{Lx}\int_{0}^{Ly}\left(\left(w_{xx}+w_{yy}\right)^2+2\left(1-\nu\right)\cdot\left(w_{xy}^2-w_{xx}\cdot w_{yy}\right)\right)\,dydx$$

Stiffness Matrix

$Q_o := Vector\left(1..m_1\cdot m_2\right):$

$k := 0:;$
for i **from** 1 **by** 1 **to** m_1 **do**
for j **from** 1 **by** 1 **to** m_2 **do**
$k := k+1;$
$Q_o[k] := q_{i,j}(t);$
$V := subs\left(Q_o[k]=p_k, V\right);$
end do;
end do;

$k := 0:;$
for i **from** 1 **by** 1 **to** m_1 **do**
for j **from** 1 **by** 1 **to** m_2 **do**
$k := k+1;$
$g_k := \frac{\partial}{\partial p_k}V;$
end do;
end do;

$G := \left[seq\left(g_k, k=1..m_1\cdot m_2\right)\right]$
$P := \left[seq\left(p_k, k=1..m_1\cdot m_2\right)\right]$

$K, Z := GenerateMatrix(G, P)$

Numerical Solutions

Properties

$$Ly := 0.18$$
$$Lx := 0.24$$
$$Lb := 0.012$$
$$x_1 := \frac{Lx}{2} - \frac{Lb}{2}$$
$$x_2 := x_1 + Lb$$
$$h_b := 0.012$$
$$h_p := 0.003$$
$$h_c := h_b + h_p$$
$$\mu := 403.2$$
$$\rho_p := \mu \cdot h_p$$
$$\rho_c := \mu \cdot h_c$$
$$E := 10.89e9$$
$$\nu := 0.372$$
$$d_p := \frac{E \cdot h_p^3}{12\left(1 - \nu^2\right)}$$
$$d_c := \frac{E \cdot h_c^3}{12\left(1 - \nu^2\right)}$$

Natural Frequencies

$$M2 := evalf(M)$$
$$K2 := evalf(K)$$
$$\lambda, A := Eigenvectors(K2, M2) :$$
$$\lambda := \Re(\lambda)$$
$$A := \Re(A)$$
$$\omega := map(\mathrm{sqrt}, \lambda)$$

Plots

$\Phi := Vector(1..m_1 \cdot m_2)$:
$U := Vector(1..m_1 \cdot m_2)$:
$w2 := Vector(1..m_1 \cdot m_2)$:

for l **from** 1 **by** 1 **to** $m_1 \cdot m_2$ **do**
$k := 0$;
for n_1 **from** 1 **by** 1 **to** m_1 **do**
for n_2 **from** 1 **by** 1 **to** m_2 **do**
$k := k + 1$;
$\Phi[k] := \sin\left(n_1 \cdot \pi \cdot \frac{x}{Lx}\right) \cdot \sin\left(n_2 \cdot \pi \cdot \frac{y}{Ly}\right)$;
$U[k] := A[k, l]$;
end do;
end do;
$w2[l] := w1[l] = U^{+} . \Phi$;
end do:;

$with(plots)$:
for l **from** 1 **by** 1 **to** $m_1 \cdot m_2$ **do**
$implicitplot3d(w2[l], x = 0..Lx, y = 0..Ly, w1[l] = -2..2, title = convert(Natural\ Frequency = \omega[l], string), titlefont = [TIMES, 12], axes = boxed, orientation = [134, 45])$
end do;

D.4 Maple Code for the Simply Supported Orthotropic Modified Plate

Orthotropic Modified Plate

$with(LinearAlgebra)$:

Assumed Shape

Direction 1 = x

$m_1 := 6$

Direction 2 = y

$m_2 := 6$

$$\phi_{n_1, n_2} := \sin\left(n_1 \cdot \pi \cdot \frac{x}{Lx}\right) \cdot \sin\left(n_2 \cdot \pi \cdot \frac{y}{Ly}\right)$$

$$w_o := \sum_{n_1=1}^{m_1} \sum_{n_2=1}^{m_2} \phi_{n_1, n_2} \cdot q_{n_1, n_2}(t)$$

$$w_d := \dot{w}_o$$

$$w_x := \frac{\partial}{\partial x} w_o$$

$$w_y := \frac{\partial}{\partial y} w_o$$

$$w_{xx} := \frac{\partial^2}{\partial x^2} w_o$$

$$w_{yy} := \frac{\partial^2}{\partial y^2} w_o$$

$$w_{xy} := \frac{\partial}{\partial x} \frac{\partial}{\partial y} w_o$$

Kinetic Energy

$$T := \frac{1}{2} \int_0^{x_1} \int_0^{Ly} w_d^2 \cdot \rho_p \, dy dx + \frac{1}{2} \int_{x_1}^{x_2} \int_0^{Ly} w_d^2 \cdot \rho_c \, dy dx + \frac{1}{2} \int_{x_2}^{Lx} \int_0^{Ly} w_d^2 \cdot \rho_p \, dy dx$$

Mass Matrix

$Q_d := Vector(1..m_1 \cdot m_2)$:

$k := 0$:;
for i **from** 1 **by** 1 **to** m_1 **do**
for j **from** 1 **by** 1 **to** m_2 **do**
$k := k + 1$;
$Q_d[k] := \dot{q}_{i,j}(t)$;
$T := subs(Q_d[k] = p_k, T)$;
end do;
end do;

$k := 0$:;
for i **from** 1 **by** 1 **to** m_1 **do**
for j **from** 1 **by** 1 **to** m_2 **do**
$k := k + 1$;
$g_k := \frac{\partial}{\partial p_k} T$;
end do;
end do;

$G := [seq(g_k, k = 1..m_1 \cdot m_2)]$
$P := [seq(p_k, k = 1..m_1 \cdot m_2)]$

$M, Z := GenerateMatrix(G, P)$

Potential Energy

$$V := \frac{1}{2}\int_0^{x_1}\int_0^{Ly} \left(dxp \cdot w_{xx}^2 + dyp \cdot w_{yy}^2 + 4 \cdot dxyp \cdot w_{xy}^2 + 2 \cdot d1p \cdot w_{xx} \cdot w_{yy}\right) \mathrm{dydx}$$

$$+\frac{1}{2}\int_{x_1}^{x_2}\int_{0}^{Ly}\left(dxc\cdot w_{xx}^2+dyc\cdot w_{yy}^2+4\cdot dxyc\cdot w_{xy}^2+2\cdot d1c\cdot w_{xx}\cdot w_{yy}\right)\,\mathrm{dydx}$$

$$+\frac{1}{2}\int_{x_2}^{Lx}\int_{0}^{Ly}\left(dxp\cdot w_{xx}^2+dyp\cdot w_{yy}^2+4\cdot dxyp\cdot w_{xy}^2+2\cdot d1p\cdot w_{xx}\cdot w_{yy}\right)\,\mathrm{dydx}$$

Stiffness Matrix

$Q_o := Vector(1..m_1\cdot m_2)$:

$k := 0$:;
for i **from** 1 **by** 1 **to** m_1 **do**
for j **from** 1 **by** 1 **to** m_2 **do**
$k := k+1$;
$Q_o[k] := q_{i,j}(t)$;
$V := subs(Q_o[k] = p_k, V)$;
end do;
end do;

$k := 0$:;
for i **from** 1 **by** 1 **to** m_1 **do**
for j **from** 1 **by** 1 **to** m_2 **do**
$k := k+1$;
$g_k := \frac{\partial}{\partial p_k} V$;
end do;
end do;

$G := [seq(g_k, k = 1..m_1\cdot m_2)]$
$P := [seq(p_k, k = 1..m_1\cdot m_2)]$

$K, Z := GenerateMatrix(G, P)$

Numerical Solutions

Properties

$$Ly := 0.18$$
$$Lx := 0.24$$
$$Lb := 0.012$$
$$x_1 := \frac{Lx}{2} - \frac{Lb}{2}$$
$$x_2 := x_1 + Lb$$
$$h_b := 0.012$$
$$h_p := 0.003$$
$$h_c := h_b + h_p$$
$$\mu := 403.2$$
$$\rho_p := \mu \cdot h_p$$
$$\rho_c := \mu \cdot h_c$$
$$Eyp := 850e6$$
$$Exp := \frac{Eyp}{0.078}$$
$$Gxyp := Exp \cdot 0.064$$
$$\nu xyp := 0.372$$
$$\nu yxp := \frac{\nu xyp \cdot Eyp}{Exp}$$
$$Sxxp := \frac{Exp}{1 - \nu xyp \cdot \nu yxp}$$
$$Syyp := \frac{Eyp}{1 - \nu xyp \cdot \nu yxp}$$
$$Sxyp := \frac{\nu yxp \cdot Exp}{1 - \nu xyp \cdot \nu yxp}$$
$$dxp := \frac{Sxxp \cdot h_p^3}{12}$$
$$dyp := \frac{Syyp \cdot h_p^3}{12}$$
$$d1p := \frac{Sxyp \cdot h_p^3}{12}$$

$$dxyp := \frac{Gxyp \cdot h_p^3}{12}$$

$$Eyc := Exp$$

$$Exc := Eyp$$

$$Gyxc := Gxyp$$

$$\nu yxc := \nu xyp$$

$$\nu xyc := \frac{\nu yxc \cdot Exc}{Eyc}$$

$$Syyc := \frac{Eyc}{1 - \nu xyc \cdot \nu yxc}$$

$$Sxxc := \frac{Exc}{1 - \nu xyc \cdot \nu yxc}$$

$$Sxyc := \frac{\nu yxc \cdot Exc}{1 - \nu xyc \cdot \nu yxc}$$

$$dyc := \frac{Syyc \cdot h_c^3}{12}$$

$$dxc := \frac{Sxxc \cdot h_c^3}{12}$$

$$d1c := \frac{Sxyc \cdot h_c^3}{12}$$

$$dxyc := \frac{Gyxc \cdot h_c^3}{12}$$

Natural Frequencies

$$M2 := evalf(M)$$

$$K2 := evalf(K)$$

$$\lambda, A := Eigenvectors(K2, M2) :$$

$$\lambda := \Re(\lambda)$$

$$A := \Re(A)$$

$$\omega := map(\mathrm{sqrt}, \lambda)$$

Plots

$\Phi := Vector(1..m_1 \cdot m_2)$:
$U := Vector(1..m_1 \cdot m_2)$:
$w2 := Vector(1..m_1 \cdot m_2)$:

for l **from** 1 **by** 1 **to** $m_1 \cdot m_2$ **do**
$k := 0$;
for n_1 **from** 1 **by** 1 **to** m_1 **do**
for n_2 **from** 1 **by** 1 **to** m_2 **do**
$k := k + 1$;
$\Phi[k] := \sin\left(n_1 \cdot \pi \cdot \frac{x}{Lx}\right) \cdot \sin\left(n_2 \cdot \pi \cdot \frac{y}{Ly}\right)$;
$U[k] := A[k, l]$;
end do;
end do;
$w2[l] := w1[l] = U^{+} . \Phi$;
end do:;

$with(plots)$:
for l **from** 1 **by** 1 **to** $m_1 \cdot m_2$ **do**
$implicitplot3d(w2[l], x = 0..Lx, y = 0..Ly, w1[l] = -2..2, title$
$= convert(Natural\ Frequency = \omega[l], string), titlefont = [TIMES, 12], axes$
$= boxed, orientation = [134, 45])$
end do;

Appendix E

Maple Code for the Assumed Shape Method Scalloped Brace Plate Model

Scalloped Brace Plate

$with(LinearAlgebra)$:

Assumed Shape

Direction 1 = x

$m_1 := 2$

Direction 2 = y

$m_2 := 2$

$$\phi_{n_1, n_2} := \sin\left(n_1 \cdot \pi \cdot \frac{x}{Lx}\right) \cdot \sin\left(n_2 \cdot \pi \cdot \frac{y}{Ly}\right)$$

$$w_o := \sum_{n_1=1}^{m_1} \sum_{n_2=1}^{m_2} \phi_{n_1, n_2} \cdot q_{n_1, n_2}(t)$$

$$w_d := \dot{w}_o$$

$$w_x := \frac{\partial}{\partial x} w_o$$

$$w_y := \frac{\partial}{\partial y} w_o$$

$$w_{xx} := \frac{\partial^2}{\partial x^2} w_o$$

$$w_{yy} := \frac{\partial^2}{\partial y^2} w_o$$

$$w_{xy} := \frac{\partial}{\partial x} \frac{\partial}{\partial y} w_o$$

Scalloped Brace

$$y1 := \frac{Ly}{4}$$

$$y2 := \frac{3 \cdot Ly}{4}$$

$$h_{y1} := y^2 + h_b + h_p$$

$$h_{y2} := \left(y - \frac{Ly}{2}\right)^2 + h_b + h_p$$

$$h_{y3} := (y - Ly)^2 + h_b + h_p$$

$$\rho_{y1} := \mu \cdot h_{y1}$$

$$\rho_{y2} := \mu \cdot h_{y2}$$

$$\rho_{y3} := \mu \cdot h_{y3}$$

$$d_{y1} := \frac{E \cdot h_{y1}^3}{12\left(1 - \nu^2\right)}$$

$$d_{y2} := \frac{E \cdot h_{y2}^3}{12\left(1 - \nu^2\right)}$$

$$d_{y3} := \frac{E \cdot h_{y3}^3}{12\left(1 - \nu^2\right)}$$

Kinetic Energy

$$T := \frac{1}{2}\int_0^{x_1}\int_0^{Ly} w_d^2 \cdot \rho_p \, dydx + \frac{1}{2}\int_{x_1}^{x_2}\int_0^{y1} w_d^2 \cdot \rho_{y1} \, dydx$$

$$+ \frac{1}{2}\int_{x_1}^{x_2}\int_{y1}^{y2} w_d^2 \cdot \rho_{y2} \, dydx + \frac{1}{2}\int_{x_1}^{x_2}\int_{y2}^{Ly} w_d^2 \cdot \rho_{y3} \, dydx$$

$$+ \frac{1}{2}\int_{x_2}^{Lx}\int_0^{Ly} w_d^2 \cdot \rho_p \, dydx$$

Mass Matrix

$$Q_d := Vector\left(1..m_1 \cdot m_2\right) :$$

```
k := 0 :;
for i from 1 by 1 to m1 do
for j from 1 by 1 to m2 do
k := k + 1;
Qd[k] := q̇i,j(t);
T := subs(Qd[k] = pk, T);
end do;
end do;

k := 0 :;
for i from 1 by 1 to m1 do
for j from 1 by 1 to m2 do
k := k + 1;
gk := ∂/∂pk T;
end do;
end do;

G := [seq(gk, k = 1 .. m1 · m2)]
P := [seq(pk, k = 1 .. m1 · m2)]


M, Z := GenerateMatrix(G, P)
```

Potential Energy

$$V := \frac{1}{2} d_p \int_0^{x_1} \int_0^{Ly} \left(\left(w_{xx} + w_{yy} \right)^2 + 2(1-\nu) \cdot \left(w_{xy}^2 - w_{xx} \cdot w_{yy} \right) \right) \mathrm{d}y\mathrm{d}x$$

$$+ \frac{1}{2} \int_{x_1}^{x_2} \int_0^{y1} d_{y1} \cdot \left(\left(w_{xx} + w_{yy} \right)^2 + 2(1-\nu) \cdot \left(w_{xy}^2 - w_{xx} \cdot w_{yy} \right) \right) \mathrm{d}y\mathrm{d}x$$

$$+ \frac{1}{2} \int_{x_1}^{x_2} \int_{y1}^{y2} d_{y2} \cdot \left(\left(w_{xx} + w_{yy} \right)^2 + 2(1-\nu) \cdot \left(w_{xy}^2 - w_{xx} \cdot w_{yy} \right) \right) \mathrm{d}y\mathrm{d}x$$

$$+\frac{1}{2}\int_{x_1}^{x_2}\int_{y2}^{Ly} d_{y3}\cdot\left(\left(w_{xx}+w_{yy}\right)^2+2(1-\nu)\cdot\left(w_{xy}^2-w_{xx}\cdot w_{yy}\right)\right)\,dydx$$

$$+\frac{1}{2}d_p\int_{x_2}^{Lx}\int_{0}^{Ly}\left(\left(w_{xx}+w_{yy}\right)^2+2(1-\nu)\cdot\left(w_{xy}^2-w_{xx}\cdot w_{yy}\right)\right)\,dydx$$

Stiffness Matrix

$Q_o := Vector(1..m_1\cdot m_2)$:

$k := 0$:;
for i **from** 1 **by** 1 **to** m_1 **do**
for j **from** 1 **by** 1 **to** m_2 **do**
$k := k+1$;
$Q_o[k] := q_{i,j}(t)$;
$V := subs(Q_o[k]=p_k, V)$;
end do;
end do;

$k := 0$:;
for i **from** 1 **by** 1 **to** m_1 **do**
for j **from** 1 **by** 1 **to** m_2 **do**
$k := k+1$;
$g_k := \frac{\partial}{\partial p_k} V$;
end do;
end do;

$G := [seq(g_k\ k=1..m_1\cdot m_2)]$
$P := [seq(p_k\ k=1..m_1\cdot m_2)]$

$K, Z := GenerateMatrix(G, P)$

Numerical Solutions

Properties

$$Ly := 0.18$$
$$Lx := 0.24$$
$$Lb := 0.012$$
$$x_1 := \frac{Lx}{2} - \frac{Lb}{2}$$
$$x_2 := x_1 + Lb$$
$$h_p := 0.003$$
$$h_b := 0.012$$
$$\mu := 403.2$$
$$E := 10.89e9$$
$$\nu := 0.372$$
$$\rho_p := \mu \cdot h_p$$
$$d_p := \frac{E \cdot h_p^3}{12\left(1 - \nu^2\right)}$$

Natural Frequencies

$$M2 := evalf(M)$$
$$K2 := evalf(K)$$
$$\lambda, A := Eigenvectors(K2, M2) :$$
$$\lambda := \Re(\lambda)$$
$$A := \Re(A)$$
$$\omega := map(\mathrm{sqrt}, \lambda)$$

Plots

$$\Phi := Vector\left(1..m_1 \cdot m_2\right) :$$

$U := Vector(1..m_1 \cdot m_2)$:
$w2 := Vector(1..m_1 \cdot m_2)$:

for l **from** 1 **by** 1 **to** $m_1 \cdot m_2$ **do**
$k := 0$;
for n_1 **from** 1 **by** 1 **to** m_1 **do**
for n_2 **from** 1 **by** 1 **to** m_2 **do**
$k := k + 1$;
$\Phi[k] := \sin\left(n_1 \cdot \pi \cdot \frac{x}{Lx}\right) \cdot \sin\left(n_2 \cdot \pi \cdot \frac{y}{Ly}\right)$;
$U[k] := A[k, l]$;
end do;
end do;
$w2[l] := w1[l] = U^{+} . \Phi$;
end do:;

$with(plots)$:
for l **from** 1 **by** 1 **to** $m_1 \cdot m_2$ **do**
$implicitplot3d(w2[l], x = 0..Lx, y = 0..Ly, w1[l] = -2..2, title$
$= convert(Natural\ Frequency = \omega[l], string), titlefont = [TIMES, 12], axes$
$= boxed, orientation = [134, 45])$
end do;

Appendix F

ANSYS Code for the Finite Element Method Plate Models

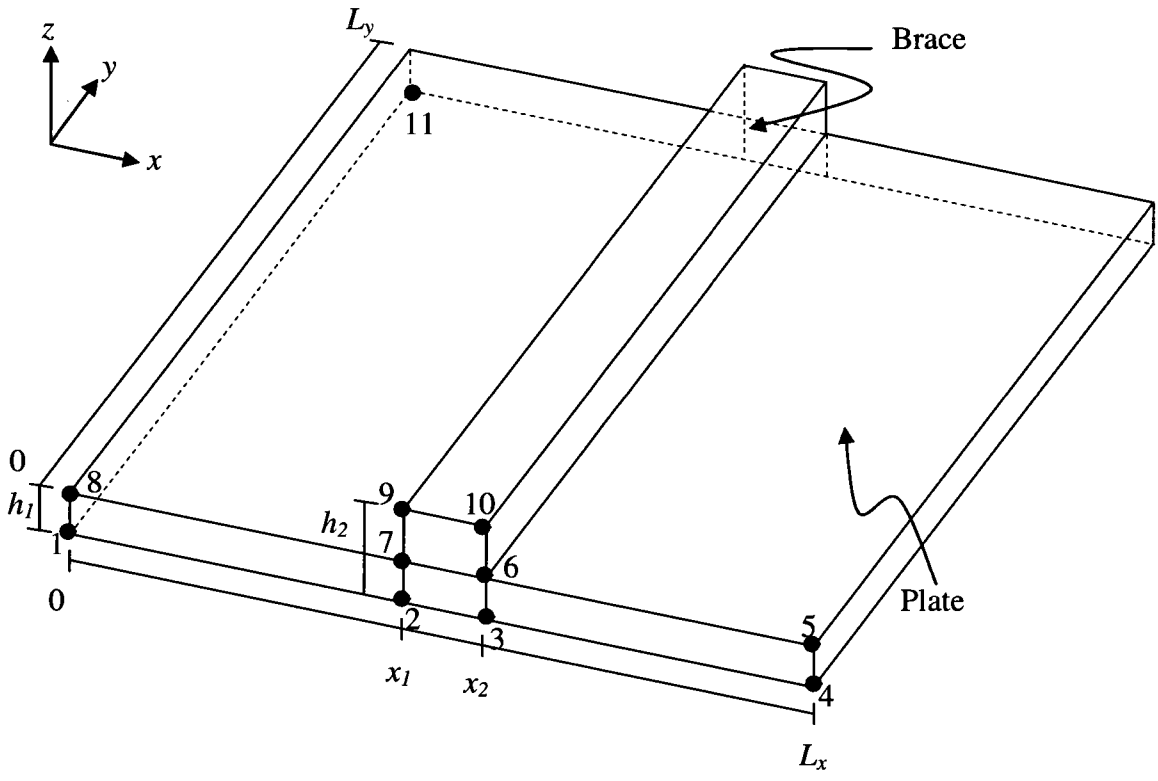

Figure F.1: Location of keypoints on the modified plate model

F.1 Prep7 Input File for the Simply Supported Isotropic Modified Plate

```
/prep7

!Variables
lx=0.24
ly=0.18
h1=0.003
offset=h1/2
h2=h1+0.012
x1=lx/2-0.012/2
x2=lx/2+0.012/2
e1=850e6
e2=e1/0.078
divs=8
divm=20
divb=40

!Keypoints
k,1,0,0,-offset
k,2,x1,0,-offset
k,3,x2,0,-offset
k,4,lx,0,-offset
k,5,lx,0,h1-offset
k,6,x2,0,h1-offset
k,7,x1,0,h1-offset
k,8,0,0,h1-offset
k,9,x1,0,h2-offset
k,10,x2,0,h2-offset
k,11,0,ly,-offset

!Lines
lstr,1,2
lstr,2,3
lstr,3,4
lstr,4,5
lstr,5,6
lstr,6,7
lstr,7,8
lstr,8,1
lstr,2,7
lstr,3,6
lstr,7,9
lstr,9,10
lstr,10,6
lstr,1,11

!Areas
al,8,1,9,7
al,9,2,10,6
al,10,3,4,5
al,11,6,13,12

!Number of elements
lesize,1,,,divm
lesize,3,,,divm
lesize,5,,,divm
lesize,7,,,divm
lesize,8,,,divs
lesize,9,,,divs
lesize,10,,,divs
lesize,4,,,divs
lesize,2,,,divs
lesize,6,,,divs
lesize,12,,,divs
lesize,11,,,divs
lesize,13,,,divs

lesize,14,,,divb

!Element type and mesh
et,1,shell181
mshape,0,2D
amesh,1,4,1
et,2,solid45

!Material Properties
mp,ex,1,e2
mp,prxy,1,0.372
mp,dens,1,403.2
mat,1
!Make 3D
```

```
vdrag,1,2,3,4,,,,14

!Select nodes for boundary conditions
aclear,1,4,1

asel,s,area,,1
asel,a,area,,2
asel,a,area,,3
asel,a,area,,5
asel,a,area,,9
asel,a,area,,13
asel,a,area,,15
asel,a,area,,17
nsla,s,1
nsel,r,loc,z,-0.0001,0.0001

!Boundary conditions
d,all,ux,0
d,all,uy,0
d,all,uz,0
allsel

/PNUM,area,1

!Modal solution
finish
/solu
antype,modal
modopt,lanb,6,0,3000

solve
```

F.2 Prep7 Input File for the Simply Supported Orthotropic Modified Plate

```
/prep7

!Variables
lx=0.24
ly=0.18
h1=0.003
offset=h1/2
h2=h1+0.012
x1=lx/2-0.012/2
x2=lx/2+0.012/2
e1=850e6
e2=e1/0.078
divs=8
divm=20
divb=40

!Keypoints
k,1,0,0,-offset
k,2,x1,0,-offset
k,3,x2,0,-offset
k,4,lx,0,-offset
k,5,lx,0,h1-offset
k,6,x2,0,h1-offset
k,7,x1,0,h1-offset
k,8,0,0,h1-offset
k,9,x1,0,h2-offset
k,10,x2,0,h2-offset
k,11,0,ly,-offset

!Lines
lstr,1,2
lstr,2,3
lstr,3,4
lstr,4,5
lstr,5,6
lstr,6,7
lstr,7,8
lstr,8,1
lstr,2,7
lstr,3,6
lstr,7,9
lstr,9,10
lstr,10,6
lstr,1,11

!Areas
```

```
al,8,1,9,7
al,9,2,10,6
al,10,3,4,5
al,11,6,13,12

!Number of elements
lesize,1,,,divm
lesize,3,,,divm
lesize,5,,,divm
lesize,7,,,divm
lesize,8,,,divs
lesize,9,,,divs
lesize,10,,,divs
lesize,4,,,divs
lesize,2,,,divs
lesize,6,,,divs
lesize,12,,,divs
lesize,11,,,divs
lesize,13,,,divs

lesize,14,,,divb

!Element type and mesh
et,1,shell181
mshape,0,2D
amesh,1,4,1
et,2,solid45

!Material Properties of the plate
mp,ex,1,e2
mp,ey,1,e1
mp,ez,1,e2*0.043
mp,gxy,1,e2*0.064
mp,gyz,1,e2*0.003
mp,gxz,1,e2*0.061
mp,prxy,1,0.372
mp,pryz,1,0.435
mp,prxz,1,0.467
mp,dens,1,403.2
mat,1
!Make plate 3D
vdrag,1,2,3,,,,14

!Material Properties of the brace
mp,ex,2,e1
mp,ey,2,e2
mp,ez,2,e2*0.043
mp,gxy,2,e2*0.064
mp,gyz,2,e2*0.061
mp,gxz,2,e2*0.003
mp,prxy,2,0.040
mp,pryz,2,0.467
mp,prxz,2,0.435
mp,dens,2,403.2
mat,2
!Make brace 3D
vdrag,4,,,,,,14

!Coincide node between the plate and
brace
nummrg,node

!Select nodes for boundary conditions
aclear,1,4,1

asel,s,area,,1
asel,a,area,,2
asel,a,area,,3
asel,a,area,,5
asel,a,area,,9
asel,a,area,,13
asel,a,area,,15
asel,a,area,,17
nsla,s,1
nsel,r,loc,z,-0.0001,0.0001
!Boundary conditions
d,all,ux,0
d,all,uy,0
d,all,uz,0
allsel

/PNUM,area,1

!Modal solution
finish
/solu
antype,modal
modopt,lanb,6,0,2000

solve
```

References

[1] N. H. Fletcher and T. D. Rossing, *The Physics of Musical Instruments*, 2nd ed. New York: Springer, 1999.

[2] W. R. Cumpiano and J. D. Natelson, *Guitarmaking, Tradition and Technology: A Complete Reference for the Design & Construction of the Steel-String Folk Guitar & the Classical Guitar.* San Francisco: Chronicle Books, 1993.

[3] R. H. Siminoff, *The Luthier's Handbook: A Guide to Building Great Tone in Acoustic Stringed Instruments.* Milwaukee, Wisconsin: Hal Leonard, 2002.

[4] M. J. Elejabarrieta, C. Santamaría, and A. Ezcurra, "Air Cavity Modes in the Resonance Box of the Guitar: the Effect of the Sound Hole," *Journal of Sound and Vibration,* vol. 252, pp. 584-590, May 2002.

[5] R. H. Siminoff, *The Art of Tap Tuning: How to Build Great Sound into Instruments.* Milwaukee, Wisconsin: Hal Leonard, 2006.

[6] C. M. Hutchins and D. Voskuil, "Mode Tuning for the Violin Maker," *CAS Journal,* vol. 2, pp. 5-9, November 1993.

[7] C. M. Hutchins, "Musical Acoustics, Part 2," in *Benchmark Papers in Acoustics.* vol. 6, R. B. Lindsay, Ed. Stroudsburg, Pennsylvania: Dowden, Hutchinson & Ross, Inc., 1975.

[8] E. Jansson, "Acoustics for Violin and Guitar Makers," 4th ed: Kungl Tekniska Högskolan, Dept of Speech, Music and Hearing, 2002.

[9] H. Fastl and E. Zwicker, *Psychoacoustics : Facts and Models*, 3rd ed. New York: Springer, 2007.

[10] R. M. French, *Engineering the Guitar.* New York: Springer, 2009.

[11] A. Chaigne, "Recent Advances in Vibration and Radiation of Musical Instruments," *Flow, Turbulence and Combustion,* vol. 61, pp. 31-41, 1999.

[12] C. M. Hutchins, "Musical Acoustics, Part 1," in *Benchmark Papers in Acoustics.* vol. 5, R. B. Lindsay, Ed. Stroudsburg, Pennsylvania: Dowden, Hutchinson & Ross, Inc., 1975.

[13] A. H. Benade, *Fundamentals of Musical Acoustics*, 2nd ed. New York: Dover Publications, Inc., 1990.

[14] Forest Products Laboratory (US), *Wood Handbook: Wood as an Engineering Material.* Madison, Wisconsin.: U.S. Dept. of Agriculture, Forest Service, Forest Products Laboratory, 1999.

[15] R. L. Bisplinghoff, H. Ashley, and R. L. Halfman, *Aeroelasticity.* Reading, Massachusetts: Addison-Wesley Publishing Company, 1955.

[16] J. P. D. Hartog, *Mechanical Vibrations.* New York: Dover Publications, Inc., 1985.

[17] L. Meirovitch, *Principles and Techniques of Vibrations.* Upper Saddle River, New Jersey: Prentice Hall, 2000.

[18] C. M. Wang, J. N. Reddy, and K. H. Lee, *Shear Deformable Beams and Plates: Relationships with Classical Solutions.* New York: Elsevier Science Ltd, 2000.

[19] W. F. Riley, L. D. Sturges, and D. H. Morris, *Mechanics of Materials*, 6th ed. Hoboken, New Jersey: Wiley, 2007.

[20] S. Timoshenko and S. Woinowsky-Krieger, *Theory of Plates and Shells*, 2nd ed. New York: McGraw-Hill, 1959.

[21] A. W. Leissa, *Vibration of plates.* Washington: Scientific and Technical Information Division, National Aeronautics and Space Administration, 1969.

[22] L. Meirovitch, *Fundamentals of Vibrations.* New York: McGraw-Hill, 2001.

[23] F. Vigneron, "Assumed Shape Method for Beam Divided into Two Equal Sections," in *Appendix C*, Ed. Ottawa: Frank Vigneron, 2009, p. 23.

[24] L. E. Malvern, *Introduction to the Mechanics of a Continuous Medium.* Englewood Cliffs, New Jersey: Prentice-Hall, 1969.